



**Calhoun: The NPS Institutional Archive**

---

Theses and Dissertations

Thesis Collection

---

1988

The performance of conventional and DBD receivers for MFSK/QPSK modulation when operating in the presence of noise and Rayleigh fading.

Rudy, Larry J.

Monterey, California. Naval Postgraduate School

---



Calhoun is a project of the Dudley Knox Library at NPS, furthering the precepts and goals of open government and government transparency. All information contained herein has been approved for release by the NPS Public Affairs Officer.

**Dudley Knox Library / Naval Postgraduate School**  
**411 Dyer Road / 1 University Circle**  
**Monterey, California USA 93943**

<http://www.nps.edu/library>







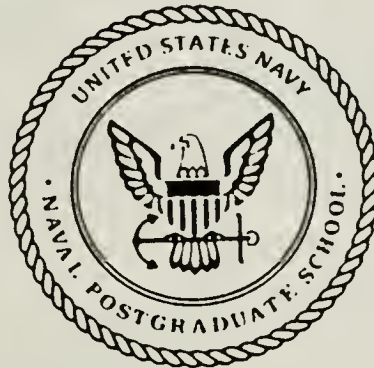






# NAVAL POSTGRADUATE SCHOOL

## Monterey, California



## THESIS

R8375

THE PERFORMANCE OF CONVENTIONAL AND  
DBD RECEIVERS FOR  
MFSK/QPSK MODULATION WHEN OPERATING  
IN THE PRESENCE OF NOISE  
AND RAYLEIGH FADING

by

Larry J. Rudy

December 1988

Thesis Advisor

Daniel C. Bukofzer

Approved for public release; distribution is unlimited.

T242316





| REPORT DOCUMENTATION PAGE  |       |   |  |   |
|--|-------|---|--|---|
| 1a Report Security Classification <b>Unclassified</b>  |       | 1b Restrictive Markings   |  |   |
| 2a Security Classification Authority   |       | 3 Distribution, Availability of Report                            |  |   |
| 2b Declassification Downgrading Schedule   |       | Approved for public release; distribution is unlimited.           |  |   |
| 4 Performing Organization Report Number(s)   |       | 5 Monitoring Organization Report Number(s)                        |  |   |
| 6a Name of Performing Organization<br>Naval Postgraduate School  |       | 6b Office Symbol<br>(if applicable) 32                            |  | 7a Name of Monitoring Organization<br>Naval Postgraduate School |
| 6c Address (city, state, and ZIP code)<br>Monterey, CA 93943-5000  |       | 7b Address (city, state, and ZIP code)<br>Monterey, CA 93943-5000 |  |   |
| 8a Name of Funding, Sponsoring Organization  |       | 8b Office Symbol<br>(if applicable)                               |  | 9 Procurement Instrument Identification Number                  |
| 8c Address (city, state, and ZIP code)   |       | 10 Source of Funding Numbers                                      |  |   |
|  |       | Program Element No  | Project No   | Task No   |
|  |       | Work Unit Accession No  |  |   |
| 11 Title (include security classification) <b>THE PERFORMANCE OF CONVENTIONAL AND DBD RECEIVERS FOR MFSK/QPSK MODULATION WHEN OPERATING IN THE PRESENCE OF NOISE AND RAYLEIGH FADING</b>   |       |   |  |   |
| 12 Personal Author(s) <b>Rudy, Larry J</b>   |       |   |  |   |
| 13a Type of Report<br>Master's Thesis  |       | 13b Time Covered<br>From To                                       |  | 14 Date of Report (year, month, day)<br>December 1988           |
| 15 Page Count<br>105   |       |   |  |   |
| 16 Supplementary Notation The views expressed in this thesis are those of the author and do not reflect the official policy or position of the Department of Defense or the U.S. Government.   |       |   |  |   |
| 17 Cosati Codes  |       |   | 18 Subject Terms (continue on reverse if necessary and identify by block number) |   |
| Field  | Group | Subgroup  | Biorthogonal Signaling, Digital Modulation, Phase Modulation, Rayleigh fading.   |   |
|  |       |   |  |   |
|  |       |   |  |   |
| 19 Abstract (continue on reverse if necessary and identify by block number) This thesis devoted to studying the properties of a digital M-ary signaling scheme called MFSK/QPSK which combines the features of M-ary FSK and QPSK modulation. This scheme is shown to be a form of biorthogonal signaling, and a receiver that is optimum in error rate sense is introduced and analyzed in order to obtain its bit error rate (BER) performance when signal interference can be modeled as additive white Gaussian noise. The bandwidth of the MFSK QPSK signaling scheme is derived and compared with that of M-ary PSK and M-ary FSK signaling. MFSK/QPSK signaling results in receivers that provide error rates much lower than corresponding receivers for M-ary PSK and slightly lower than those for M-ary FSK, while maintaining a bandwidth efficiency at least three times greater than that of M-ary FSK though not as great as that of M-ary PSK signaling. A significant effort has been devoted to examining a detection method known as direct bit detection (DBD) which has been applied to M-ary PSK and MFSK/QPSK signaling. DBD receivers are introduced, and the BER of the MFSK/QPSK DBD receiver is derived and compared with that of the optimum (symbol discrimination) receiver. Lastly, the effects on performance due to Rayleigh fading are analyzed and evaluated for M-ary PSK DBD receivers as well as for the MFSK/QPSK optimum (symbol discrimination) and DBD receiver. |       |   |  |   |
| 20 Distribution/Availability of Abstract<br><input checked="" type="checkbox"/> unclassified unlimited <input type="checkbox"/> same as report <input type="checkbox"/> DTIC users   |       |   | 21 Abstract Security Classification<br>Unclassified                              |   |
| 22a Name of Responsible Individual<br>Daniel C. Bukofzer   |       |   | 22b Telephone (include Area code)<br>(408) 646-2859                              | 22c Office Symbol<br>62Bh                                       |

Approved for public release; distribution is unlimited.

The Performance of Conventional and DBD Receivers for  
MFSK/QPSK Modulation When Operating in the Presence of Noise  
and Rayleigh Fading

by

Larry J. Rudy  
Lieutenant, United States Coast Guard  
B.S., U.S. Coast Guard Academy, 1981

Submitted in partial fulfillment of the  
requirements for the degree of

MASTER OF SCIENCE IN ELECTRICAL ENGINEERING

from the

NAVAL POSTGRADUATE SCHOOL  
December 1988

## ABSTRACT

This thesis devoted to studying the properties of a digital M-ary signaling scheme called MFSK/QPSK which combines the features of M-ary FSK and QPSK modulation. This scheme is shown to be a form of biorthogonal signaling, and a receiver that is optimum in error rate sense is introduced and analyzed in order to obtain its bit error rate (BER) performance when signal interference can be modeled as additive white Gaussian noise. The bandwidth of the MFSK/QPSK signaling scheme is derived and compared with that of M-ary PSK and M-ary FSK signaling. MFSK/QPSK signaling results in receivers that provide error rates much lower than corresponding receivers for M-ary PSK and slightly lower than those for M-ary FSK, while maintaining a bandwidth efficiency at least three times greater than that of M-ary FSK though not as great as that of M-ary PSK signaling. A significant effort has been devoted to examining a detection method known as direct bit detection (DBD) which has been applied to M-ary PSK and MFSK/QPSK signaling. DBD receivers are introduced, and the BER of the MFSK/QPSK DBD receiver is derived and compared with that of the optimum (symbol discrimination) receiver. Lastly, the effects on performance due to Rayleigh fading are analyzed and evaluated for M-ary PSK DBD receivers as well as for the MFSK/QPSK optimum (symbol discrimination) and DBD receiver.

## TABLE OF CONTENTS

|   |    |
|---|----|
| I. INTRODUCTION .....   | 1  |
| A. BACKGROUND .....   | 1  |
| B. CONTENTS AND SUMMARY OF RESULTS .....                            | 1  |
| C. M-ARY PHASE-SHIFT KEYING .....                                   | 2  |
| D. M-ARY FREQUENCY-SHIFT KEYING .....                               | 3  |
| E. RECEIVERS OF M-ARY PSK AND M-ARY FSK .....                       | 3  |
| F. SYMBOL ERROR RATES FOR M-ARY PSK AND M-ARY FSK .....             | 7  |
| G. BANDWIDTH REQUIREMENTS .....                                     | 10 |
| II. DIRECT BIT DETECTION METHODS FOR M-ARY PSK .....                | 12 |
| A. M-ARY PSK DIRECT BIT DETECTION RECEIVERS .....                   | 12 |
| B. PERFORMANCE OF DBD RECEIVERS FOR M-ARY PSK .....                 | 12 |
| III. MFSK/QPSK .....  | 20 |
| A. MFSK/QPSK AS A BIORTHOGONAL SIGNAL SET .....                     | 20 |
| B. OPTIMUM RECEIVER .....   | 27 |
| C. OPTIMUM RECEIVER BER .....                                       | 33 |
| D. DBD RECEIVER FOR MFSK/QPSK .....                                 | 41 |
| E. MFSK/QPSK DBD RECEIVER BER .....                                 | 43 |
| F. BANDWIDTH OF MFSK/QPSK .....                                     | 46 |
| IV. RAYLEIGH FADING .....   | 50 |
| A. THE RAYLEIGH FADING MODEL .....                                  | 50 |
| B. EFFECT ON BER OF M-ARY PSK USING DBD RECEIVER .....              | 50 |
| C. EFFECT ON BER OF MFSK/QPSK USING DBD RECEIVER .....              | 61 |
| D. EFFECT ON BER OF MFSK/QPSK USING THE OPTIMUM RE-<br>CEIVER ..... | 62 |
| V. RESULTS .....  | 64 |
| A. PERFORMANCE COMPARISONS .....                                    | 64 |
| B. BANDWIDTH EFFICIENCY .....                                       | 70 |



C. EFFECTS OF RAYLEIGH FADING ..... 70

VI. CONCLUSIONS ..... 77

APPENDIX A. INTEGRAL IDENTITY ..... 78

APPENDIX B. MFSK/QPSK BER COMPUTER PROGRAM ..... 82

APPENDIX C. 16-PSK RAYLEIGH FADING BER COMPUTER PROGRAM 85

APPENDIX D. MFSK/QPSK RAYLEIGH FADING BER COMPUTER  
PROGRAM ..... 91

LIST OF REFERENCES ..... 95

INITIAL DISTRIBUTION LIST ..... 96

## LIST OF TABLES

|          |   |    |
|----------|---|----|
| Table 1. | FUNCTION DEFINITIONS .....  | 18 |
| Table 2. | PERFORMANCE COMPARISONS AT KEY SYMBOL ERROR<br>RATES .....              | 64 |
| Table 3. | PERFORMANCE COMPARISONS OF MFSK/QPSK RECEIVERS .                        | 65 |
| Table 4. | BANDWIDTH EFFICIENCIES FOR M-ARY PSK, M-ARY FSK,<br>AND MFSK/QPSK ..... | 70 |
| Table 5. | EFFECT OF RAYLEIGH FADING USING VARIOUS RECEIVERS                       | 76 |

## LIST OF FIGURES

|            |   |    |
|------------|---|----|
| Figure 1.  | Signal Constellations for a) QPSK and b) 8-PSK                    | 4  |
| Figure 2.  | Magnitude Spectrum for QFSK                                       | 5  |
| Figure 3.  | Magnitude Spectrum for M-ary FSK                                  | 6  |
| Figure 4.  | Receiver Structure for M-ary PSK                                  | 8  |
| Figure 5.  | Receiver Structure for M-ary FSK                                  | 9  |
| Figure 6.  | Block Diagram of the 8-PSK DBD Receiver                           | 13 |
| Figure 7.  | Block Diagram of the 16-PSK DBD Receiver                          | 14 |
| Figure 8.  | Signal Constellation for 8-PSK Showing Variable Phase Parameters  | 15 |
| Figure 9.  | Signal Constellation for 16-PSK Showing Variable Phase Parameters | 16 |
| Figure 10. | Vector Representation of 2FSK/QPSK                                | 28 |
| Figure 11. | Diagram of a General Correlation Receiver                         | 30 |
| Figure 12. | Diagram of Correlation Receiver for 2FSK/QPSK                     | 32 |
| Figure 13. | Diagram of DBD Receiver for 2FSK/QPSK                             | 42 |
| Figure 14. | Magnitude Spectrum for 2FSK/QPSK                                  | 47 |
| Figure 15. | Magnitude Spectrum for MFSK/QPSK                                  | 48 |
| Figure 16. | 2FSK/QPSK Bit Error Performance ( $k = 3$ bits/symbol)            | 66 |
| Figure 17. | 4FSK/QPSK Bit Error Performance ( $k = 4$ bits/symbol)            | 67 |
| Figure 18. | 8FSK/QPSK Bit Error Performance ( $k = 5$ bits/symbol)            | 68 |
| Figure 19. | 16FSK/QPSK Bit Error Performance ( $k = 6$ bits/symbol)           | 69 |
| Figure 20. | 8-PSK DBD Receiver Bit Error Performance in Rayleigh Fading       | 72 |
| Figure 21. | 16-PSK DBD Receiver Bit Error Performance in Rayleigh Fading      | 73 |
| Figure 22. | MFSK/QPSK DBD Rcvr. Bit Error Performance in Rayleigh Fading      | 74 |
| Figure 23. | MFSK/QPSK Opt. Rcvr. Bit Error Performance in Rayleigh Fading     | 75 |





## **I. INTRODUCTION**

### **A. BACKGROUND**

There exists an increasing need for high-data-rate, reliable digital communication systems. The reasons for this need stem from the desire by an increased number of users to transmit larger amounts of data via digital communication schemes which provide more reliability, flexibility, and lower cost when compared with analog communication systems. These increased demands come at a time when the available bandwidth in the free space channel is becoming a limited resource. These data transmission requirements coupled with limited channel resources are the driving force behind the continual search for digital modulation techniques which operate at low error rates and are bandwidth efficient. Present signaling schemes in use are the well known M-ary Phase Shift Keying (M-PSK) and M-ary Frequency Shift Keying (M-FSK). These signaling schemes are briefly described in Sections C and D of this chapter, and the corresponding receiver structures for recovering the digital information are described in Section E, while the performance of these receivers, specified in terms of the symbol error rates, for both M-ary PSK and M-ary FSK modulation are given in Section F. The bandwidth requirements associated with these two modulation schemes are given in Section G.

### **B. CONTENTS AND SUMMARY OF RESULTS**

This thesis explores a hybrid form of digital modulation, namely MFSK/QPSK, which embodies features of both M-ary FSK and Quaternary (or four phase) PSK. The analysis compares and contrasts the properties of this modulation scheme to the widely known M-ary PSK and M-ary FSK modulation. In Chapter 3, MFSK/QPSK is shown to be a form of biorthogonal signaling, and therefore its corresponding receiver performance is easily revealed given what is already known for this class of signals. The optimum MFSK/QPSK receiver that recovers the digital information with minimum probability of error under specific noise interference assumptions is analyzed from a performance standpoint, which traditionally has been given in terms of the Symbol Error Rate (SER). Because a more meaningful performance parameter is the receiver's Bit Error Rate (BER), Chapter 3 has been devoted to deriving the receiver's BER as a function of signal-to-noise ratio, along with the bandwidth requirements and the bandwidth efficiency of the MFSK/QPSK scheme. Comparisons are made between the MFSK/QPSK scheme and conventional phase and frequency modulation methods with

respect to SER performance and bandwidth efficiency in Chapter 5. The results show that the MFSK/QPSK scheme when compared to M-ary PSK, does not attain the high bandwidth efficiencies achieved by M-ary PSK, yet outperforms M-ary PSK substantially in terms of SER performance, while performing slightly better than M-ary FSK in terms of SER performance and only requiring one third to one fourth the bandwidth required by an M-ary FSK system.

Additionally, this thesis addresses the properties of a class of digital communication receivers which decode the individual bits that make up a symbol directly, without need for symbol-to-bit mapping post-detection circuitry. These are referred to as direct bit detection (DBD) receivers, because each of the bits that make up a symbol are determined independently. These receivers have been proposed and analyzed for M-ary PSK Ref. 1 [pp. 461-463] as well as for the MFSK/QPSK signaling scheme Ref. 2 [pp. 16-101] under discussion here. DBD receiver structures for M-ary PSK are introduced in Chapter 2, and previously derived expressions for their BER performance are presented. In Chapter 3, a DBD receiver structure for MFSK/QPSK signaling is described, and analysis is carried out in order to derive its BER performance, with corresponding results presented in graphical form in Chapter 5. Also in Chapter 5 the BER performance of the MFSK/QPSK DBD receiver is compared to that of the optimum receiver that performs symbol detection followed by symbol-to-bit mappings prior to delivering binary data to the intended user. Furthermore, the results demonstrate that while the DBD receiver does not perform as well as the optimum receiver in BER sense, its simplified receiver structure and direct bit detection properties offer other potential advantages.

In choosing a modulation method, it is important that the effect of system disturbances such as Rayleigh fading, which is common in digital microwave radio transmission applications, be analyzed in order to fully understand all aspects of expected system performance for the different signaling schemes under consideration. The effect of Rayleigh fading on the BER performance of the MFSK/QPSK receivers as well as of the M-ary PSK DBD receivers is analyzed and evaluated in Chapter 4. The results demonstrate that in all cases, Rayleigh fading can severely degrade receiver performance.

### **C. M-ARY PHASE-SHIFT KEYING**

M-ary signaling techniques involve forming groups of  $k$  bits to generate  $M = 2^k$  symbols which are assigned to  $M$  different waveforms suitable for transmission over a channel. One form of M-ary signaling, namely M-ary Phase-Shift Keying (M-PSK), is a bandwidth efficient digital modulation scheme. The phase of the transmitted



sinusoidal carrier waveform can take on one of  $M$  different phases to represent  $M$  different symbols. The  $M$ -ary PSK waveform can be described mathematically as

$$s_i(t) = \sqrt{\frac{2E}{T_s}} \cos\left[2\pi f_0 t + \frac{2\pi i}{M}\right] \quad (1.1)$$

for  $i = 0, 1, \dots, M-1$  and  $0 \leq t \leq T_s$ , where generally (as is the case here) the phase difference between waveform pairs is taken to be constant. Each symbol or waveform  $s_i(t)$  is transmitted at a rate of  $R_s = \frac{1}{T_s}$  symbols/sec, where  $T_s$  is the time duration of each waveform  $s_i(t)$ . For  $k=2$  and  $M=4$ , the resulting modulation form is known as Quaternary Phase-Shift Keying (QPSK), where the phase difference between waveform pairs is  $\frac{\pi}{2}$  radians. For 8-PSK, in which  $k=3$  and  $M=8$ , waveform pairs are separated by a phase of  $\frac{\pi}{4}$  radians. Signal constellations for QPSK and 8-PSK as well as symbol assignments for each signal (or phasor representation) are presented in Figure 1 on page 4.

#### D. M-ARY FREQUENCY-SHIFT KEYING

$M$ -ary Frequency-Shift Keying ( $M$ -FSK) is another form of  $M$ -ary signaling, in which the waveforms are mathematically expressed as

$$s_i(t) = \sqrt{\frac{2E}{T_s}} \cos 2\pi f_i t \quad (1.2)$$

where the frequencies  $f_i$ , typically are given by

$$f_i = f_0 + i\Delta f \quad (1.3)$$

for  $i = 0, 1, \dots, M-1$  and  $0 \leq t \leq T_s$ . The signal duration is normally chosen so that  $f_i T_s$  is an integer or at least  $f_i T_s \gg 1$  holds. The frequency separation  $\Delta f$  is often set equal to  $R_s$ , providing minimum frequency spacing between signals  $s_i(t)$ , while forming a set of orthogonal signals. For  $k=2$  and  $M=4$ , the resulting modulation is Quadrature Frequency-Shift Keying (QFSK). Magnitude spectra for QFSK and  $M$ -ary FSK (for arbitrary  $M$ ) are shown in Figure 2 on page 5 and in Figure 3 on page 6, respectively.

#### E. RECEIVERS OF M-ARY PSK AND M-ARY FSK

Signals transmitted through a physical channel always encounter interference. The SER results given later in this chapter and the BER analysis presented in Chapter 3 are obtained under the assumption that this interference can be modeled as a sample function of an additive white Gaussian noise (AWGN) process having double sided power

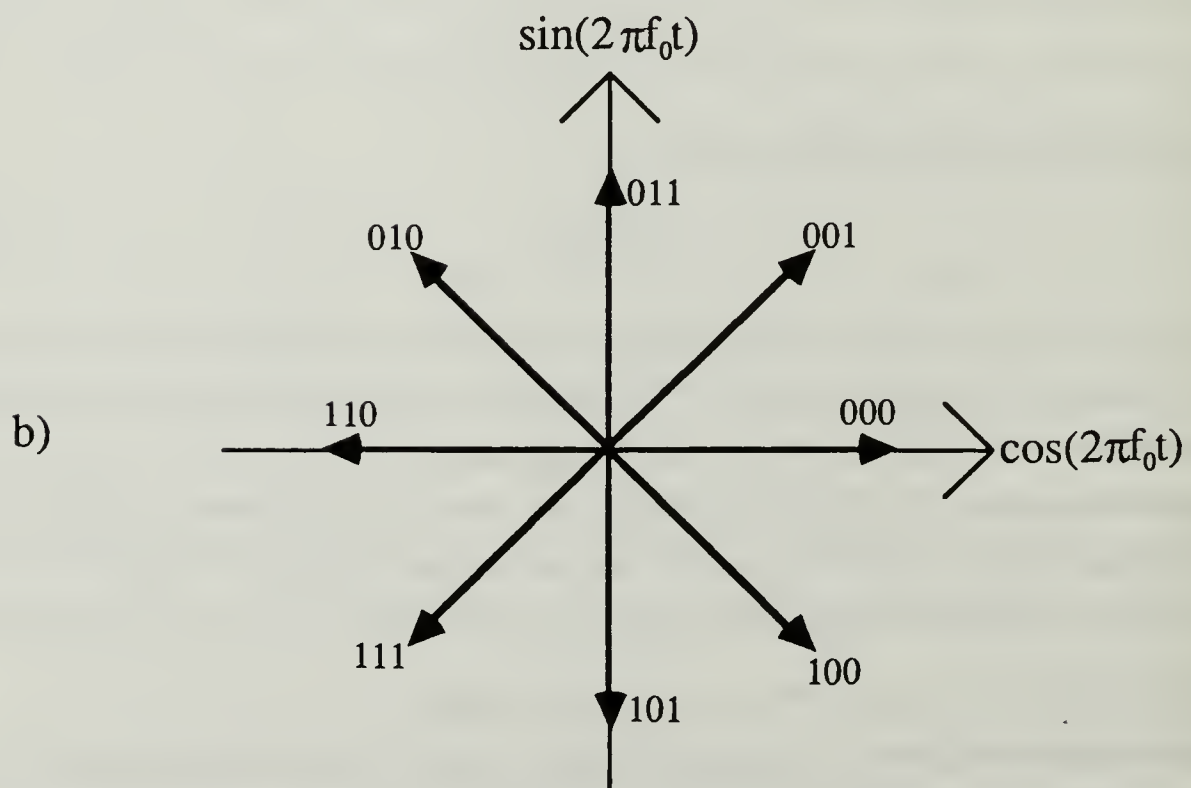
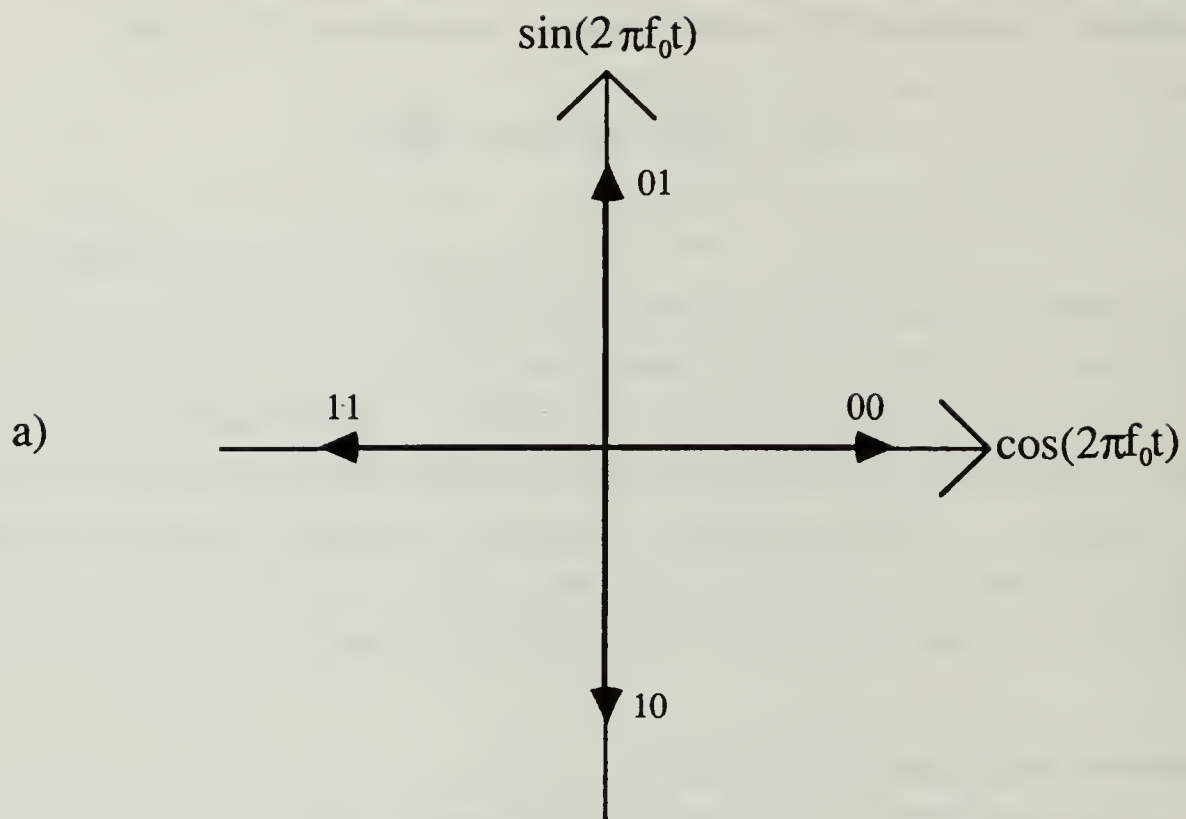


Figure 1. Signal Constellations for a) QPSK and b) 8-PSK

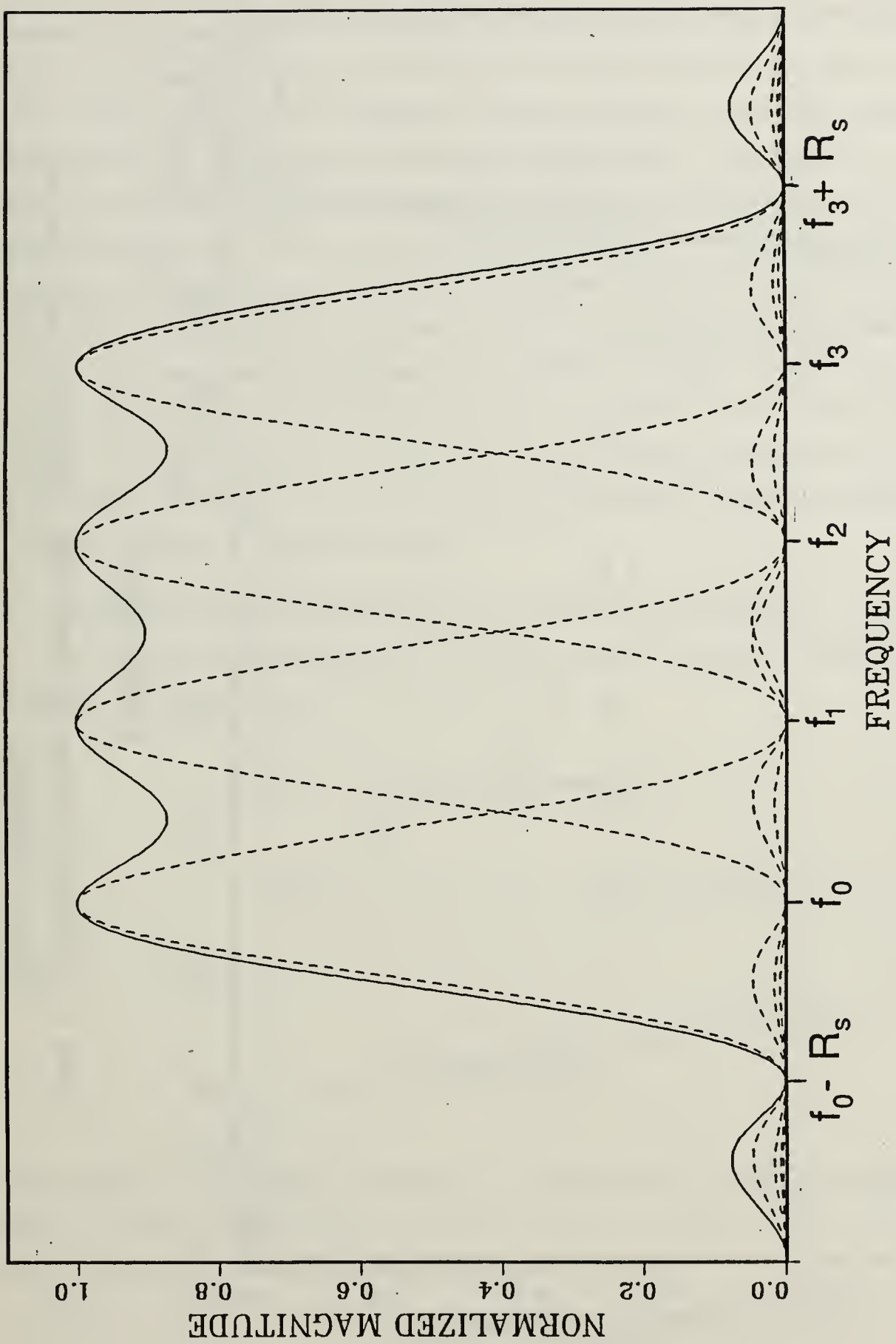


Figure 2. Magnitude Spectrum for QFSK: Dashed lines show individual spectral components.

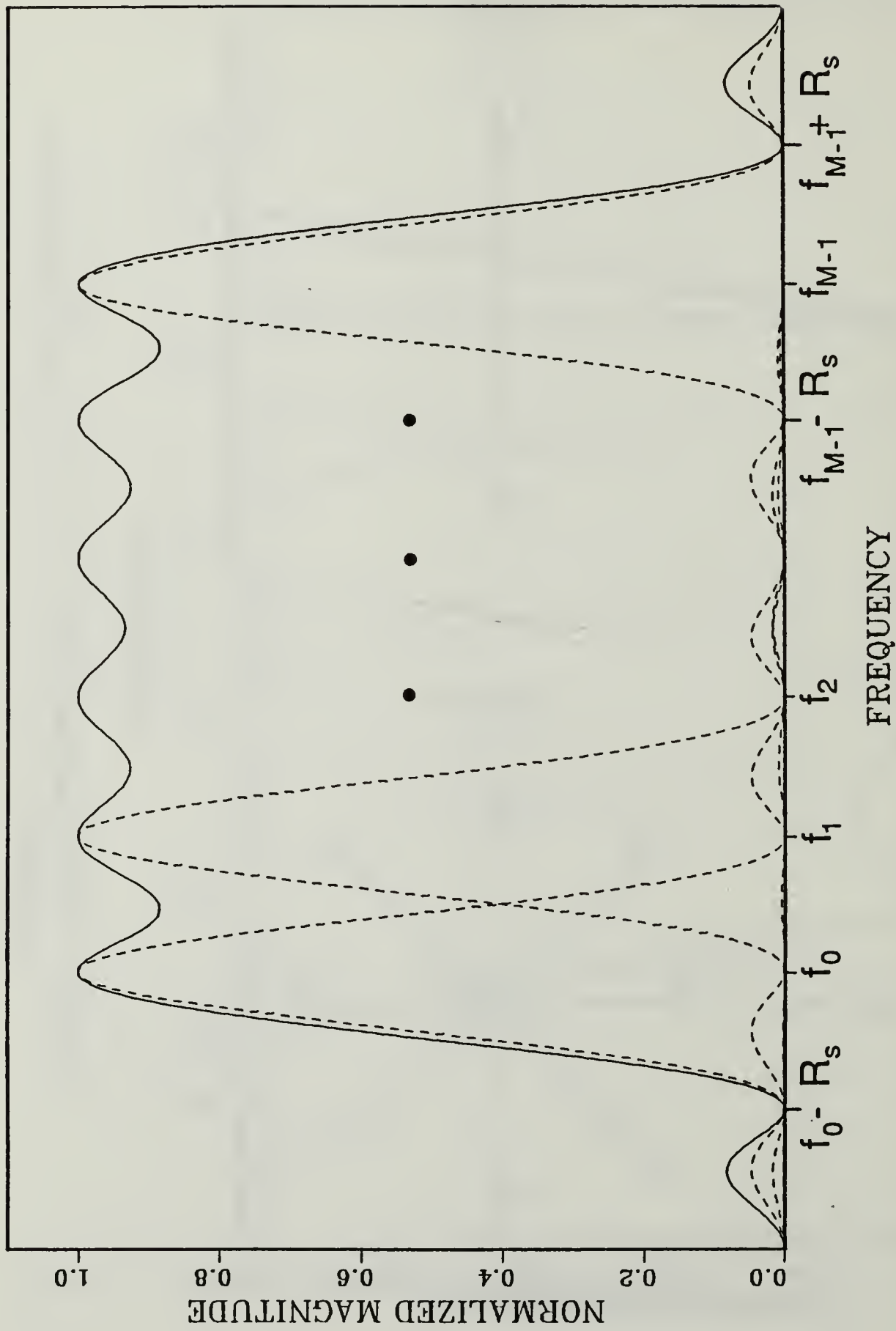


Figure 3. Magnitude Spectrum for M-ary FSK: Dashed lines show individual spectral components.

spectral density (PSD) of  $\frac{N_0}{2}$ . Under this assumption, receivers can be derived that are optimum in the sense that the probability of a symbol error is minimized. One structural form of an optimum receiver for M-ary PSK is shown in Figure 4 on page 8. This receiver as well as all receivers considered herein is assumed to be coherent, meaning that the phase of the sinusoidal carrier is known at the receiver. The concept of coherence applies to this receiver in that the cosine and sine functions which are correlated with the received signal are in phase with the unmodulated carrier sinusoid. Because the receiver correlates the received signal with a set of sinusoidal functions, which in this case consists of each of the possible transmitted signals, it is referred to as a correlation receiver.

An optimum receiver structure for M-ary FSK is shown in Figure 5 on page 9, which also corresponds to a correlation receiver. The correlator with a local signal input which most closely matches the incoming signal, will produce in the absence of interference, the largest output so that the receiver can decide which signal was sent according to which correlator output is the largest.

## F. SYMBOL ERROR RATES FOR M-ARY PSK AND M-ARY FSK

For coherent demodulation of M-ary PSK using the optimum receiver shown in Figure 4, the SER is given by Ref. 3 [pp. 204-207]

$$P_s\{e\} = \frac{1}{2} - \frac{1}{M} + Q\left(\sqrt{\frac{2E}{N_0}} \sin \frac{\pi}{M}\right) - \frac{1}{\sqrt{\pi}} \int_0^{\sqrt{\frac{E}{N_0}}} \exp(-y^2) \left[1 - 2Q\left(y\sqrt{2} \cot \frac{\pi}{M}\right)\right] dy \quad (1.4)$$

where

$$Q(\xi) \equiv \int_{\xi}^{\infty} g(\zeta) d\zeta \quad (1.5)$$

The integral on the right hand side of Eq. 1.4 has no known closed form, and therefore must be evaluated numerically if plotting of  $P_s\{e\}$  as a function of  $\frac{E}{N_0}$  is desired. For high values of  $\frac{E}{N_0}$ , the SER can be tightly upperbounded by

$$P_s\{e\} < 2Q\left(\sqrt{\frac{2E}{N_0}} \sin \frac{\pi}{M}\right) \quad (1.6)$$



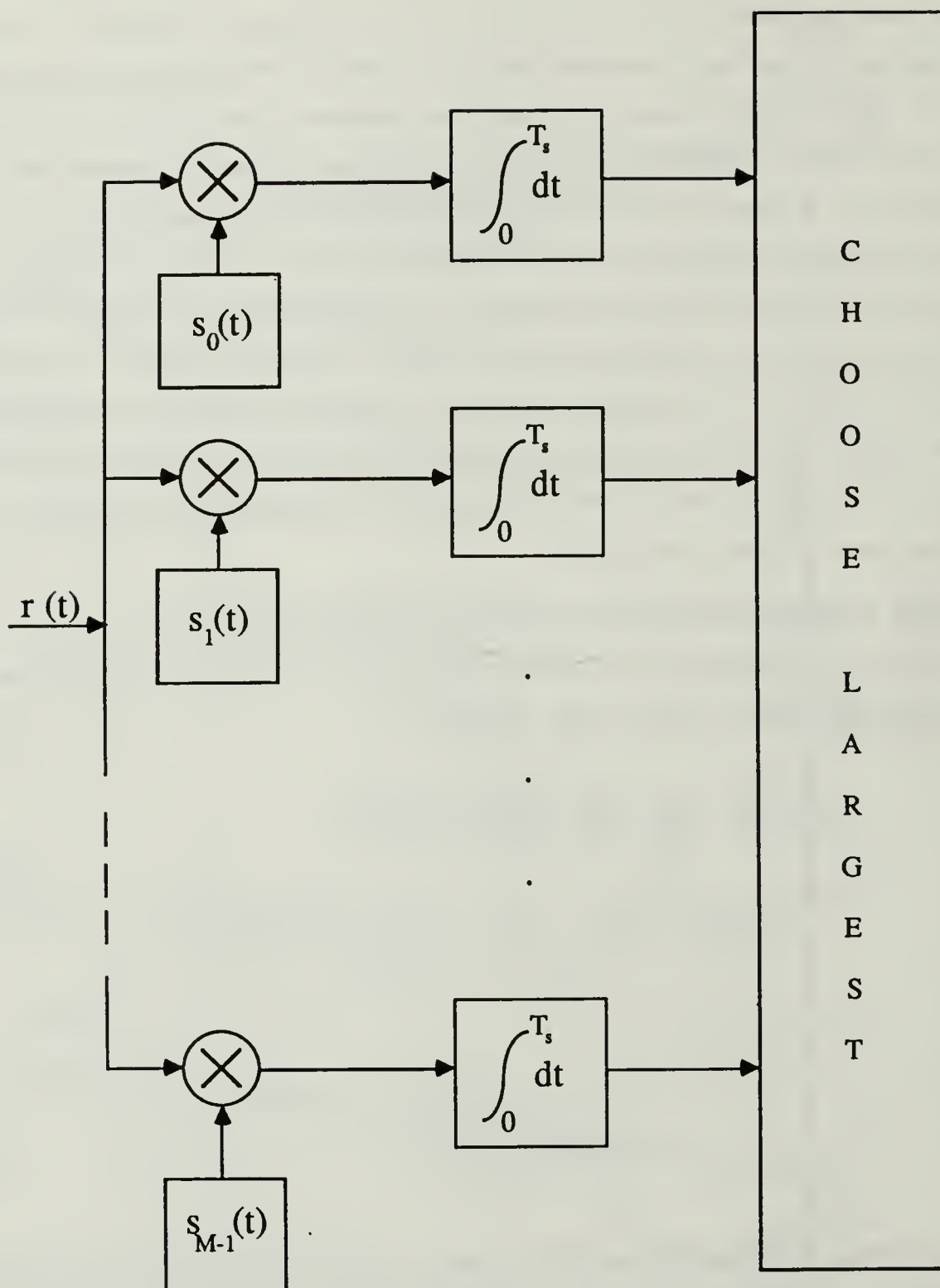


Figure 4. Receiver Structure for M-ary PSK

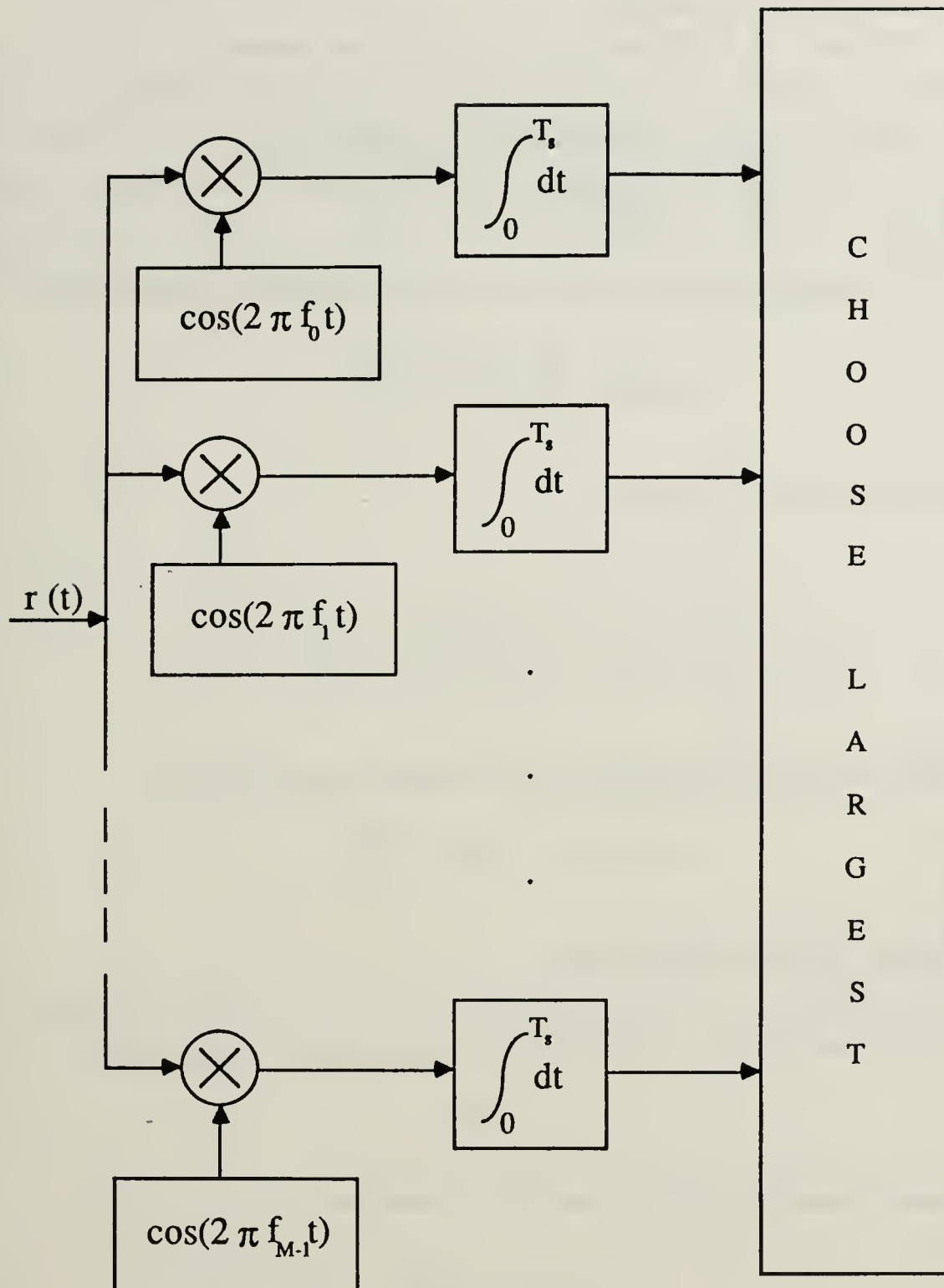


Figure 5. Receiver Structure for M-ary FSK

For M-ary FSK modulation and an AWGN interference model, the optimum coherent receiver of Figure 5 on page 9 achieves a probability of correctly decoding a symbol given by Ref. 3 [pp. 200-203]

$$P_s\{C\} = \int_{-\infty}^{\infty} \left[ \int_{-\infty}^{y + \sqrt{\frac{E}{\sigma}}} g(x) dx \right]^{M-1} g(y) dy \quad (1.7)$$

where  $\sigma = \frac{N_0}{2}$ , and  $g(\zeta)$  is the zero mean unit variance Gaussian distribution, or

$$g(\zeta) \equiv \frac{1}{\sqrt{2\pi}} \exp\left(-\frac{\zeta^2}{2}\right) \quad (1.8)$$

This expression can be rewritten as

$$P_s\{C\} = \int_{-\infty}^{\infty} \left[ 1 - Q\left(y + \sqrt{\frac{E}{\sigma}}\right) \right]^{M-1} g(y) dy = 1 - P_s\{e\} \quad (1.9)$$

Also, the SER can be closely upperbounded for high values of  $\frac{E}{N_0}$  by

$$P_s\{e\} \leq (M-1)Q\left(\sqrt{\frac{E}{N_0}}\right) \quad (1.10)$$

## G. BANDWIDTH REQUIREMENTS

For M-ary PSK, the carrier is switched at the rate of  $R_s$  times per second. Since there are  $k$  bits associated with each symbol, the bit rate  $R_b$  can be expressed as

$$R_b = kR_s \quad (1.11)$$

The null-to-null bandwidth  $W$  for M-ary PSK is given by

$$W = 2R_s = \frac{2R_b}{k} \quad (1.12)$$

For M-ary FSK the carrier is also switched at the symbol rate  $R_s$ . Looking at Figure 3 it can be seen that the total null-to-null bandwidth left-most main lobe to right-most main lobe for M-ary FSK can be written as

$$W = (M + 1)R_s = \frac{(2^k + 1)R_b}{k} \quad (1.13)$$

From Eq. 1.13 it is apparent that the null-to-null bandwidth of M-ary FSK increases with increasing values of  $k$ , however Eq. 1.12 shows that the null-to-null bandwidth of M-ary PSK decreases with increasing  $k$ . This property makes M-ary PSK a desirable modulation method when bandwidth must be minimized. In the next chapter M-ary PSK receivers of a different structure than the one shown in Figure 4 are introduced, and their bit error rates presented.

## II. DIRECT BIT DETECTION METHODS FOR M-ARY PSK

### A. M-ARY PSK DIRECT BIT DETECTION RECEIVERS

M-ary PSK modulation as discussed in Chapter 1, Section A, is a signaling scheme that achieves bandwidth conservation at the expense of signal-to-noise ratio required to maintain a certain bit error rate performance level. The two forms of M-ary PSK signaling discussed in this chapter are 8-PSK and 16-PSK. For 8-PSK,  $k = 3$  bits/symbol and  $M = 8$  symbols, while for 16-PSK,  $k = 4$  bits/symbol and  $M = 16$  symbols. The M-ary PSK receiver discussed in Chapter 1, Section E and most other optimum receiver structures discussed in the literature, require symbol-to-bit mapping to be carried out after a decision has been made as to what signal was transmitted. A receiver structure which does not require this symbol-to-bit mapping is proposed in Ref. 4 [pp. 3-5] and in Ref. 1 [pp. 461-463] for 8-PSK and 16-PSK, respectively. Block diagrams for these receivers are shown in Figure 6 on page 13 for 8-PSK, and in Figure 7 on page 14 for 16-PSK. Because each of the bits are determined independently by these receivers by appropriate processing of the correlator outputs, these receivers are referred to as direct bit detection (DBD) receivers. The processes used by DBD receivers for recovering bits make it possible to adjust the BER of the individual bits within a symbol by means of varying the angles between the signal waveforms. These angle adjustments are shown in Figure 8 on page 15 for 8-PSK, and in Figure 9 on page 16 for 16-PSK, where  $\alpha$  and  $\beta$  are the adjustable phase parameters.

### B. PERFORMANCE OF DBD RECEIVERS FOR M-ARY PSK

A BER analysis for the 8-PSK DBD receiver was carried out by Ref. 4 [pp. 5-14] in which a coherent receiver was assumed, and AWGN used as the interference model. The three bits associated with each symbol are identified as 1B, 2B and 3B corresponding to the most significant bit, the second-most significant bit and the least significant bit, respectively. The results of the BER analysis showed that the individual bit error probabilities were not equal for the 1B, 2B and 3B. In fact these probabilities are given by

$$\begin{aligned} Pr\{1B \text{ incorrect}\} &= \frac{1}{2} Q\left(\sqrt{\frac{2E}{N_0}} \cos \alpha\right) + \frac{1}{2} Q\left(\sqrt{\frac{2E}{N_0}} \sin \alpha\right) \\ &= Pr\{3B \text{ incorrect}\} \end{aligned} \quad (2.1)$$

and

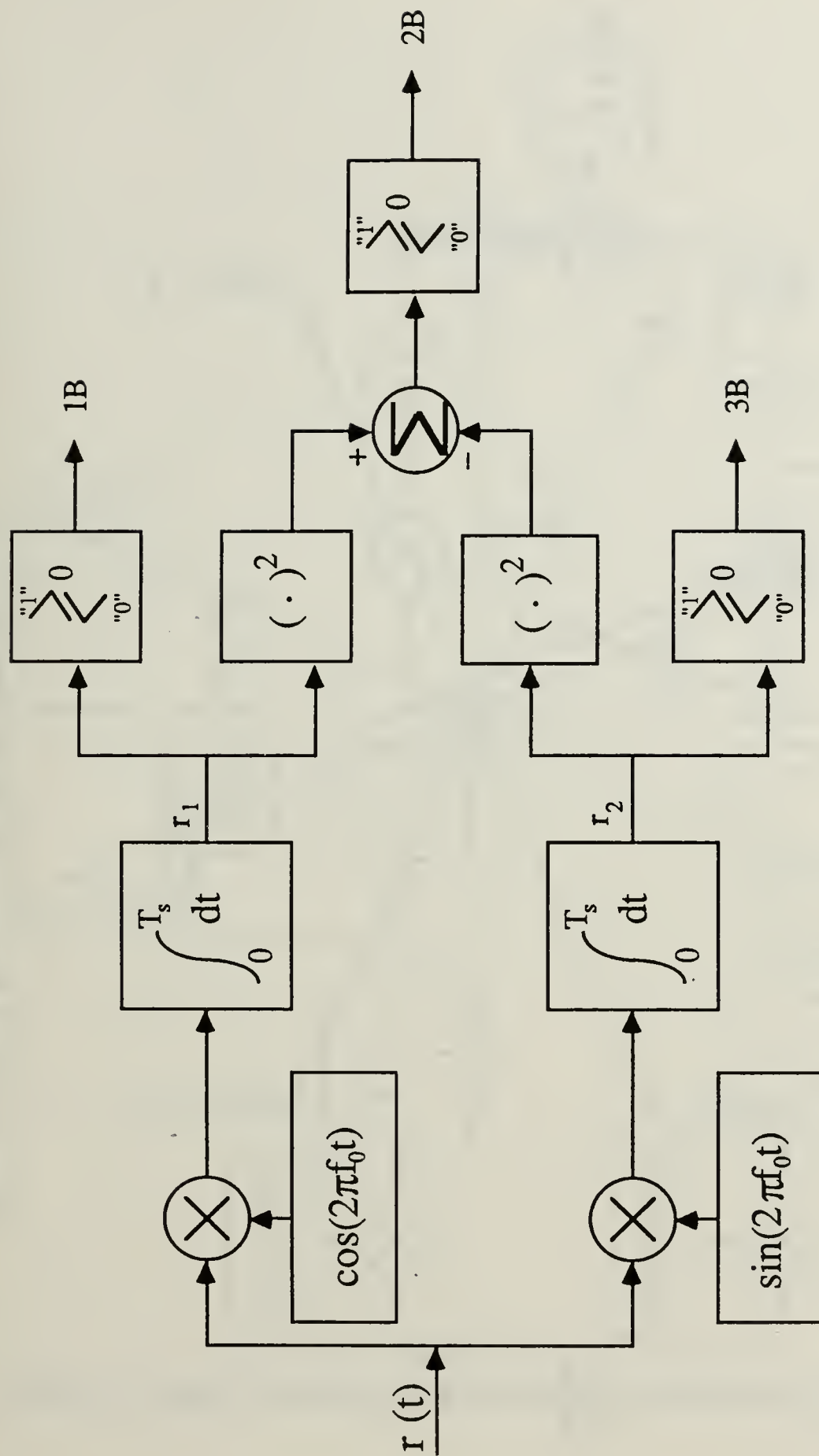


Figure 6. Block Diagram of the 8-PSK DBD Receiver



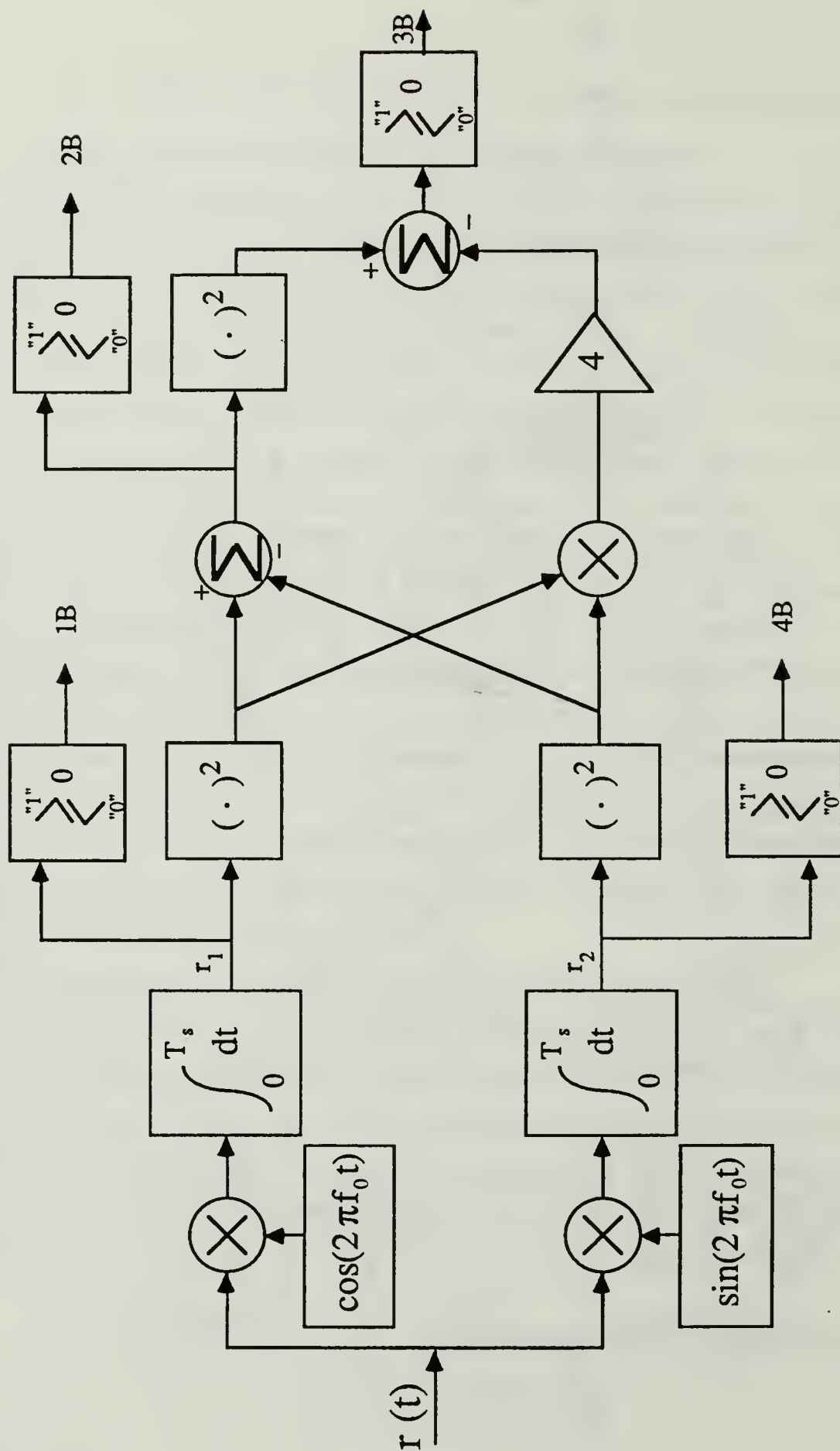


Figure 7. Block Diagram of the 16-PSK DBD Receiver

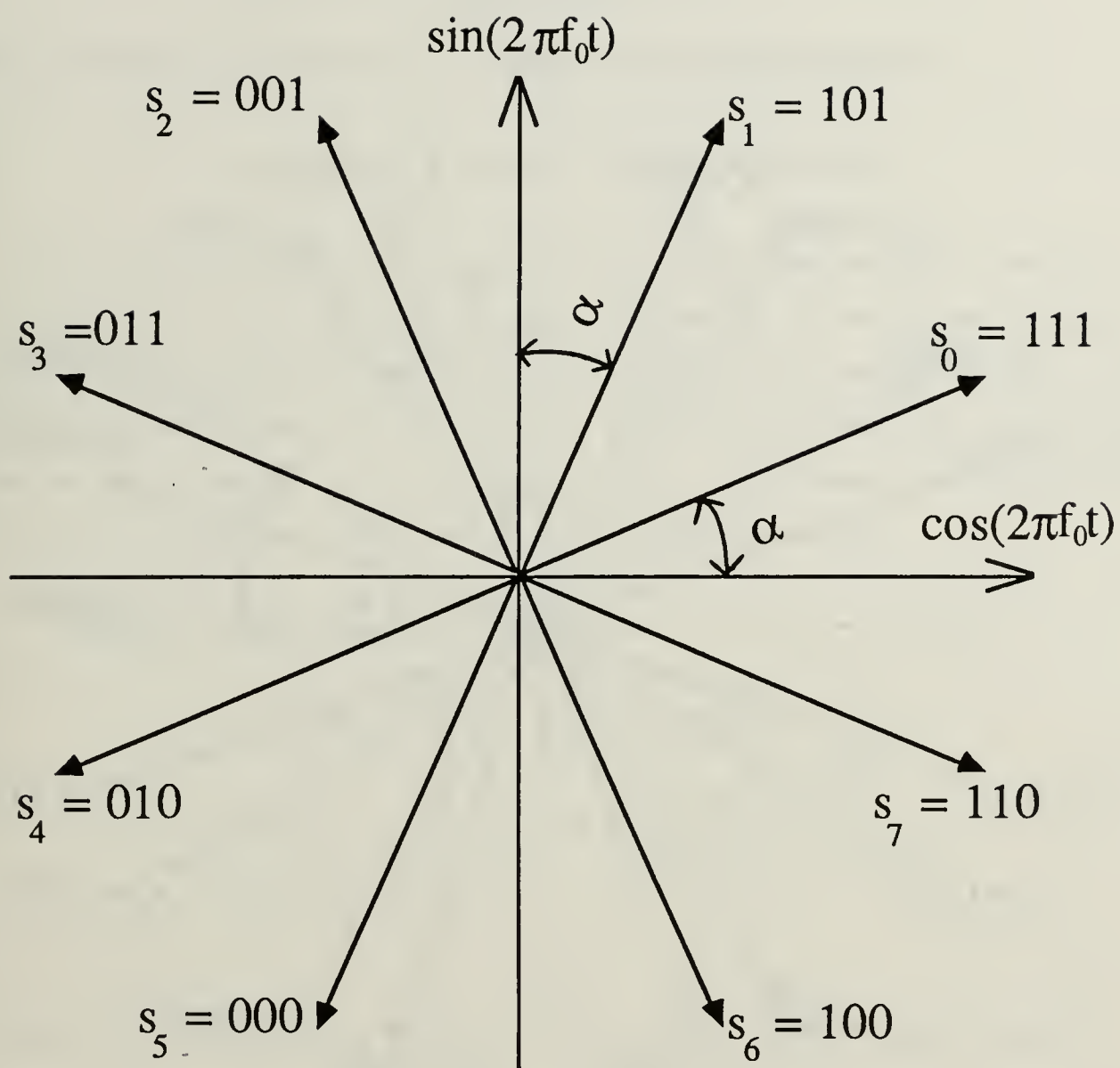


Figure 8. Signal Constellation for 8-PSK Showing Variable Phase Parameters



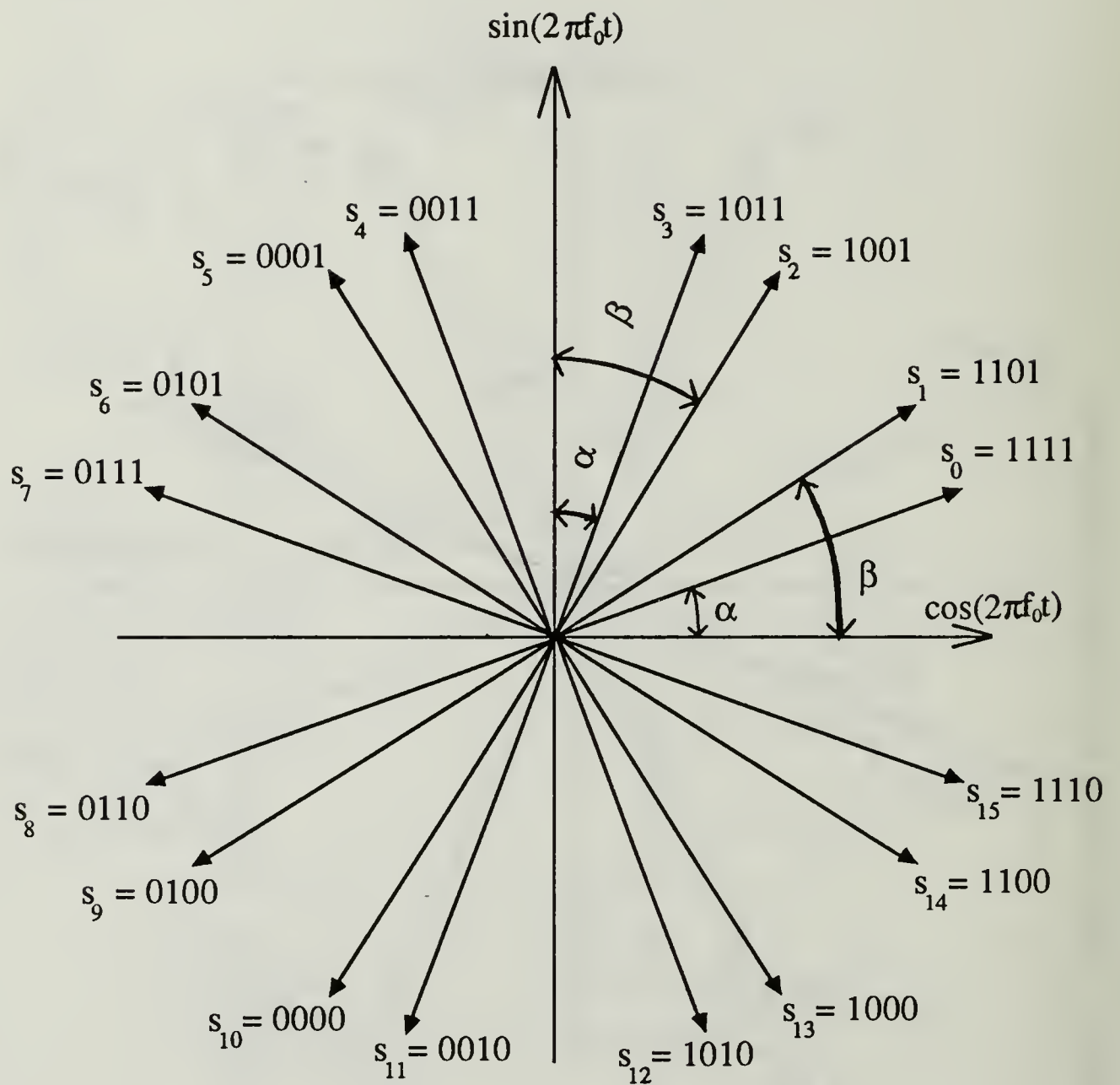


Figure 9. Signal Constellation for 16-PSK Showing Variable Phase Parameters

$$\begin{aligned}
Pr\{2B \text{ incorrect}\} = & \\
& Q\left(\sqrt{\frac{E}{N_0}} [\cos \alpha + \sin \alpha]\right) + Q\left(\sqrt{\frac{E}{N_0}} [\cos \alpha - \sin \alpha]\right) \\
& - 2Q\left(\sqrt{\frac{E}{N_0}} [\cos \alpha + \sin \alpha]\right)Q\left(\sqrt{\frac{E}{N_0}} [\cos \alpha - \sin \alpha]\right)
\end{aligned} \tag{2.2}$$

The overall BER for 8-PSK using the DBD receiver can be expressed as

$$P_b\{e\} = \frac{2}{3} Pr\{1B \text{ incorrect}\} + \frac{1}{3} Pr\{2B \text{ incorrect}\} \tag{2.3}$$

For 16-PSK, there are four bits associated with each symbol which are identified as 1B, 2B, 3B and 4B corresponding to the most significant bit, the second-most significant bit, the third-most significant bit, and the least significant bit, respectively. The error probability associated with each of these bits is different as given by Ref. 1 [pp. 461-463], under the assumption of a coherent receiver and an AWGN interference model. The bit error probabilities for the individual bits in 16-PSK are given by

$$\begin{aligned}
Pr\{1B \text{ incorrect}\} = & \\
& \frac{1}{4} \left[ Q\left(\sqrt{\frac{2E}{N_0}} \cos \alpha\right) + Q\left(\sqrt{\frac{2E}{N_0}} \cos \beta\right) \right] \\
& + \frac{1}{4} \left[ Q\left(\sqrt{\frac{2E}{N_0}} \sin \alpha\right) + Q\left(\sqrt{\frac{2E}{N_0}} \sin \beta\right) \right] \\
= & Pr\{4B \text{ incorrect}\}
\end{aligned} \tag{2.4}$$

$$\begin{aligned}
Pr\{2B \text{ incorrect}\} = & \frac{1}{2} Q\left(\sqrt{\frac{E}{N_0}} [\cos \alpha - \sin \alpha]\right) + Q\left(\sqrt{\frac{E}{N_0}} [\cos \alpha + \sin \alpha]\right) \cdot \\
& \left[ \frac{1}{2} - Q\left(\sqrt{\frac{E}{N_0}} [\cos \alpha - \sin \alpha]\right) \right] \\
& + \frac{1}{2} Q\left(\sqrt{\frac{E}{N_0}} [\cos \beta - \sin \beta]\right) + Q\left(\sqrt{\frac{E}{N_0}} [\cos \beta + \sin \beta]\right) \cdot \\
& \left[ \frac{1}{2} - Q\left(\sqrt{\frac{E}{N_0}} [\cos \beta - \sin \beta]\right) \right]
\end{aligned} \tag{2.5}$$

$$\begin{aligned}
Pr\{3B \text{ incorrect}\} = & \frac{1}{2} - \sum_{i=1}^4 \sqrt{\frac{E}{\pi N_0}} \int_0^{\frac{\pi}{8}} \exp\left(-\frac{E}{N_0} f_i^2(\Gamma, \alpha, \beta)\right) g_i(\Gamma, \alpha, \beta) \cdot \\
& \left\{ \frac{1}{2} - \mathcal{Q}\left(\sqrt{\frac{2E}{N_0}} g_i(\Gamma, \alpha, \beta)\right) \right\} d\Gamma \\
& + \sum_{i=5}^8 \sqrt{\frac{E}{\pi N_0}} \int_0^{\frac{\pi}{8}} \exp\left(-\frac{E}{N_0} f_i^2(\Gamma, \alpha, \beta)\right) g_i(\Gamma, \alpha, \beta) \cdot \\
& \left\{ \frac{1}{2} - \mathcal{Q}\left(\sqrt{\frac{2E}{N_0}} g_i(\Gamma, \alpha, \beta)\right) \right\} d\Gamma
\end{aligned} \tag{2.6}$$

where the integral in Eq. 2.6 has not been solved analytically, but has been evaluated numerically in Ref. 1 [pp. 466-467], and the functions  $f_i(\Gamma, \alpha, \beta)$  and  $g_i(\Gamma, \alpha, \beta)$  are defined in Table 1.

**Table 1. FUNCTION DEFINITIONS**

| Index<br>i | $f_i(\Gamma, \alpha, \beta)$ | $g_i(\Gamma, \alpha, \beta)$ |
|------------|------------------------------|------------------------------|
| 1          | $\sin(\Gamma - \alpha)$      | $\cos(\Gamma - \alpha)$      |
| 2          | $\cos(\Gamma - \alpha)$      | $\sin(\Gamma - \alpha)$      |
| 3          | $\cos(\Gamma + \alpha)$      | $\sin(\Gamma + \alpha)$      |
| 4          | $\sin(\Gamma + \alpha)$      | $\cos(\Gamma + \alpha)$      |
| 5          | $\sin(\Gamma - \beta)$       | $\cos(\Gamma - \beta)$       |
| 6          | $\cos(\Gamma - \beta)$       | $\sin(\Gamma - \beta)$       |
| 7          | $\cos(\Gamma + \beta)$       | $\sin(\Gamma + \beta)$       |
| 8          | $\sin(\Gamma + \beta)$       | $\cos(\Gamma + \beta)$       |

The overall BER for 16-PSK can then be expressed as

$$P_b\{e\} = \frac{1}{2} Pr\{1B \text{ incorrect}\} + \frac{1}{4} Pr\{2B \text{ incorrect}\} + \frac{1}{4} Pr\{3B \text{ incorrect}\} \tag{2.7}$$

These results have been presented here so that results in the sequel can be compared to the BER results associated with DBD coherent receivers for 8-PSK and 16-PSK signaling.

### III. MFSK/QPSK

#### A. MFSK/QPSK AS A BIORTHOGONAL SIGNAL SET

If the features of M-ary FSK and QPSK modulation are combined, a hybrid digital modulation scheme results where signals are both phase modulated and frequency shifted. This new modulation technique will have four signals at each of the operating frequencies corresponding to the four different possible phase modulations. The signal set can be expressed as

$$s_i(t) = \sqrt{\frac{2E}{T_s}} \cos[2\pi f_1 t + i \frac{\pi}{2}] \quad (3.1)$$

for  $i = 0, 1, 2, 3$  and  $0 \leq t \leq T_s$ , and

$$s_i(t) = \sqrt{\frac{2E}{T_s}} \cos[2\pi f_2 t + (i - 4) \frac{\pi}{2}] \quad (3.2)$$

for  $i = 4, 5, 6, 7$  and  $0 \leq t \leq T_s$ .

Integrating the square of the signal  $s_0(t)$  over the interval  $0 \leq t \leq T_s$  yields

$$\begin{aligned} \int_0^{T_s} s_0^2(t) dt &= \int_0^{T_s} \frac{2E}{T_s} \cos^2[2\pi f_1 t] dt \\ &= E \left[ 1 + \frac{\sin[4\pi f_1 T_s]}{4\pi f_1 T_s} \right] \end{aligned} \quad (3.3)$$

If the product  $f_1 T_s$  is an integer, or if  $f_1 T_s \gg 1$ , then

$$\int_0^{T_s} s_0^2(t) dt = E \quad (3.4)$$

which corresponds to the signal energy. Similar integration yields identical results for  $s_i(t)$ ,  $i = 1, 2, \dots, 7$ .

Applying the Gram-Schmidt orthonormalization procedure Ref. 5 [pp. 266-269] to the signal set described by Eqs. 3.1 and 3.2 generates a set of orthonormal basis functions  $\{\phi_j(t)\}$  having the property

$$\int_0^{T_s} \phi_i(t) \phi_j(t) dt = \begin{cases} 1; & \text{for } i=j \\ 0; & \text{for } i \neq j \end{cases} \quad (3.5)$$

so that the signals  $s_i(t)$  can be synthesized using a linear combination of basis functions, i.e.,

$$s_i(t) = \sum_{j=1}^N s_{ij} \phi_j(t); \quad i = 0, 1, \dots, 7 \quad (3.6)$$

where the  $s_{ij}$  coefficients are defined as

$$s_{ij} \equiv \int_0^{T_s} s_i(t) \phi_j(t) dt \quad (3.7)$$

The first basis function is obtained by normalizing  $s_0(t)$ . From Eq. 3.4, we have

$$\phi_1(t) = \frac{s_0(t)}{\sqrt{E}} = \sqrt{\frac{2}{T_s}} \cos[2\pi f_1 t] \quad (3.8)$$

so that  $s_0(t) = \sqrt{E} \phi_1(t)$ , and the coefficient  $s_{01} = \sqrt{E}$ . From Eq. 3.7,  $s_{11}$  is given by

$$\begin{aligned} s_{11} &= \int_0^{T_s} s_1(t) \phi_1(t) dt \\ &= \int_0^{T_s} \sqrt{\frac{2E}{T_s}} \cos(2\pi f_1 t + \frac{\pi}{2}) \sqrt{\frac{2}{T_s}} \cos(2\pi f_1 t) dt \\ &= \frac{\sqrt{E}}{T_s} \int_0^{T_s} \{ \cos[\frac{\pi}{2}] + \cos[2\pi(2f_1)t + \frac{\pi}{2}] \} dt = 0 \end{aligned} \quad (3.9)$$

Defining the auxiliary function  $\gamma_1(t)$  as

$$\begin{aligned} \gamma_1(t) &= s_1(t) - s_{11} \phi_1(t) \\ &= s_1(t) \end{aligned} \quad (3.10)$$

where the second equality follows from Eq. 3.9, the second basis function can be obtained by normalizing the auxiliary function. That is

$$\phi_2(t) = \frac{\gamma_1(t)}{\sqrt{E_{\gamma_1}}} = \frac{s_1(t)}{\sqrt{E}} = \sqrt{\frac{2}{T_s}} \cos(2\pi f_1 t + \frac{\pi}{2}) \quad (3.11)$$

Using next the coefficients  $s_{21}$  and  $s_{22}$  to obtain the auxiliary function  $\gamma_2(t)$  as

$$\gamma_2(t) = s_2(t) - s_{21}\phi_1(t) - s_{22}\phi_2(t) \quad (3.12)$$

where

$$\begin{aligned} s_{21} &= \int_0^{T_s} s_2(t)\phi_1(t)dt \\ &= \int_0^{T_s} \sqrt{\frac{2E}{T_s}} \cos(2\pi f_1 t + \pi) \sqrt{\frac{2}{T_s}} \cos(2\pi f_1 t) dt \\ &= \frac{\sqrt{E}}{T_s} \int_0^{T_s} \{ \cos[\pi] + \cos[2\pi(2f_1)t + \pi] \} dt = -\sqrt{E} \end{aligned} \quad (3.13)$$

and

$$\begin{aligned} s_{22} &= \int_0^{T_s} s_2(t)\phi_2(t)dt \\ &= \int_0^{T_s} \sqrt{\frac{2E}{T_s}} \cos(2\pi f_1 t + \pi) \sqrt{\frac{2}{T_s}} \cos(2\pi f_1 t + \frac{\pi}{2}) dt \\ &= \frac{\sqrt{E}}{T_s} \int_0^{T_s} \{ \cos[\frac{\pi}{2}] + \cos[2\pi(2f_1)t + \frac{3\pi}{2}] \} dt = 0 \end{aligned} \quad (3.14)$$

results in Eq. 3.12 becoming equal to

$$\begin{aligned} \gamma_2(t) &= s_2(t) + \sqrt{E} \phi_1(t) \\ &= \sqrt{\frac{2E}{T_s}} \cos(2\pi f_1 t + \pi) + \sqrt{\frac{2E}{T_s}} \cos(2\pi f_1 t) \\ &= \sqrt{\frac{2E}{T_s}} [ -\cos(2\pi f_1 t) + \cos(2\pi f_1 t) ] = 0 \end{aligned} \quad (3.15)$$

This indicates that  $s_2(t)$  is completely described as



$$s_2(t) = -\sqrt{E} \phi_1(t) \quad (3.16)$$

and thus no new basis function is introduced by  $s_2(t)$  .

The coefficients for  $s_3(t)$  are given by

$$\begin{aligned} s_{31} &= \int_0^{T_s} s_3(t) \phi_1(t) dt \\ &= \int_0^{T_s} \sqrt{\frac{2E}{T_s}} \cos(2\pi f_1 t + \frac{3\pi}{2}) \sqrt{\frac{2}{T_s}} \cos(2\pi f_1 t) dt \\ &= \frac{\sqrt{E}}{T_s} \int_0^{T_s} \{ \cos[\frac{3\pi}{2}] + \cos[2\pi(2f_1)t + \frac{3\pi}{2}] \} dt = 0 \end{aligned} \quad (3.17)$$

and

$$\begin{aligned} s_{32} &= \int_0^{T_s} s_3(t) \phi_2(t) dt \\ &= \int_0^{T_s} \sqrt{\frac{2E}{T_s}} \cos(2\pi f_1 t + \frac{3\pi}{2}) \sqrt{\frac{2}{T_s}} \cos(2\pi f_1 t + \frac{\pi}{2}) dt \\ &= \frac{\sqrt{E}}{T_s} \int_0^{T_s} \{ \cos[\pi] + \cos[2\pi(2f_1)t] \} dt = -\sqrt{E} \end{aligned} \quad (3.18)$$

so that the auxiliary function  $\gamma_3(t)$  becomes

$$\begin{aligned} \gamma_3(t) &= s_3(t) - s_{32} \phi_2(t) \\ &= \sqrt{\frac{2E}{T_s}} \cos(2\pi f_1 t + 3 \frac{\pi}{2}) + \sqrt{\frac{2E}{T_s}} \cos(2\pi f_1 t + \frac{\pi}{2}) \\ &= \sqrt{\frac{2E}{T_s}} [ -\cos(2\pi f_1 t + \frac{\pi}{2}) + \cos(2\pi f_1 t + \frac{\pi}{2}) ] = 0 \end{aligned} \quad (3.19)$$

Thus, as with  $s_2(t)$ ,  $s_3(t)$  introduces no new basis functions. Continuing this procedure for the signal  $s_4(t)$  , we have



$$\begin{aligned}
s_{41} &= \int_{-\infty}^{\infty} s_4(t) \phi_1(t) dt \\
&= \int_0^{T_s} \sqrt{\frac{2E}{T_s}} \cos(2\pi f_2 t) \sqrt{\frac{2}{T_s}} \cos(2\pi f_1 t) dt \\
&= \frac{2\sqrt{E}}{T_s} \int_0^{T_s} \cos(2\pi f_2 t) \cos(2\pi f_1 t) dt = 0
\end{aligned} \tag{3.20}$$

where the last equality is due to the assumption that the frequencies  $f_1$  and  $f_2$  are spread far enough apart to maintain orthogonality as in binary FSK modulation. Similarly

$$\begin{aligned}
s_{42} &= \int_0^{T_s} s_4(t) \phi_2(t) dt \\
&= \int_0^{T_s} \sqrt{\frac{2E}{T_s}} \cos(2\pi f_2 t) \sqrt{\frac{2}{T_s}} \cos(2\pi f_1 t + \frac{\pi}{2}) dt \\
&= \frac{2\sqrt{E}}{T_s} \int_0^{T_s} \cos(2\pi f_2 t) \cos(2\pi f_1 t + \frac{\pi}{2}) dt = 0
\end{aligned} \tag{3.21}$$

so that the auxiliary function  $\gamma_4(t)$  becomes

$$\gamma_4(t) = s_4(t) - \sum_{j=1}^2 s_{4j} \phi_j(t) = s_4(t) \tag{3.22}$$

Normalizing  $\gamma_4(t)$  in order to obtain the third basis function, results in

$$\phi_3(t) = \frac{s_4(t)}{\sqrt{E}} = \sqrt{\frac{2}{T_s}} \cos(2\pi f_2 t) \tag{3.23}$$

Next, evaluating  $s_{5j}$  for  $j = 1, 2, 3$  yields

$$\begin{aligned}
s_{51} &= \int_0^{T_s} s_5(t) \phi_1(t) dt \\
&= \int_0^{T_s} \sqrt{\frac{2E}{T_s}} \cos(2\pi f_2 t + \frac{\pi}{2}) \sqrt{\frac{2}{T_s}} \cos(2\pi f_1 t) dt \\
&= \frac{2\sqrt{E}}{T_s} \int_0^{T_s} \cos(2\pi f_2 t + \frac{\pi}{2}) \cos(2\pi f_1 t) dt = 0
\end{aligned} \tag{3.24}$$

and

$$\begin{aligned}
s_{52} &= \int_0^{T_s} s_5(t) \phi_2(t) dt \\
&= \int_0^{T_s} \sqrt{\frac{2E}{T_s}} \cos(2\pi f_2 t + \frac{\pi}{2}) \sqrt{\frac{2}{T_s}} \cos(2\pi f_1 t + \frac{\pi}{2}) dt \\
&= \frac{2\sqrt{E}}{T_s} \int_0^{T_s} \cos(2\pi f_2 t + \frac{\pi}{2}) \cos(2\pi f_1 t + \frac{\pi}{2}) dt = 0
\end{aligned} \tag{3.25}$$

where again, the frequencies  $f_1$  and  $f_2$  are chosen to maintain orthogonality as explained above. Furthermore,

$$\begin{aligned}
s_{53} &= \int_0^{T_s} s_5(t) \phi_3(t) dt \\
&= \int_0^{T_s} \sqrt{\frac{2E}{T_s}} \cos(2\pi f_2 t + \frac{\pi}{2}) \sqrt{\frac{2}{T_s}} \cos(2\pi f_2 t) dt \\
&= \frac{\sqrt{E}}{T_s} \int_0^{T_s} \{ \cos[\frac{\pi}{2}] + \cos[2\pi(2f_2)t + \frac{\pi}{2}] \} dt = 0
\end{aligned} \tag{3.26}$$

so that with all three of the coefficients equal to zero,  $s_5(t)$  must be orthogonal to all of the basis functions generated thus far. The fourth basis function is then obtained by normalizing  $s_5(t)$ , that is

$$\phi_4(t) = \frac{s_5(t)}{\sqrt{E}} = \sqrt{\frac{2}{T_s}} \cos(2\pi f_2 t + \frac{\pi}{2}) \tag{3.27}$$

It can be easily shown that the remaining signals  $s_6(t)$  and  $s_7(t)$  can be expressed as

$$\begin{aligned}
s_6(t) &= -\sqrt{E} \phi_3(t) \\
s_7(t) &= -\sqrt{E} \phi_4(t)
\end{aligned} \tag{3.28}$$

Thus the coefficients  $s_{63}$  and  $s_{74}$  are both equal to  $-\sqrt{E}$ . Since the set  $\{\phi_i(t)\}$  represents an orthonormal basis in a vector space, the signals  $s_i(t)$  can now be interpreted geometrically as vectors having components equal to the  $s_{ij}$ , namely

$$s_i(t) \rightarrow \vec{s}_i = (s_{i1}, s_{i2}, \dots, s_{iN}); \quad i = 0, 1, \dots, M-1 \tag{3.29}$$

where  $N$  is the number of linearly independent orthonormal basis vectors, and  $M$  is the number of signal vectors.<sup>1</sup> It is well known that

$$\int_0^{T_s} s_i^2(t) dt = \sum_{j=1}^N (s_{ij})^2 = |\vec{s}_i|^2 = E_i \quad (3.30)$$

where  $E_i$  is the energy of the  $i$ th signal. For the case of 2FSK/QPSK,  $M$  is equal to 8,  $N$  is equal to 4, and the vectors representing the signals are

$$\begin{aligned} \vec{s}_0 &= (+\sqrt{E}, 0, 0, 0) \\ \vec{s}_1 &= (0, +\sqrt{E}, 0, 0) \\ \vec{s}_2 &= (-\sqrt{E}, 0, 0, 0) \\ \vec{s}_3 &= (0, -\sqrt{E}, 0, 0) \\ \vec{s}_4 &= (0, 0, +\sqrt{E}, 0) \\ \vec{s}_5 &= (0, 0, 0, +\sqrt{E}) \\ \vec{s}_6 &= (0, 0, -\sqrt{E}, 0) \\ \vec{s}_7 &= (0, 0, 0, -\sqrt{E}) \end{aligned} \quad (3.31)$$

Since there are eight different possible transmitted signals, each signal can represent three bits of information.

The average energy and also the dimensionality of the signal set can be minimized, by subtracting from each signal a constant vector  $\vec{a}$  such that

$$\sum_{i=0}^{M-1} P\{\vec{s}_i\} |\vec{s}_i - \vec{a}|^2 \quad (3.32)$$

is minimized, where  $P\{\vec{s}_i\}$  is the *a priori* probability that the signal  $s_i(t)$  has been transmitted. Such vector  $\vec{a}$  can be obtained from

$$\vec{a} = \sum_{i=0}^{M-1} P\{\vec{s}_i\} \vec{s}_i \equiv E\{\vec{s}\} \quad (3.33)$$

---

<sup>1</sup> The general practice of labeling the number of signals as  $M$  is followed here, but the letter  $M$  in "MFSK/QPSK" represents the number of frequency shifts.

For a signal set of the type described above, assuming all *a priori* probabilities  $P\{\vec{s}_i\}$  are equal, Eq. 3.33 for  $\vec{a}$  reduces to

$$\vec{a} = \frac{1}{8} \sum_{i=0}^{M-1} \vec{s}_i = 0 \quad (3.34)$$

so that there is no minimum energy transformation that would reduce the dimensionality or the average energy of the signal set.

Figure 10 on page 28 shows the vector representation of the 2FSK/QPSK signal set shown as eight vectors in a four dimensional vector space. A signal set consisting of  $N$  orthogonal signals augmented with the negative of each signal is referred to as a biorthogonal signal set. As shown by Figure 10, the 2FSK/QPSK signals form this type of set. For a general biorthogonal signal set, the number of dimensions of the vector space is always equal to half the number of signal vectors. That is

$$M = 2N \quad (3.35)$$

while the number  $k$  of bits represented by each signal is given by

$$k = \log_2 M \quad (3.36)$$

Finally, the number  $K_f$  of signal frequencies in the MFSK/QPSK scheme is one-fourth the number of signals or

$$M = 4K_f \quad (3.37)$$

The best assignment of bits to the  $M$  signals of the biorthogonal signal set is to match those signals separated by the greatest Euclidean distance in the vector space, with symbols having the greatest Hamming distance. With this rule in mind the bit assignments become obvious. That is, signals which are antipodal are assigned symbols which correspond to binary complements. Once this assignment is done, all other vectors' Euclidean distances are equal, so that any other assignment patterns can be freely chosen. A typical bit assignment is shown for the case of  $M = 8$  in Figure 10.

## B. OPTIMUM RECEIVER

With the basis functions having been specified, available analytical results on the structure and performance of receivers for discriminating biorthogonal signals received

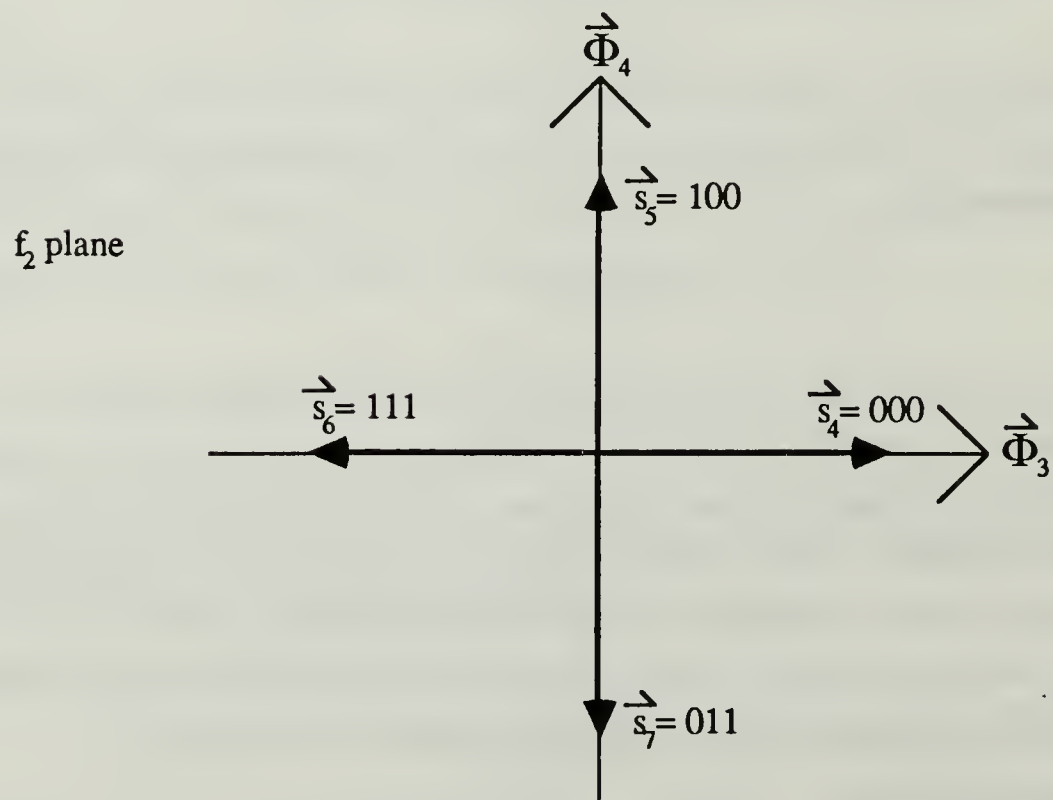
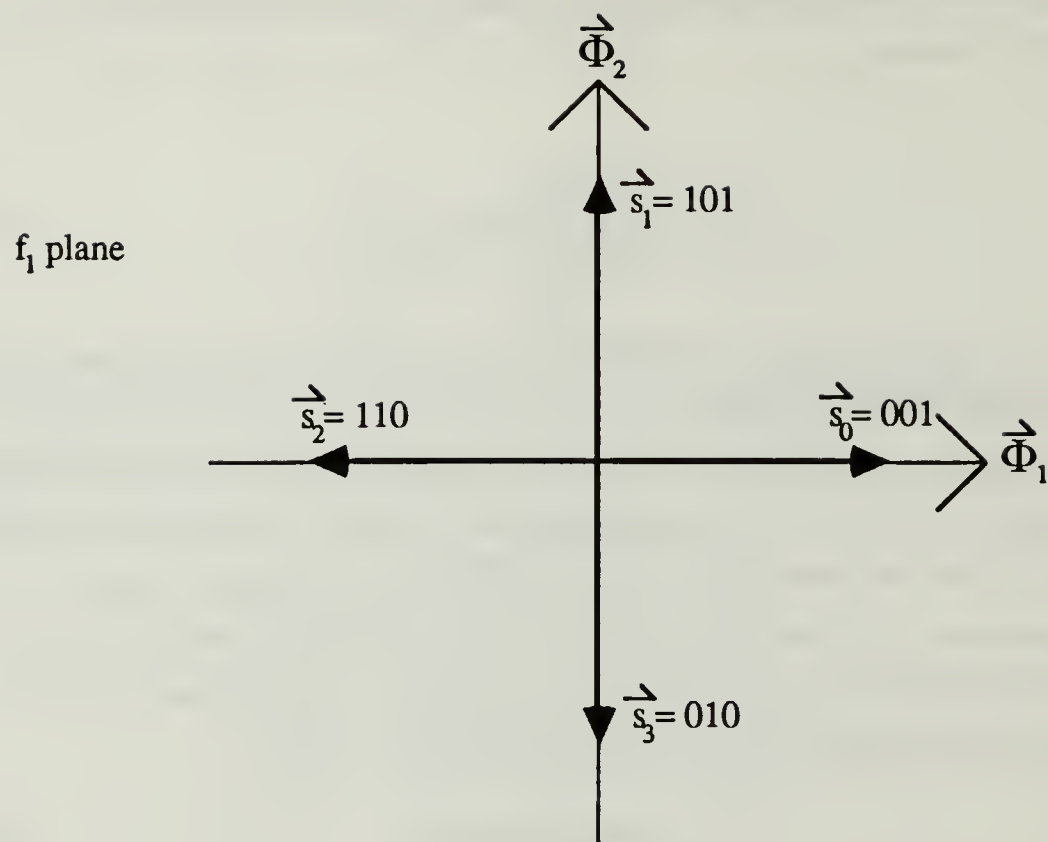


Figure 10. Vector Representation of 2FSK/QPSK



in additive white Gaussian noise make it possible to design an optimum receiver for the discrimination of MFSK/QPSK signals. The received signal  $r(t)$  is assumed to consist of a signal component  $s_i(t)$  plus a sample function of a white Gaussian noise process  $n(t)$ . That is,

$$r(t) = s_i(t) + n(t) \quad (3.38)$$

As shown by Ref. 5 [pp. 211-235] the optimum receiver takes on the structure of a correlation receiver. A block diagram of the general correlation receiver is shown in Figure 11 on page 30. The signal  $r(t)$  is processed by a bank of correlators, where the number of correlators in the receiver is equal to  $N$ , the number of dimensions in the signal vector space model. The effect of the additive white Gaussian noise is to add to the signal vector a noise vector  $\vec{n}$  having  $N$  independent components, each of which is a zero mean, Gaussian random variable with variance  $\frac{N_0}{2}$ . Thus the correlator outputs  $r_j$  form the components of a random vector  $\vec{r}$ , i.e.,

$$\vec{r} = \vec{s}_i + \vec{n} = (r_1, r_2, \dots, r_N) \quad (3.39)$$

After generating the vector  $\vec{r}$ , the components  $r_j$  are processed through a weighting matrix to generate the dot products  $d_i$  which are given by

$$d_i = \vec{r} \cdot \vec{s}_i \equiv \sum_{j=1}^N r_j s_{ij} \quad (3.40)$$

The  $d_i$  are then summed with bias terms  $c_i$  where

$$c_i \equiv \frac{1}{2} (N_0 \ln[P\{m_i\}] - |\vec{s}_i|^2); \quad i = 0, 1, \dots, M-1 \quad (3.41)$$

Finally, all summer outputs  $l_i$  are routed to circuitry which decides which signal was sent according to the rule:

$$\begin{aligned} & \text{If } l_i > l_k; \quad \forall \quad k = 0, 1, \dots, M-1; \quad k \neq i \\ & \text{Then decide } s_i(t) \text{ was the transmitted signal.} \end{aligned} \quad (3.42)$$

For the signal vectors of Eq. 3.31, assuming  $P\{s_i(t)\} = \frac{1}{M}$  for all  $i$ , the structure of the optimum receiver simplifies from that of the general correlation receiver to the 2FSK/QPSK receiver shown in Figure 12 on page 32. The 2FSK/QPSK scheme can be



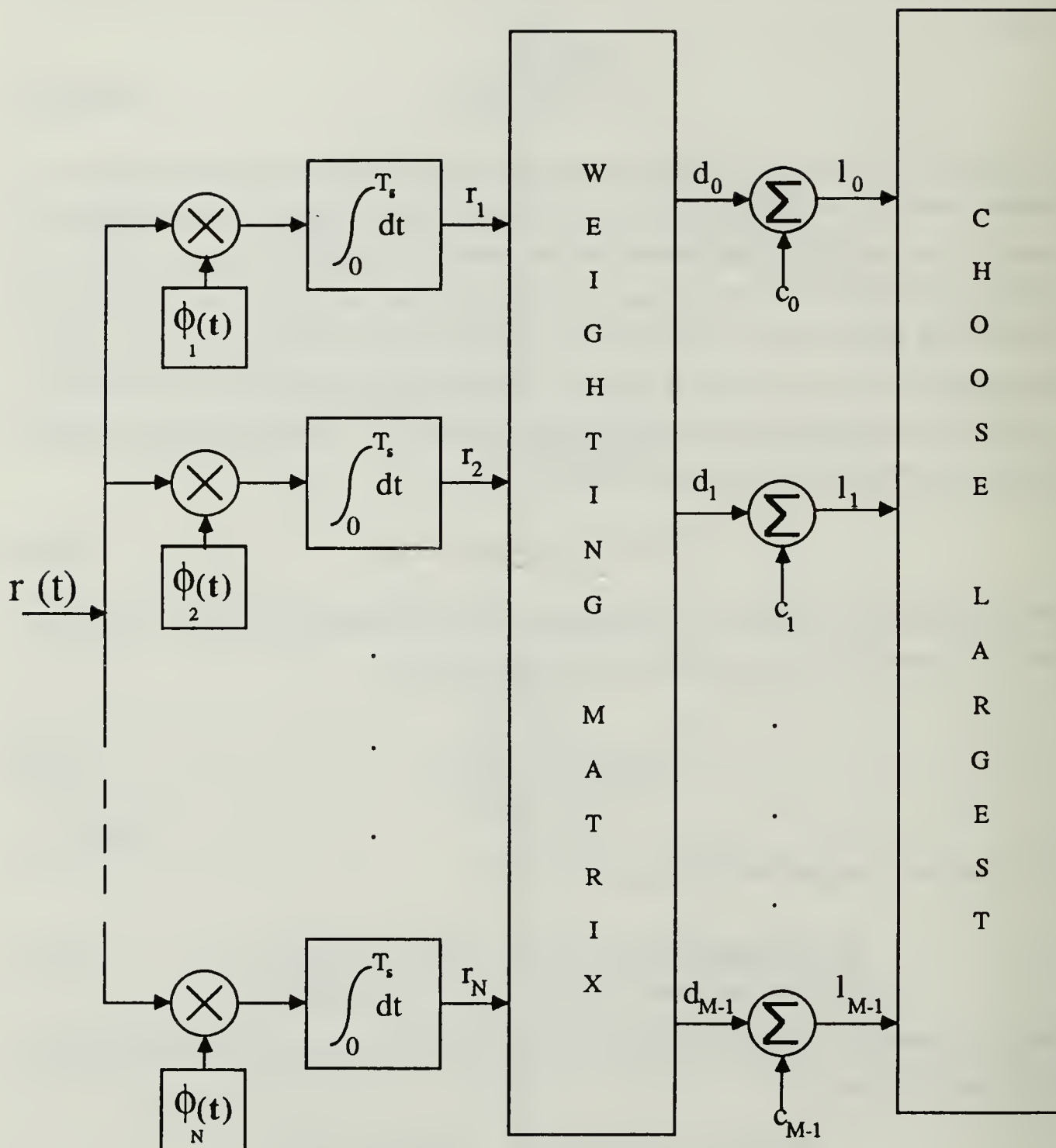


Figure 11. Diagram of a General Correlation Receiver

extended beyond the case considered by increasing the number of signal frequencies. For example, in order to increase the number of bits per signal from three to four, the number of signals  $M$  must be doubled to 16. This is accomplished by doubling the number of frequencies  $K_f$  from two to four, and thus doubling the number of basis functions from four to eight. This change will be reflected in the receiver structure by a doubling of the number of correlators to eight. The new signal set is also biorthogonal, and further extensions to MFSK/QPSK result in  $N$  basis functions,  $K_f$  frequencies,  $M$  signals, and  $k$  bits per signal. The formula for the probability of a correct symbol decision for the biorthogonal set is given by Ref. 5 [pp. 261-263] as

$$P_s\{C\} = \int_0^\infty f_n(\alpha - \sqrt{E}) d\alpha \left[ 1 - 2 \int_\alpha^\infty f_n(\beta) d\beta \right]^{N-1} \quad (3.43)$$

where  $f_n(x)$  is a Gaussian distribution function expressed as

$$f_n(x) = \frac{1}{\sqrt{2\pi\sigma^2}} \exp\left(-\frac{x^2}{2\sigma^2}\right) \quad (3.44)$$

and where

$$\sigma = \sqrt{\frac{N_0}{2}} \quad (3.45)$$

Using the transformation  $y = \frac{\alpha - \sqrt{E}}{\sigma}$  and rearranging the terms in Eq. 3.43 yields

$$P_s\{C\} = \int_{-\frac{\sqrt{E}}{\sigma}}^\infty \left[ 1 - 2 \int_{\sigma y + \sqrt{E}}^\infty f_n(\beta) d\beta \right]^{N-1} g(y) dy \quad (3.46)$$

Using another variable transformation the inner integral becomes

$$\int_{\sigma y + \sqrt{E}}^\infty f_n(\beta) d\beta = \int_{y + \frac{\sqrt{E}}{\sigma}}^\infty g(x) dx = Q\left(y + \frac{\sqrt{E}}{\sigma}\right) \quad (3.47)$$

Substituting this result into Eq. 3.46 gives

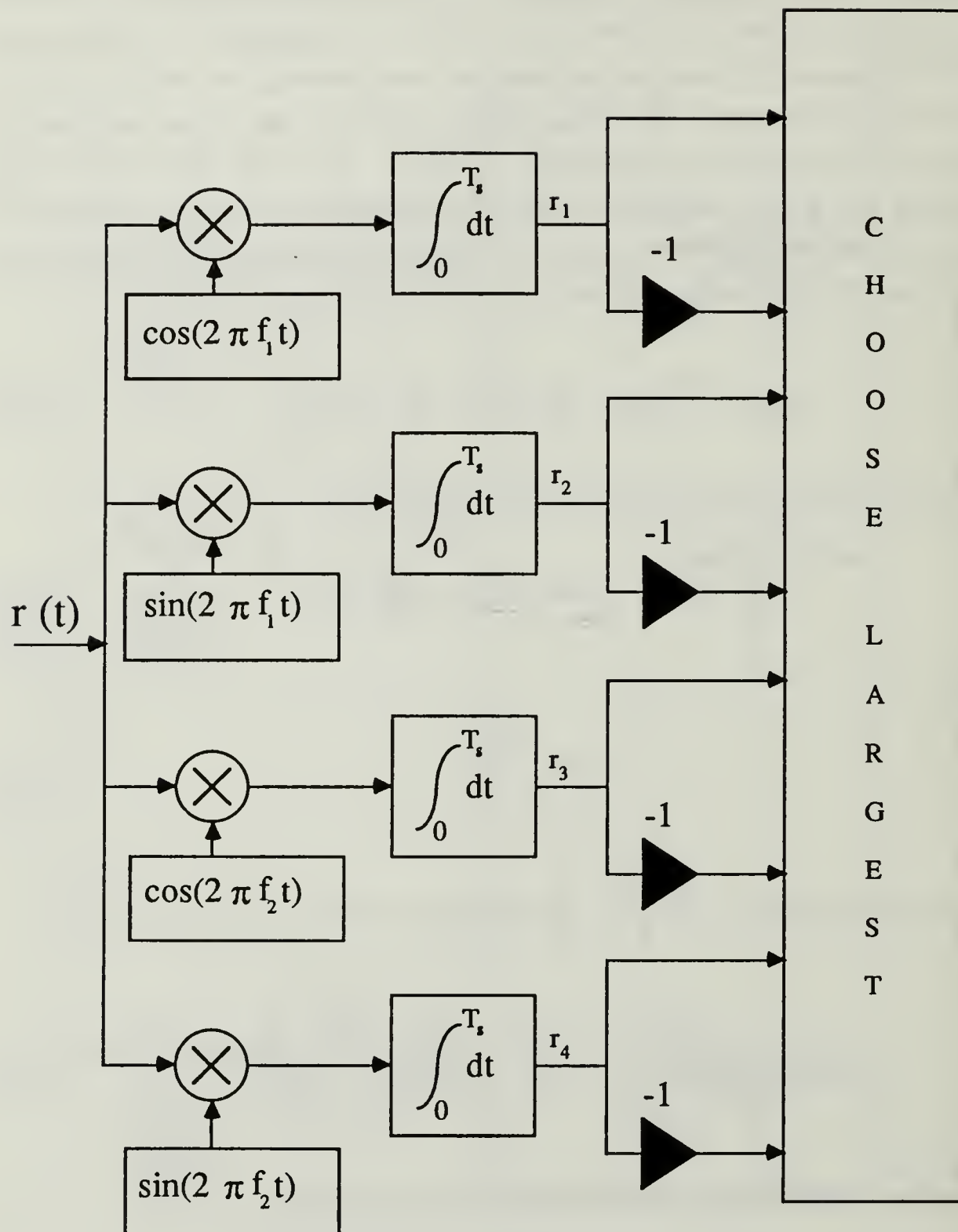


Figure 12. Diagram of Correlation Receiver for 2FSK/QPSK

$$P_s\{C\} = \int_{-\frac{\sqrt{E}}{\sigma}}^{\infty} \left[ 1 - 2Q\left(y + \frac{\sqrt{E}}{\sigma}\right) \right]^{N-1} g(y) dy \quad (3.48)$$

Thus we have the probability of a correct symbol decision associated with the optimum receiver expressed in terms of the Q function.

### C. OPTIMUM RECEIVER BER

In order to compute the Bit Error Rate (BER) of the optimum receiver shown in Figure 12, it is necessary to determine under what conditions a chosen bit will be correctly identified by the receiver for a given transmitted signal. The three bits assigned to each 2FSK/QPSK signal are identified as 1B, 2B and 3B corresponding to the most significant bit, the second-most significant bit, and the least significant bit respectively. We can assume without any loss in generality that  $s_0(t)$  is transmitted. The probability that the 1B is correctly identified at the receiver, conditioned on the assumption that  $s_0(t)$  was transmitted can be written as

$$\begin{aligned} Pr\{1B \text{ Correct} | \vec{s}_0\} &= Pr\{r_1 = \max_j r_j | \vec{s}_0\} + Pr\{-r_2 = \max_j r_j | \vec{s}_0\} \\ &\quad + Pr\{r_3 = \max_j r_j | \vec{s}_0\} + Pr\{-r_4 = \max_j r_j | \vec{s}_0\} \end{aligned} \quad (3.49)$$

Now

$$\begin{aligned} &Pr\{r_1 = \max_j r_j | \vec{s}_0\} \\ &= Pr\{r_1 > -r_1, r_1 > r_2, r_1 > -r_2, r_1 > r_3, r_1 > -r_3, r_1 > r_4, r_1 > -r_4 | \vec{s}_0\} \end{aligned} \quad (3.50)$$

If we further condition on  $r_1$ , that is  $r_1 = R_1$ , since  $r_1 > -r_1$  only for  $R_1 > 0$ , then this conditioning will be

$$\begin{aligned} &Pr\{r_1 = \max_j r_j | \vec{s}_0, r_1 = R_1 > 0\} \\ &= Pr\{R_1 > r_2, R_1 > -r_2, R_1 > r_3, R_1 > -r_3, R_1 > r_4, R_1 > -r_4 | \vec{s}_0, r_1 = R_1 > 0\} \end{aligned} \quad (3.51)$$

Observe that

$$R_1 > r_j, R_1 > -r_j \Rightarrow -R_1 < r_j < R_1 \quad (3.52)$$

so that

$$\begin{aligned}
& Pr\{\mathbf{r}_1 = \max_j \mathbf{r}_j | \vec{s}_0, \mathbf{r}_1 = R_1 > 0\} \\
& = Pr\{-R_1 < \mathbf{r}_2 < R_1, -R_1 < \mathbf{r}_3 < R_1, -R_1 < \mathbf{r}_4 < R_1 | \vec{s}_0, \mathbf{r}_1 = R_1 > 0\}
\end{aligned} \tag{3.53}$$

Assuming  $s_0(t)$  was transmitted, then from Eqs. 3.8 and 3.38 we have

$$r(t) = \sqrt{E} \phi_1(t) + n(t) \tag{3.54}$$

so that

$$\mathbf{r}_1 = \sqrt{E} + \mathbf{n}_1, \quad \mathbf{r}_2 = \mathbf{n}_2, \quad \mathbf{r}_3 = \mathbf{n}_3, \quad \mathbf{r}_4 = \mathbf{n}_4 \tag{3.55}$$

Due to the independence of the random variables  $\mathbf{n}_j$ , the set  $\{\mathbf{r}_j\}$  consists of independent Gaussian random variables having probability density functions (p.d.f.'s)

$$f_{\mathbf{r}_1}(R_1) = \frac{1}{\sqrt{2\pi\sigma^2}} \exp\left[ \frac{-(R_1 - \sqrt{E})^2}{2\sigma^2} \right] \tag{3.56}$$

and

$$f_{\mathbf{r}_j}(R_j) = \frac{1}{\sqrt{2\pi\sigma^2}} \exp\left[ \frac{-R_j^2}{2\sigma^2} \right]; \quad \text{for } j = 2, 3, 4 \tag{3.57}$$

So that Eq. 3.53 simplifies to

$$\begin{aligned}
& Pr\{-R_1 < \mathbf{r}_2 < R_1, -R_1 < \mathbf{r}_3 < R_1, -R_1 < \mathbf{r}_4 < R_1 | \vec{s}_0, \mathbf{r}_1 = R_1 > 0\} \\
& = \prod_{j=2}^4 Pr\{-R_1 < \mathbf{r}_j < R_1 | \vec{s}_0, \mathbf{r}_1 = R_1 > 0\}
\end{aligned} \tag{3.58}$$

Furthermore, from Eq. 3.57

$$\begin{aligned}
Pr\{-R_1 < \mathbf{r}_j < R_1 | \vec{s}_0, \mathbf{r}_1 = R_1 > 0\} &= \int_{-R_1}^{R_1} \frac{1}{\sqrt{2\pi\sigma^2}} \exp\left(\frac{-R_j^2}{2\sigma^2}\right) dR_j \\
&= 2 \left[ \frac{1}{2} - \int_{\frac{R_1}{\sigma}}^{\infty} \frac{1}{\sqrt{2\pi}} \exp\left(\frac{-x^2}{2}\right) dx \right] \quad (3.59) \\
&= 1 - 2Q\left(\frac{R_1}{\sigma}\right); \text{ for } j = 2, 3, 4
\end{aligned}$$

Using this result with Eqs. 3.53 and 3.58 yields

$$Pr\{\mathbf{r}_1 = \max_j \mathbf{r}_j | \vec{s}_0, \mathbf{r}_1 = R_1 > 0\} = \left[ 1 - 2Q\left(\frac{R_1}{\sigma}\right) \right]^3 \quad (3.60)$$

so that integrating over all  $R_1 > 0$  yields

$$\begin{aligned}
Pr\{\mathbf{r}_1 = \max_j \mathbf{r}_j | \vec{s}_0\} &= \int_0^\infty \left[ 1 - 2Q\left(\frac{R_1}{\sigma}\right) \right]^3 \frac{1}{\sqrt{2\pi\sigma^2}} \exp\left[\frac{-(R_1 - \sqrt{E})^2}{2\sigma^2}\right] dR_1 \\
&= \int_{-\frac{\sqrt{E}}{\sigma}}^\infty \left[ 1 - 2Q\left(y + \frac{\sqrt{E}}{\sigma}\right) \right]^3 \frac{1}{\sqrt{2\pi}} \exp\left(\frac{-y^2}{2}\right) dy \quad (3.61)
\end{aligned}$$

Note that this expression approaches unity as  $\frac{E}{\sigma^2} \rightarrow \infty$  as expected. Consider now

$$\begin{aligned}
Pr\{-\mathbf{r}_2 = \max_j \mathbf{r}_j | \vec{s}_0\} &= Pr\{-\mathbf{r}_2 > \mathbf{r}_1, -\mathbf{r}_2 > -\mathbf{r}_1, -\mathbf{r}_2 > \mathbf{r}_2, -\mathbf{r}_2 > \mathbf{r}_3, -\mathbf{r}_2 > -\mathbf{r}_3, -\mathbf{r}_2 > \mathbf{r}_4, -\mathbf{r}_2 > -\mathbf{r}_4 | \vec{s}_0\} \quad (3.62)
\end{aligned}$$

If we further condition on  $\mathbf{r}_2$ , that is  $\mathbf{r}_2 = R_2$ , since  $-\mathbf{r}_2 > \mathbf{r}_2$  can only be satisfied for  $R_2 < 0$ , then this conditioning will be

$$\begin{aligned}
Pr\{-\mathbf{r}_2 = \max_j \mathbf{r}_j | \vec{s}_0, \mathbf{r}_2 = R_2 < 0\} &= Pr\{\mathbf{r}_1 < -R_2, \mathbf{r}_1 > R_2, \mathbf{r}_3 < -R_2, \mathbf{r}_3 > R_2, \mathbf{r}_4 < -R_2, \mathbf{r}_4 > R_2 | \vec{s}_0, \mathbf{r}_2 = R_2 < 0\} \quad (3.63)
\end{aligned}$$

Let  $R'_2 = -R_2$ , so that in terms of  $R'_2$ ,



$$r_j < -R_2, r_j > R_2 \Rightarrow r_j < R'_2, r_j > -R'_2 \Rightarrow -R'_2 < r_j < R'_2; \quad j = 1, 3, 4 \quad (3.64)$$

and the requirement  $R_2 < 0 \Rightarrow R'_2 > 0$ , so

$$\begin{aligned} & Pr\{-r_2 = \max_j r_j | \vec{s}_0, r_2 = -R'_2, R'_2 > 0\} \\ &= \prod_{\substack{j=1 \\ j \neq 2}}^4 Pr\{-R'_2 < r_j < R'_2 | \vec{s}_0, r_2 = -R'_2, R'_2 > 0\} \end{aligned} \quad (3.65)$$

For  $j = 1$ ,

$$\begin{aligned} & Pr\{-R'_2 < r_1 < R'_2\} \\ &= \int_{-R'_2}^{R'_2} \frac{1}{\sqrt{2\pi\sigma^2}} \exp\left[-\frac{(R_1 - \sqrt{E})^2}{2\sigma^2}\right] dR_1 = \int_{\frac{(-R'_2 - \sqrt{E})}{\sigma}}^{\frac{(R'_2 - \sqrt{E})}{\sigma}} \frac{1}{\sqrt{2\pi}} \exp\left(\frac{-x^2}{2}\right) dx \\ &= 1 - \int_{-\infty}^{-\frac{(R'_2 + \sqrt{E})}{\sigma}} \frac{1}{\sqrt{2\pi}} \exp\left(\frac{-x^2}{2}\right) dx - \int_{\frac{(R'_2 - \sqrt{E})}{\sigma}}^{\infty} \frac{1}{\sqrt{2\pi}} \exp\left(\frac{-x^2}{2}\right) dx \\ &= 1 - Q\left(\frac{R'_2 + \sqrt{E}}{\sigma}\right) - Q\left(\frac{R'_2 - \sqrt{E}}{\sigma}\right) \end{aligned} \quad (3.66)$$

since  $R'_2 > 0$ . For  $j = 3, 4$

$$\begin{aligned} Pr\{-R'_2 < r_j < R'_2\} &= \int_{-R'_2}^{R'_2} \frac{1}{\sqrt{2\pi\sigma^2}} \exp\left(\frac{-R_j^2}{2\sigma^2}\right) dR_j \\ &= \int_{-\frac{R'_2}{\sigma}}^{\frac{R'_2}{\sigma}} \frac{1}{\sqrt{2\pi}} \exp\left(\frac{-x^2}{2}\right) dx \\ &= 1 - 2Q\left(\frac{R'_2}{\sigma}\right) \end{aligned} \quad (3.67)$$

so that

$$\begin{aligned}
& Pr\{-r_2 = \max_j r_j | \vec{s}_0, r_2 = -R'_2, R'_2 > 0\} \\
& = \left[1 - 2Q\left(\frac{R'_2}{\sigma}\right)\right]^2 \left[1 - Q\left(\frac{R'_2 + \sqrt{E}}{\sigma}\right) - Q\left(\frac{R'_2 - \sqrt{E}}{\sigma}\right)\right] \quad (3.68)
\end{aligned}$$

Since  $r_2$  takes on values  $R_2$ , we can define a new random variable  $r'_2 = -r_2$  where  $r'_2$  takes on values  $R'_2$ , i.e., if  $r_2 = R_2$ , then  $r'_2 = -R_2 = R'_2$ . So the condition

$$r_2 = -R'_2, R'_2 > 0 \Rightarrow -r'_2 = -R'_2, R'_2 > 0 \Rightarrow r'_2 = R'_2, R'_2 > 0 \quad (3.69)$$

and given the symmetric p.d.f. for  $r_2$  conditioned on  $\vec{s}_0$ , we see that the conditional p.d.f. of  $r'_2$  is no different than the conditional p.d.f. of  $r_2$ , so

$$\begin{aligned}
& Pr\{-r_2 = \max_j r_j | \vec{s}_0\} = Pr\{r'_2 = \max_j r_j | \vec{s}_0\} \\
& = \int_0^\infty \left[1 - 2Q\left(\frac{R'_2}{\sigma}\right)\right]^2 \left[1 - Q\left(\frac{R'_2 + \sqrt{E}}{\sigma}\right) - Q\left(\frac{R'_2 - \sqrt{E}}{\sigma}\right)\right] f_{r_j}(R'_2) dR'_2 \quad (3.70)
\end{aligned}$$

Through a transformation of variables this expression is reduced to

$$\begin{aligned}
& Pr\{-r_2 = \max_j r_j | \vec{s}_0\} \\
& = \int_0^\infty [1 - 2Q(y)]^2 \left[1 - Q\left(y + \frac{\sqrt{E}}{\sigma}\right) - Q\left(y - \frac{\sqrt{E}}{\sigma}\right)\right] \frac{1}{\sqrt{2\pi}} \exp\left(-\frac{y^2}{2}\right) dy \quad (3.71)
\end{aligned}$$

Note that this last expression approaches zero as  $\frac{E}{\sigma^2} \rightarrow \infty$ . Consider now

$$\begin{aligned}
& Pr\{r_3 = \max_j r_j | \vec{s}_0\} \\
& = Pr\{r_3 > r_1, r_3 > -r_1, r_3 > r_2, r_3 > -r_2, r_3 > -r_3, r_3 > r_4, r_3 > -r_4 | \vec{s}_0\} \quad (3.72) \\
& = Pr\{r_1 < r_3, r_1 > -r_3, r_2 < r_3, r_2 > -r_3, 2r_3 > 0, r_4 < r_3, r_4 > -r_3 | \vec{s}_0\}
\end{aligned}$$

If we condition on  $r_3$  that is  $r_3 = R_3$ , we must have  $R_3 > 0$ , or we cannot satisfy the  $2r_3 > 0$  condition. Thus

$$\begin{aligned}
& Pr\{r_3 = \max_j r_j | \vec{s}_0, r_3 = R_3 > 0\} \\
& = Pr\{-R_3 < r_1 < R_3, -R_3 < r_2 < R_3, -R_3 < r_4 < R_3 | \vec{s}_0, r_3 = R_3 > 0\} \quad (3.73)
\end{aligned}$$

From the mathematical form of this equation, it is obvious that this probability, when averaged over all  $R_3 > 0$  produces the same probability as that given by Eq. 3.71, which also is identical to  $Pr\{-r_4 = \max_j r_j | \vec{s}_0\}$ . Thus, we obtain from Eqs. 3.49, 3.61 and 3.71

$$\begin{aligned}
& Pr\{1B \text{ Correct} | \vec{s}_0\} \\
&= \int_{-\frac{\sqrt{E}}{\sigma}}^{\infty} \left[ 1 - 2Q\left(y + \frac{\sqrt{E}}{\sigma}\right) \right]^3 g(y) dy \\
&+ 3 \int_0^{\infty} [1 - 2Q(y)]^2 \left[ 1 - Q\left(y + \frac{\sqrt{E}}{\sigma}\right) - Q\left(y - \frac{\sqrt{E}}{\sigma}\right) \right] g(y) dy
\end{aligned} \tag{3.74}$$

If the 2B is selected then

$$\begin{aligned}
Pr\{2B \text{ Correct} | \vec{s}_0\} &= Pr\{r_1 = \max_j r_j | \vec{s}_0\} + Pr\{r_2 = \max_j r_j | \vec{s}_0\} \\
&+ Pr\{r_3 = \max_j r_j | \vec{s}_0\} + Pr\{r_4 = \max_j r_j | \vec{s}_0\}
\end{aligned} \tag{3.75}$$

The first term on the right hand side of Eq. 3.75 is given by Eq. 3.61, while the last three terms are all of the same form as  $Pr\{r_3 = \max_j r_j | \vec{s}_0\}$  from Eq. 3.72 and will all yield the same probability as given by Eq. 3.71. Therefore, the probability that the 2B is correct is the identical to the probability that the 1B is correct. It can be shown in similar fashion that the probability of correctly identifying the 3B is also equal to that for the 1B. Thus Eq. 3.74 is also the expression for  $P_b\{\text{Correct} | \vec{s}_0\}$  the average probability of decoding a bit correctly given that  $s_0(t)$  was transmitted.

Now consider the case of a given signal  $s_k(t)$  being transmitted, where  $s_k(t)$  can be any one of the signals  $s_i(t)$ ,  $i = 0, 1, \dots, 7$ . For any chosen bit, the probability that this bit is correct conditioned on the hypothesis that  $s_k(t)$  was transmitted can be expressed in a form

$$Pr\{\text{Chosen Bit Correct} | \vec{s}_k\} = Pr\{r_l = \max_j r_j | \vec{s}_k\} + \sum_{\substack{m=1 \\ m \neq l}}^4 Pr\{r_m = \max_j r_j | \vec{s}_k\} \tag{3.76}$$

where  $r_l$  and the  $r_m$  terms are the signed correlator outputs  $\pm r_j$ . The output  $r_l$  corresponds to  $\vec{s}_k$  in that if  $r_l$  is the maximum of all the  $\pm r_j$ , then the receiver decides  $s_k(t)$  was transmitted. The outputs  $r_m$  correspond to three other  $\vec{s}_i$  which if selected by the receiver, would result in the chosen bit still being correct. The first term on the right

hand side will again yield the same probability as that given by Eq. 3.61. The terms in the summation are all of the same mathematical form as Eq. 3.72, and so are equal to the probability given by Eq. 3.71. Thus Eq. 3.74 is the expression for the probability that any chosen bit is correct for any given signal transmitted, and therefore yields the overall average probability of a correct bit,  $P_b\{C\}$ .

Some insight into the total probability of a correct bit decision  $P_b\{C\}$ , may be gained by comparing Eq. 3.74 with the probability of a correct symbol decision  $P_s\{C\}$  given by Eq. 3.48. Since  $N$ , the number of basis functions is equal to 4, the first term in the expression for  $P_b\{C\}$  is equal to  $P_s\{C\}$ . This should come as no surprise, since the derivation for the probability of the 1B being correct began with Eq. 3.43 where the first term is in fact the probability that this bit is correct because the receiver made the correct symbol decision.

The second term in Eq. 3.74 represents the probability that the bit is correctly identified even though the receiver has made a symbol error. Recall from Figure 10 that only those signals which have vector representations orthogonal to each other have bits in common, and for 2FSK/QPSK there are three such signals meeting this requirement for any one fixed signal. The probabilities of erroneously choosing one of these signals over say  $s_0(t)$ , are all equal as discussed above. Furthermore, the conditional probability of (incorrectly) choosing any of the signals orthogonal to  $s_0(t)$ , can be shown to have the mathematical form of Eq. 3.72. Thus Eq. 3.71 specifies the probability of erroneously choosing any one of the signals orthogonal to  $s_0(t)$ .

The above results for 2FSK/QPSK can be extended to MFSK/QPSK, that is, a multi-frequency/four-phase signaling scheme. The structure of the optimum MFSK/QPSK receiver is the same as that of the general correlation receiver shown in Figure 11 on page 30 where the bank of  $N$  correlators corresponds to a pair of correlators, one each for the In-phase and Quadrature channels, for each of the  $K_f$  frequencies. The expression for the conditional probability of a correct signal decision has already been given in Eq. 3.48. The expression for the conditional probability of deciding in favor of a signal that is orthogonal to the transmitted signal, yet does not result in a bit error takes on a form similar to that derived for the 2FSK/QPSK case. To demonstrate this, assume that  $s_0(t)$  has been transmitted and examine the probability that one of the signals orthogonal to  $s_0(t)$  is erroneously chosen over  $s_0(t)$ . This corresponds to the probability that for some  $r_k$ ,  $k = 2, 3, \dots, N$



$$\begin{aligned}
& Pr\{\mathbf{r}_k = \max_j \mathbf{r}_j | \vec{s}_0\} \\
& = Pr\{\mathbf{r}_k > \mathbf{r}_1, \mathbf{r}_k > -\mathbf{r}_1, \mathbf{r}_k > \mathbf{r}_2, \mathbf{r}_k > -\mathbf{r}_2, \dots, \mathbf{r}_k > -\mathbf{r}_k, \dots, \mathbf{r}_k > \mathbf{r}_N, \mathbf{r}_k > -\mathbf{r}_N | \vec{s}_0\} \quad (3.77)
\end{aligned}$$

Further conditioning on  $\mathbf{r}_k$  yields

$$\begin{aligned}
& Pr\{\mathbf{r}_k = \max_j \mathbf{r}_j | \vec{s}_0, \mathbf{r}_k = R_k, R_k > 0\} \\
& = \prod_{\substack{j=1 \\ j \neq k}}^N Pr\{-R_k < \mathbf{r}_j < R_k | \vec{s}_0, \mathbf{r}_k = R_k, R_k > 0\} \quad (3.78)
\end{aligned}$$

The first term in the summation ( $j = 1$ ) is the same as that given by Eq. 3.66 for 2FSK/QPSK. All the other terms ( $j = 2, 3, \dots, N; j \neq k$ ) are given by Eq. 3.67, so that

$$\begin{aligned}
& Pr\{\mathbf{r}_k = \max_j \mathbf{r}_j | \vec{s}_0, \mathbf{r}_k = R_k, R_k > 0\} \\
& = \left[ 1 - 2Q\left(\frac{R'_2}{\sigma}\right) \right]^{N-2} \left[ 1 - Q\left(\frac{R'_2 + \sqrt{E}}{\sigma}\right) - Q\left(\frac{R'_2 - \sqrt{E}}{\sigma}\right) \right] \quad (3.79)
\end{aligned}$$

Now, integrating over all  $\mathbf{r}_k > 0$  yields

$$\begin{aligned}
& Pr\{\mathbf{r}_k = \max_j \mathbf{r}_j | \vec{s}_0\} \\
& = \int_0^\infty \left[ 1 - 2Q(y) \right]^{N-2} \left[ 1 - Q\left(y + \frac{\sqrt{E}}{\sigma}\right) - Q\left(y - \frac{\sqrt{E}}{\sigma}\right) \right] \frac{1}{\sqrt{2\pi}} \exp\left(-\frac{y^2}{2}\right) dy \quad (3.80)
\end{aligned}$$

Since there are  $M - 2$  signals orthogonal to  $s_0(t)$ , and for any chosen bit, half of these signals have this chosen bit in common with the one in  $s_0(t)$ , yields  $\frac{(M-2)}{2} = N - 1$  ways of making a symbol error while correctly indentifying the bit in question. Thus the expression for the probability of a correct bit decision conditioned on the signal  $s_0(t)$  being transmitted, is given by

$$\begin{aligned}
P_b\{\text{Correct} | \vec{s}_0\} &= \int_{-\frac{\sqrt{E}}{\sigma}}^{\infty} \left[ 1 - 2Q\left(y + \frac{\sqrt{E}}{\sigma}\right) \right]^{N-1} g(y) dy \\
&+ (N-1) \int_0^{\infty} [1 - 2Q(y)]^{N-2} \left[ 1 - Q\left(y + \frac{\sqrt{E}}{\sigma}\right) - Q\left(y - \frac{\sqrt{E}}{\sigma}\right) \right] g(y) dy
\end{aligned} \tag{3.81}$$

Using steps similar to those used in the analysis of the 2FSK/QPSK receiver as well as those presented above, it can be shown that Eq. 3.81 is also the expression for the overall average probability of a bit being correctly identified by the MFSK/QPSK optimum receiver  $P_b\{C\}$ .

Since the integrals involved in calculating the bit error probability for the MFSK/QPSK optimum receiver cannot easily be expressed in closed form, the BER can only be evaluated using numerical techniques. Appendix B presents a computer program in FORTRAN language used to compute the actual bit error probability for the optimum receiver by employing numerical integration. An upper bound for the receiver's bit error probability is given by Ref. 6 [pp. 255-257] as a union bound, namely

$$P_b\{e\} \lesssim \frac{1}{2} \left[ (M-2)Q\left(\sqrt{\frac{kE_b}{N_0}}\right) + Q\left(\sqrt{\frac{2kE_b}{N_0}}\right) \right] \tag{3.82}$$

This bound is a good approximation to the actual BER for  $k > 3$  at moderate to large  $\frac{E_b}{N_0}$ .

#### D. DBD RECEIVER FOR MFSK/QPSK

Another receiver structure for MFSK/QPSK signals is implementable by using DBD techniques. Ref. 2 [pp. 19-25] A diagram of the structure of this receiver is shown in Figure 13 on page 42 for the 2FSK/QPSK case. The DBD receiver uses the same correlator subsystem as the optimum receiver Figure 12 on page 32, however the two receivers differ in the way the correlator outputs are processed. Whereas the optimum receiver processed these correlator outputs through a weighting network and then selected its largest output, the DBD receiver routes the correlator outputs through a two stage summing network and then compares the summer outputs to a zero threshold in order to arrive at binary decisions.



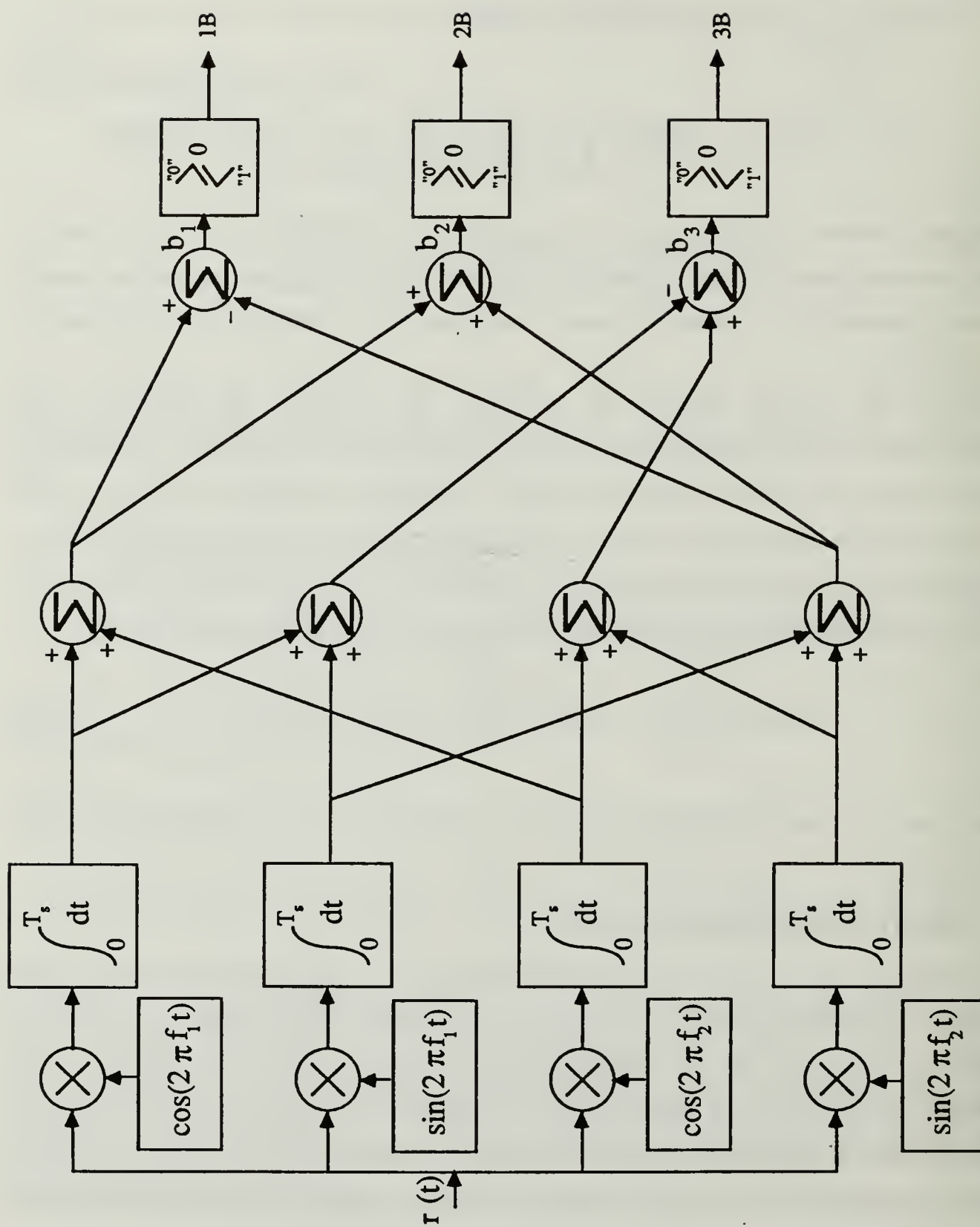


Figure 13. Diagram of DBD Receiver for 2FSK/QPSK

### E. MFSK/QPSK DBD RECEIVER BER

The analysis for the derivation of the BER performance for the 2FSK/QPSK DBD receiver is similar to that carried out for the performance analysis of the optimum (symbol discrimination) receiver. We begin by assuming  $s_0(t)$  is transmitted. Since the correlator outputs are identical for both receivers in question, the analysis on the performance of the DBD receiver can proceed with the correlator outputs, which are again characterized as independent Gaussian random variables with density functions given by Eqs. 3.56 and 3.57. Note from Figure 13 that there is a path from each correlator output to the input of all second stage summers. The outputs of these summers, denoted  $b_n$ ,  $n = 1, 2, 3$ , are given by

$$\begin{aligned} b_1 &= r_1 - r_2 + r_3 - r_4 \\ b_2 &= r_1 + r_2 + r_3 + r_4 \\ b_3 &= -r_1 - r_2 + r_3 + r_4 \end{aligned} \quad (3.83)$$

Each  $b_n$  will also be a Gaussian random variable having a mean equal to the sum of the means of the  $r_j$ , and due to the independence of the  $r_j$ , the variance of  $b_n$  will consist of the sum of the variances of the  $r_j$ , each of which equals  $\frac{N_0}{2}$ . Thus we have

$$\begin{aligned} b_1 &\sim N(\sqrt{E}, 2N_0) \\ b_2 &\sim N(\sqrt{E}, 2N_0) \\ b_3 &\sim N(-\sqrt{E}, 2N_0) \end{aligned} \quad (3.84)$$

where  $N(a, b)$  is used to denote a Gaussian probability density of mean  $a$  and variance  $b$ . With the statistics of the  $b_n$  specified comparing these random variables to a zero threshold yields the following conditional probabilities of decoding the bits correctly namely

$$\begin{aligned} Pr\{1B \text{ Correct} | \bar{s}_0\} &= Pr\{b_1 > 0\} = \int_0^\infty \frac{1}{\sqrt{2\pi(2N_0)}} \exp\left[-\frac{(x - \sqrt{E})^2}{2(2N_0)}\right] dx \\ &= Q\left(-\sqrt{\frac{E}{2N_0}}\right) = 1 - Q\left(\sqrt{\frac{E}{2N_0}}\right) \end{aligned} \quad (3.85)$$

$$\begin{aligned}
Pr\{2B \text{ Correct} | \vec{s}_0\} &= Pr\{\mathbf{b}_2 > 0\} = \int_0^{\infty} \frac{1}{\sqrt{2\pi(2N_0)}} \exp\left[-\frac{(x - \sqrt{E})^2}{2(2N_0)}\right] dx \\
&= 1 - Q\left(\sqrt{\frac{E}{2N_0}}\right)
\end{aligned} \tag{3.86}$$

$$\begin{aligned}
Pr\{3B \text{ Correct} | \vec{s}_0\} &= Pr\{\mathbf{b}_3 < 0\} = \int_{-\infty}^0 \frac{1}{\sqrt{2\pi(2N_0)}} \exp\left[-\frac{(x + \sqrt{E})^2}{2(2N_0)}\right] dx \\
&= 1 - Q\left(\sqrt{\frac{E}{2N_0}}\right)
\end{aligned} \tag{3.87}$$

Since each of the individual bits have identical probability of correct decoding, the corresponding average probability conditioned on the assumption that  $s_0(t)$  was transmitted is

$$P_b\{\text{Correct} | \vec{s}_0\} = 1 - Q\left(\sqrt{\frac{E}{2N_0}}\right) \tag{3.88}$$

and consequently the conditional bit error probability is

$$P_b\{\text{Error} | \vec{s}_0\} = 1 - P_b\{\text{Correct} | \vec{s}_0\} = Q\left(\sqrt{\frac{E}{2N_0}}\right) \tag{3.89}$$

Consider next the case in which any one of the  $s_i(t)$ ,  $i = 0, 1, \dots, 7$  is transmitted, for any of the receiver correlators. If the transmitted signal is matched to the local signal correlator, its output  $r_j$  will be

$$r_j = \sqrt{E} + n_j \tag{3.90}$$

and for the correlator having antipodal local signal matching, the output will be

$$r_j = -\sqrt{E} + n_j \tag{3.91}$$

All other correlators will have an output given by

$$r_j = n_j \tag{3.92}$$

Examining now any one of the second stage summer outputs  $b_n$ , if the bit corresponding to  $b_n$  for the signal sent is a logical zero, then  $b_n$  is statistically characterized by

$$b_n \sim N(\sqrt{E}, 2N_0) \quad (3.93)$$

In this case the bit will be correct if  $b_n$  is greater than the zero threshold, and the probability of the bit corresponding to  $b_n$  being correctly decoded is given by

$$\begin{aligned} Pr\{b_n > 0\} &= \int_0^{\infty} \frac{1}{\sqrt{2\pi(2N_0)}} \exp\left[-\frac{(x - \sqrt{E})^2}{2(2N_0)}\right] dx \\ &= 1 - Q\left(\sqrt{\frac{E}{2N_0}}\right) \end{aligned} \quad (3.94)$$

However, in the case where the bit is a logical one, then

$$b_n \sim N(-\sqrt{E}, 2N_0) \quad (3.95)$$

Now the bit will be correct if  $b_n$  is less than the zero threshold, and the probability of correct decoding is given by

$$\begin{aligned} Pr\{b_n < 0\} &= \int_{-\infty}^0 \frac{1}{\sqrt{2\pi(2N_0)}} \exp\left[-\frac{(x + \sqrt{E})^2}{2(2N_0)}\right] dx \\ &= 1 - Q\left(\sqrt{\frac{E}{2N_0}}\right) \end{aligned} \quad (3.96)$$

For both cases the probability of a bit error is the same, and it is identical for all  $b_n$  regardless of which signal  $s_i(t)$  is transmitted. Thus, we can write the total bit error probability for the 2FSK/QPSK DBD receiver as

$$P_b\{e\} = Q\left(\sqrt{\frac{E}{2N_0}}\right) \quad (3.97)$$

Extending the 2FSK/QPSK results to the general case of MFSK/QPSK in which there are  $M$  signals,  $N$  receiver correlators,  $k$  bits, and  $K_f$  frequencies where the biorthogonal signal relationships of Eqs. 3.35 - 3.37 again hold, for each of the random

variables  $\mathbf{b}_n$ ,  $n = 1, 2, \dots, k$ , the corresponding variance will be the sum of the variances of the  $\mathbf{n}_j$ , so

$$Var\{\mathbf{b}_n\} = \sum_{j=1}^N \frac{N_0}{2} = \frac{NN_0}{2} = K_f N_0 \quad (3.98)$$

and again the mean of the  $\mathbf{b}_n$  will be  $\pm \sqrt{E}$ . Following the same steps as those carried out in obtaining Eqs. 3.90 - 3.97, the total bit error probability for MFSK/QPSK DBD receiver is given by

$$P_b\{e\} = Q\left(\sqrt{\frac{E}{K_f N_0}}\right) \quad (3.99)$$

## F. BANDWIDTH OF MFSK/QPSK

The bandwidth of MFSK/QPSK signals can be derived from knowledge of QPSK and MFSK bandwidth requirements. Each carrier is switched at the symbol rate  $R_s$ , where  $R_s = \frac{1}{T_s}$ . This gives each carrier a two-sided bandwidth of  $2R_s$  Hz. To maintain orthogonality between signals at different frequencies in MFSK modulation, the frequencies are separated by  $R_s$  Hz. This same relationship must also be maintained in MFSK/QPSK. The spectrum of the 2FSK/QPSK signal is plotted in Figure 14 on page 47. From the graph, the total null-to-null bandwidth of the 2FSK/QPSK signal can be seen to be

$$W = 3R_s \quad (3.100)$$

Proceeding to the family of MFSK/QPSK signals, Figure 15 on page 48 shows the spectrum for such signals. By examining this figure, the total null-to-null bandwidth can be shown to be

$$\begin{aligned} W &= (K_f + 1)R_s \\ &= (2^{k-2} + 1)R_s \end{aligned} \quad (3.101)$$

This general result for MFSK/QPSK correctly yields the result for the special case of 2FSK/QPSK in which  $k = 3$ , namely

$$W = (2^{3-2} + 1)R_s = 3R_s \quad (3.102)$$



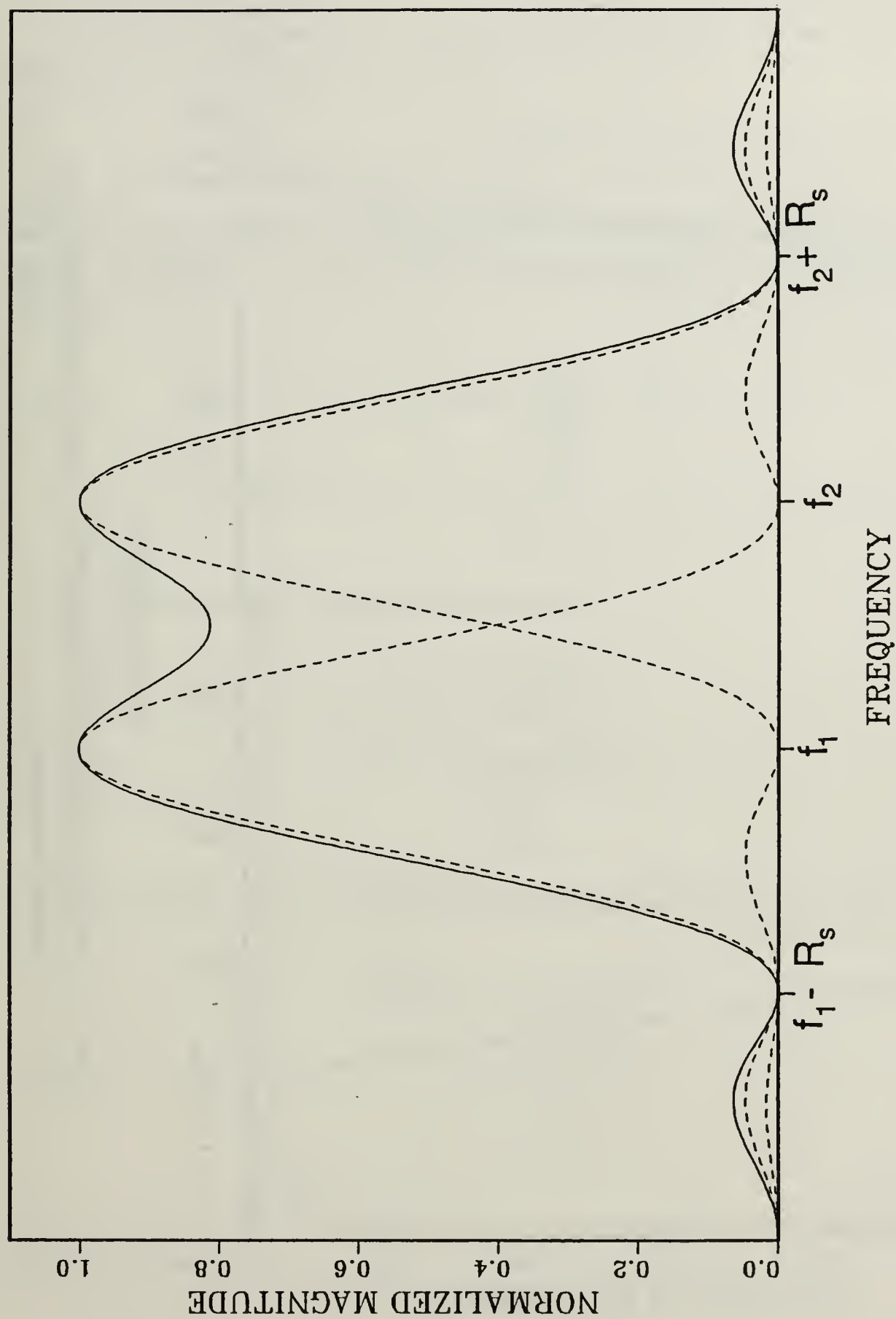


Figure 14. Magnitude Spectrum for 2FSK/QPSK: Dashed lines show individual spectral components.



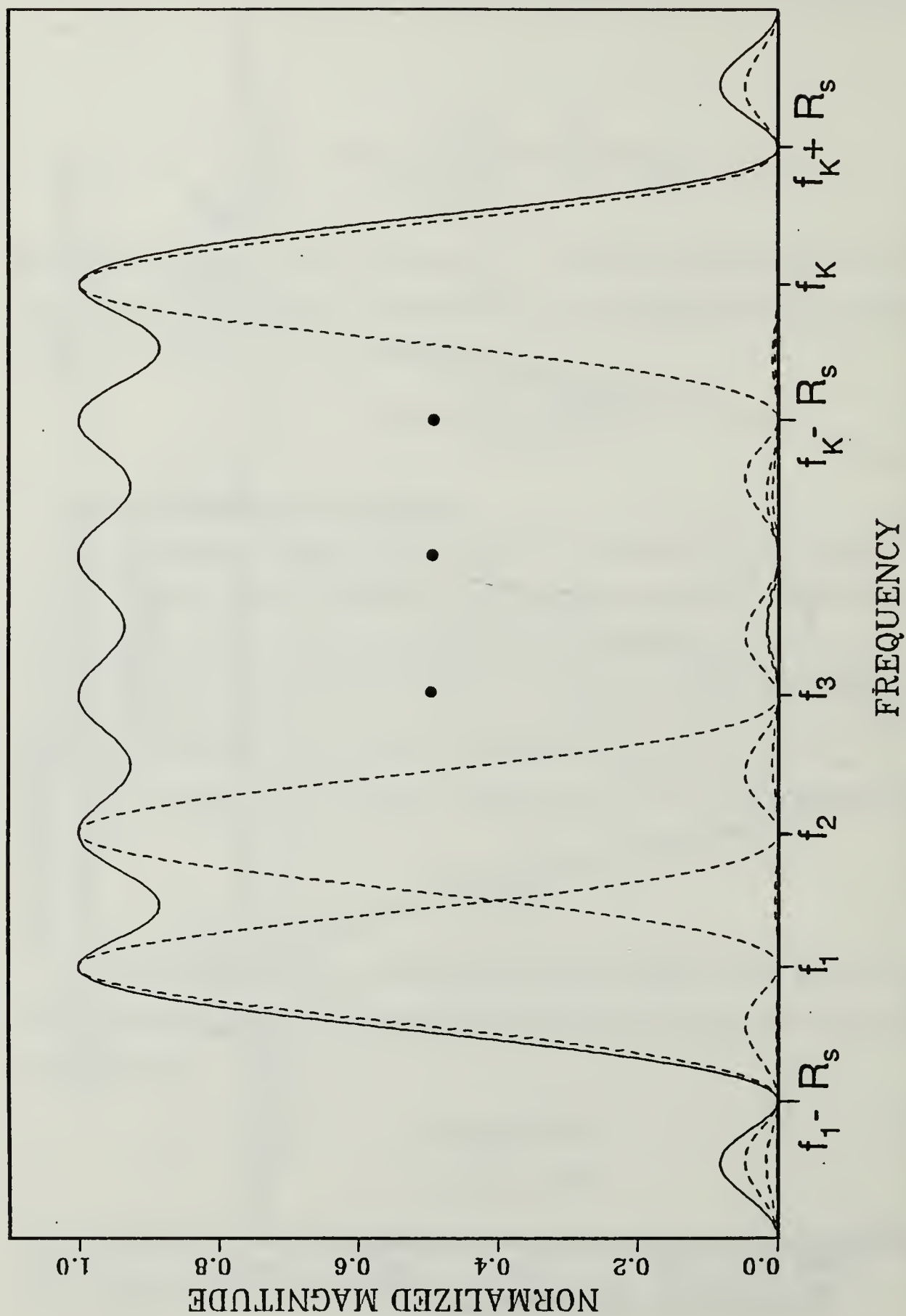


Figure 15. Magnitude Spectrum for MFSK/QPSK: Dashed lines show individual spectral components.

which agrees with Eq. 3.100.

The bandwidth efficiency of a digital modulation scheme is given by Ref. 6 [pp. 393-395] as

$$\eta = \frac{R_b}{W} \quad (3.103)$$

and is one way to evaluate how efficiently different modulation schemes use the available channel bandwidth. For M-ary PSK, bandwidth efficiency is given by Ref. 3 [pp. 211-213]

$$\begin{aligned} \eta_{MPSK} &= \frac{R_b}{2R_s} \\ &= \frac{kR_s}{2R_s} \\ &= \frac{k}{2} \end{aligned} \quad (3.104)$$

and for M-ary FSK the bandwidth efficiency is

$$\begin{aligned} \eta_{FSK} &= \frac{R_b}{(M+1)R_s} \\ &= \frac{kR_s}{(M+1)R_s} \\ &= \frac{k}{2^k + 1} \end{aligned} \quad (3.105)$$

For MFSK/QPSK, using Eq. 3.101 we obtain a bandwidth efficiency given by

$$\begin{aligned} \eta_{MFSK/QPSK} &= \frac{R_b}{(2^{k-2} + 1)R_s} \\ &= \frac{kR_s}{(2^{k-2} + 1)R_s} \\ &= \frac{k}{2^{k-2} + 1} \end{aligned} \quad (3.106)$$

A table of bandwidth efficiencies for M-ary PSK, M-ary FSK, and MFSK/QPSK is given in Chapter 5.

## IV. RAYLEIGH FADING

### A. THE RAYLEIGH FADING MODEL

Often, when a signal is transmitted through a channel in which multipath propagation and/or heavy precipitation conditions exist, fading occurs with a consequent change in the signal amplitude. One way to model this fading is to redefine the signal amplitude  $A$  which up until now has been treated as a constant, as a Rayleigh distributed random variable  $A$  with p.d.f.

$$f_A(A) = \frac{A}{A_0^2} \exp\left(-\frac{A^2}{2A_0^2}\right) u(A) \quad (4.1)$$

where  $u(\cdot)$  is the unit step function, and from Ref. 7 [pp. 110-112], the value of  $A_0$  is related to the second moment of  $A$  as

$$E\{A^2\} = 2A_0^2 \quad (4.2)$$

In order to evaluate the effect of Rayleigh fading on the BER for a given modulation scheme and corresponding receiver, the expression for BER under nonfading channel conditions must be averaged over the distribution of the signal amplitude. This requires expressing the bit error probability as a function of signal amplitude, weighting the function with the amplitude p.d.f. and integrating this product over all values of  $A$ .

### B. EFFECT ON BER OF M-ARY PSK USING DBD RECEIVER

For the 8-PSK DBD receiver, the (non-fading) bit error probabilities are given by Eqs. 2.1 - 2.2. These probabilities must now be expressed as functions of the random amplitude  $A$ . From Eq. 1.1 it is apparent that the signal amplitude is given by

$$A = \sqrt{\frac{2E}{T_s}} \quad (4.3)$$

so that

$$E = \frac{A^2 T_s}{2} \quad (4.4)$$

Since the signal amplitude is now a random variable, the signal energy also becomes a random variable  $E$ , which is expressed as

$$E = \frac{A^2 T_s}{2} \quad (4.5)$$

Substituting this result into Eqs. 2.1 through 2.3 yields

$$\begin{aligned} Pr\{1B \text{ incorrect}\} = \\ \frac{1}{2} Q\left(A\sqrt{\frac{T_s}{N_0}} \cos \alpha\right) + \frac{1}{2} Q\left(A\sqrt{\frac{T_s}{N_0}} \sin \alpha\right) \end{aligned} \quad (4.6)$$

$$\begin{aligned} Pr\{2B \text{ incorrect}\} = \\ Q\left(A\sqrt{\frac{T_s}{2N_0}} [\cos \alpha + \sin \alpha]\right) + Q\left(A\sqrt{\frac{T_s}{2N_0}} [\cos \alpha - \sin \alpha]\right) \\ - 2Q\left(A\sqrt{\frac{T_s}{2N_0}} [\cos \alpha + \sin \alpha]\right)Q\left(A\sqrt{\frac{T_s}{2N_0}} [\cos \alpha - \sin \alpha]\right) \end{aligned} \quad (4.7)$$

and as before,

$$Pr\{3B \text{ incorrect}\} = Pr\{1B \text{ incorrect}\} \quad (4.8)$$

The bit error probability under fading conditions for the most significant bit, namely 1B, is obtained by weighting the probability given in Eq. 4.6 by the p.d.f. of the random amplitude  $A$  and integrating over all  $A$ . That is

$$\begin{aligned} P_{Ray}\{1B \text{ incorrect}\} &= \int_{-\infty}^{\infty} Pr\{1B \text{ incorrect}\} f_A(A) dA \\ &= \int_{-\infty}^{\infty} \left[ \frac{1}{2} Q\left(A\sqrt{\frac{T_s}{N_0}} \cos \alpha\right) + \frac{1}{2} Q\left(A\sqrt{\frac{T_s}{N_0}} \sin \alpha\right) \right] f_A(A) dA \end{aligned} \quad (4.9)$$

This integral can be solved using the identity given by Ref. 8 [pp. 12-13] as

$$\int_{-\infty}^{\infty} Q(\alpha A) f_A(A) dA = \frac{1}{2} \left[ 1 - \frac{1}{\sqrt{1 + \frac{1}{\alpha^2 A_0^2}}} \right] \quad (4.10)$$

Using Eq. 4.2 and the linearity of the expectation operator we can write an expression for the average signal energy under fading conditions, namely  $E\{E\} = \bar{E}$  as

$$\begin{aligned}
\bar{E} &= E\left\{\frac{A^2 T_s}{2}\right\} \\
&= \frac{T_s}{2} E\{A^2\} = \frac{T_s}{2} (2A_0^2) \\
&= T_s A_0^2
\end{aligned} \tag{4.11}$$

Using Eq. 4.10 in order to evaluate Eq. 4.9 yields the bit error probability under Rayleigh fading, namely

$$\begin{aligned}
P_{Ray}\{\text{1B incorrect}\} &= \\
&\frac{1}{2} - \frac{1}{4} \left[ \frac{1}{\sqrt{\left(\frac{\bar{E}}{N_0} \cos^2 \alpha\right)^{-1} + 1}} \right] - \frac{1}{4} \left[ \frac{1}{\sqrt{\left(\frac{\bar{E}}{N_0} \sin^2 \alpha\right)^{-1} + 1}} \right]
\end{aligned} \tag{4.12}$$

Next, the BER under fading conditions for the second-most significant bit, namely 2B, is obtained by integrating the product of the BER given by Eq. 4.7 with the Rayleigh p.d.f.. The contribution from the first two terms of Eq. 4.7 can be derived using the same steps as those carried out above for the evaluation of  $P_{Ray}\{\text{1B incorrect}\}$ . Since the third term in Eq. 4.7 involves the product of two Q functions, a new identity is required. That is

$$\begin{aligned}
&\int_{-\infty}^{\infty} Q(\alpha A) Q(\beta A) f_A(A) dA = \\
&\frac{1}{4} - \frac{\beta \tan^{-1} \left[ \frac{\sqrt{\beta^2 + \frac{1}{A_0^2}}}{\alpha} \right]}{2\pi \sqrt{\beta^2 + \frac{1}{A_0^2}}} - \frac{\alpha \tan^{-1} \left[ \frac{\sqrt{\alpha^2 + \frac{1}{A_0^2}}}{\beta} \right]}{2\pi \sqrt{\alpha^2 + \frac{1}{A_0^2}}}
\end{aligned} \tag{4.13}$$

the proof of which is presented in Appendix A. Using this identity for the contribution of the third term of Eq. 4.7 and combining this with the contributions from the first two terms of Eq. 4.7 yields



$$\begin{aligned}
P_{Ray}\{2B \text{ incorrect}\} = & \frac{1}{2} - \frac{1}{2\sqrt{\left(\frac{\bar{E}}{2N_0} u_1^2\right)^{-1} + 1}} - \frac{1}{2\sqrt{\left(\frac{\bar{E}}{2N_0} u_2^2\right)^{-1} + 1}} \\
& + \frac{u_1 \tan^{-1} \left[ \frac{\sqrt{u_1^2 + 2\left(\frac{\bar{E}}{N_0}\right)^{-1}}}{u_2} \right]}{\pi\sqrt{u_1^2 + 2\left(\frac{\bar{E}}{N_0}\right)^{-1}}} + \frac{u_2 \tan^{-1} \left[ \frac{\sqrt{u_2^2 + 2\left(\frac{\bar{E}}{N_0}\right)^{-1}}}{u_1} \right]}{\pi\sqrt{u_2^2 + 2\left(\frac{\bar{E}}{N_0}\right)^{-1}}} \quad (4.14)
\end{aligned}$$

where  $u_1$  and  $u_2$  are given by

$$\begin{aligned}
u_1 &= \cos \alpha + \sin \alpha \\
u_2 &= \cos \alpha - \sin \alpha
\end{aligned} \quad (4.15)$$

The overall average bit error rate under fading conditions can be obtained from

$$P_{b, Ray}\{e\} = \frac{2}{3} P_{Ray}\{1B \text{ incorrect}\} + \frac{1}{3} P_{Ray}\{2B \text{ incorrect}\} \quad (4.16)$$

For the 16-PSK DBD receiver operating under Rayleigh fading conditions, much of the performance analysis can be carried out using the same procedure as the one used for the evaluation of the performance of the 8-PSK DBD receiver operating under similar Rayleigh fading conditions. The bit error probabilities under non-fading conditions are given by Eqs. 2.4 - 2.6. Rewriting these equations in terms of the random variable  $A$ , for the most significant bit we obtain

$$Pr\{1B \text{ incorrect}\} = \frac{1}{4} \sum_{i=1}^4 \left[ Q \left( A \sqrt{\frac{T_s}{N_0}} v_i \right) \right] \quad (4.17)$$

where the variables  $v_i$  are defined as



$$\begin{aligned}
v_1 &= \cos \alpha \\
v_2 &= \cos \beta \\
v_3 &= \sin \alpha \\
v_4 &= \sin \beta
\end{aligned} \tag{4.18}$$

and for the second-most significant bit

$$\begin{aligned}
Pr\{2B \text{ incorrect}\} = & \\
& \frac{1}{2} \sum_{i=1}^4 Q\left(A\sqrt{\frac{T_s}{2N_0}} w_i\right) - Q\left(A\sqrt{\frac{T_s}{2N_0}} w_1\right) Q\left(A\sqrt{\frac{T_s}{2N_0}} w_2\right) \\
& - Q\left(A\sqrt{\frac{T_s}{2N_0}} w_3\right) Q\left(A\sqrt{\frac{T_s}{2N_0}} w_4\right)
\end{aligned} \tag{4.19}$$

where the variables  $w_i$  are given by

$$\begin{aligned}
w_1 &= \cos \alpha - \sin \alpha \\
w_2 &= \cos \alpha + \sin \alpha \\
w_3 &= \cos \beta - \sin \beta \\
w_4 &= \cos \beta + \sin \beta
\end{aligned} \tag{4.20}$$

For the third-most significant bit

$$\begin{aligned}
Pr\{3B \text{ incorrect}\} = & \\
& \frac{1}{2} - \sum_{i=1}^4 A\sqrt{\frac{T_s}{2\pi N_0}} \int_0^{\frac{\pi}{8}} \exp\left(-\frac{A^2 T_s}{2N_0} f_i^2(\Gamma, \alpha, \beta)\right) g_i(\Gamma, \alpha, \beta) \cdot \\
& \left\{ \frac{1}{2} - Q\left(A\sqrt{\frac{T_s}{N_0}} g_i(\Gamma, \alpha, \beta)\right) \right\} d\Gamma \\
& + \sum_{i=5}^8 A\sqrt{\frac{T_s}{2\pi N_0}} \int_0^{\frac{\pi}{8}} \exp\left(-\frac{A^2 T_s}{2N_0} f_i^2(\Gamma, \alpha, \beta)\right) g_i(\Gamma, \alpha, \beta) \cdot \\
& \left\{ \frac{1}{2} - Q\left(A\sqrt{\frac{T_s}{N_0}} g_i(\Gamma, \alpha, \beta)\right) \right\} d\Gamma
\end{aligned} \tag{4.21}$$

where the functions  $f_i(\Gamma, \alpha, \beta)$  and  $g_i(\Gamma, \alpha, \beta)$  are defined in Table 1 of Chapter 2. For the least significant bit, from Eq. 2.3 it is obvious that

$$Pr\{4B \text{ incorrect}\} = Pr\{1B \text{ incorrect}\} \tag{4.22}$$

For the most significant bit, the BER under fading conditions is obtained using Eq. 4.17 and the identity given by Eq. 4.9, to yield

$$P_{Ray}\{1B \text{ incorrect}\} = \frac{1}{2} - \frac{1}{8} \sum_{i=1}^4 \left[ \frac{1}{\sqrt{\left(\frac{\bar{E}}{N_0} v_i^2\right)^{-1} + 1}} \right] \quad (4.23)$$

$$= P_{Ray}\{4B \text{ incorrect}\}$$

where the variables  $v_i$  are defined in Eq. 4.18, and the last equality in Eq. 4.23 follows from Eq. 4.22. The BER under Rayleigh fading conditions for the second-most significant bit is obtained using the identities of Eqs. 4.9 and 4.13 to yield

$$P_{Ray}\{2B \text{ incorrect}\} = \frac{1}{2} - \frac{1}{4} \sum_{i=1}^4 \left[ \frac{1}{\sqrt{\left(\frac{\bar{E}}{2N_0} w_i^2\right)^{-1} + 1}} \right]$$

$$+ \frac{w_1 \tan^{-1} \left[ \frac{\sqrt{w_1^2 + 2\left(\frac{\bar{E}}{N_0}\right)^{-1}}}{w_2} \right]}{2\pi \sqrt{w_1^2 + 2\left(\frac{\bar{E}}{N_0}\right)^{-1}}} + \frac{w_2 \tan^{-1} \left[ \frac{\sqrt{w_2^2 + 2\left(\frac{\bar{E}}{N_0}\right)^{-1}}}{w_1} \right]}{2\pi \sqrt{w_2^2 + 2\left(\frac{\bar{E}}{N_0}\right)^{-1}}} \quad (4.24)$$

$$+ \frac{w_3 \tan^{-1} \left[ \frac{\sqrt{w_3^2 + 2\left(\frac{\bar{E}}{N_0}\right)^{-1}}}{w_4} \right]}{2\pi \sqrt{w_3^2 + 2\left(\frac{\bar{E}}{N_0}\right)^{-1}}} + \frac{w_4 \tan^{-1} \left[ \frac{\sqrt{w_4^2 + 2\left(\frac{\bar{E}}{N_0}\right)^{-1}}}{w_3} \right]}{2\pi \sqrt{w_4^2 + 2\left(\frac{\bar{E}}{N_0}\right)^{-1}}}$$

where the  $w_i$  terms are defined in Eq. 4.20. For the third-most significant bit, the integrals to be evaluated are all of the basic form

$$\begin{aligned}
& \int_{-\infty}^{\infty} A \int_0^{\frac{\pi}{8}} \exp\left(-\frac{A^2 T_s}{2N_0} f_i^2(\Gamma, \alpha, \beta)\right) g_i(\Gamma, \alpha, \beta) d\Gamma f_A(A) dA \\
&= \int_0^{\frac{\pi}{8}} g_i(\Gamma, \alpha, \beta) \frac{1}{\varepsilon_i^3 A_0^2} \int_0^{\infty} x^2 \exp(-x^2) dx d\Gamma \\
&= \int_0^{\frac{\pi}{8}} g_i(\Gamma, \alpha, \beta) \frac{1}{\varepsilon_i^3 A_0^2} \left[ \frac{\sqrt{\pi}}{4} \right] d\Gamma
\end{aligned} \tag{4.25}$$

where  $\varepsilon_i$  is defined as

$$\varepsilon_i \equiv \sqrt{\rho_i + \frac{1}{2A_0^2}} \tag{4.26}$$

and

$$\rho_i \equiv \frac{T_s}{2N_0} f_i^2(\Gamma, \alpha, \beta) \tag{4.27}$$

The variable  $x$  is defined as  $x = A\varepsilon_i$ , so that the evaluation of the integral of the product of the first term in the summation of Eq. 4.21 with the Rayleigh p.d.f. becomes

$$\begin{aligned}
& \int_{-\infty}^{\infty} \frac{A}{2} \sqrt{\frac{T_s}{2\pi N_0}} \int_0^{\frac{\pi}{8}} \exp\left(-\frac{A^2 T_s}{2N_0} f_i^2(\Gamma, \alpha, \beta)\right) g_i(\Gamma, \alpha, \beta) d\Gamma f_A(A) dA \\
&= \frac{1}{8} \sqrt{\frac{T_s A_0^2}{2\pi N_0}} \cdot \frac{\sqrt{\pi}}{A_0^3} \int_0^{\frac{\pi}{8}} \frac{g_i(\Gamma, \alpha, \beta)}{\varepsilon_i^3} d\Gamma \\
&= \frac{1}{4} \sqrt{\frac{\bar{E}}{N_0}} \int_0^{\frac{\pi}{8}} \frac{g_i(\Gamma, \alpha, \beta)}{\left[ \frac{\bar{E}}{N_0} f_i^2(\Gamma, \alpha, \beta) + 1 \right]^{\frac{3}{2}}} d\Gamma
\end{aligned} \tag{4.28}$$

Multiplying the second term within the summation of Eq. 4.21 by the Rayleigh p.d.f. and integrating, yields

$$\begin{aligned}
& \int_{-\infty}^{\infty} A \sqrt{\frac{T_s}{2\pi N_0}} \int_0^{\frac{\pi}{8}} \exp\left(-\frac{A^2 T_s}{2N_0} f_i^2(\Gamma, \alpha, \beta)\right) g_i(\Gamma, \alpha, \beta) Q\left(A \sqrt{\frac{T_s}{N_0}} g_i(\Gamma, \alpha, \beta)\right) d\Gamma f_A(A) dA \\
&= \int_{-\infty}^{\infty} A \sqrt{\frac{T_s}{2\pi N_0}} \int_0^{\frac{\pi}{8}} \exp\left(-\frac{A^2 T_s}{2N_0} f_i^2(\Gamma, \alpha, \beta)\right) g_i(\Gamma, \alpha, \beta) \cdot \\
&\quad \int_{-\infty}^{\infty} \frac{g(x) dx d\Gamma f_A(A) dA}{A \sqrt{\frac{T_s}{N_0}} g_i(\Gamma, \alpha, \beta)} \\
&= \int_0^{\frac{\pi}{8}} \int_{-\infty}^{\infty} \int_{-\infty}^{\infty} \frac{A}{\sqrt{2\pi}} \xi_i \exp(-A^2 \rho_i) g(x) u(x - A \xi_i) \frac{A}{A_0^2} \exp\left(-\frac{A^2}{2A_0^2}\right) u(A) dA dx d\Gamma
\end{aligned} \tag{4.29}$$

where  $\xi_i$  is defined as

$$\xi_i \equiv \sqrt{\frac{T_s}{N_0}} g_i(\Gamma, \alpha, \beta) \tag{4.30}$$

Carrying out the integration with respect to  $A$  first, while realizing that  $u(x - A \xi_i)u(A)$  is nonzero only for  $A$  in the range  $0 < A < \frac{x}{\xi_i}$ , yields

$$\begin{aligned}
& \int_0^{\frac{x}{\xi_i}} \frac{A}{\sqrt{2\pi}} \exp(-A^2 \rho_i) \frac{A}{A_0^2} \exp\left(-\frac{A^2}{2A_0^2}\right) dA \\
&= \frac{1}{A_0^2 \sqrt{2\pi}} \int_0^{\frac{x}{\xi_i}} \frac{1}{2a_i} \exp(-a_i A^2) dA - \frac{x}{2a_i \xi_i} \exp\left(-\frac{a_i x^2}{\xi_i^2}\right)
\end{aligned} \tag{4.31}$$

where  $a_i$  is defined as

$$a_i \equiv \rho_i + \frac{1}{2A_0^2} \tag{4.32}$$

so that Eq. 4.29 becomes

$$\begin{aligned}
& \frac{1}{A_0^2 \sqrt{2\pi}} \int_0^{\frac{\pi}{8}} \int_0^\infty \xi_i \frac{1}{\sqrt{2\pi}} \exp\left(-\frac{x^2}{2}\right) \cdot \\
& \left[ \int_0^{\frac{x}{\xi_i}} \frac{1}{2a_i} \exp(-a_i A^2) dA - \frac{x}{2a_i \xi_i} \exp\left(-\frac{a_i x^2}{\xi_i^2}\right) \right] dx d\Gamma \\
& = \frac{1}{A_0^2 \sqrt{2\pi}} \int_0^{\frac{\pi}{8}} \int_0^\infty \left[ \frac{\xi_i}{\sqrt{2\pi}} \exp\left(-\frac{x^2}{2}\right) \int_0^{\frac{x}{\xi_i}} \frac{1}{2a_i} \exp(-a_i A^2) dA \right. \\
& \quad \left. - \frac{x}{2a_i \sqrt{2\pi}} \exp\left(-\left[\frac{x^2}{2} + \frac{a_i x^2}{\xi_i^2}\right]\right) \right] dx d\Gamma
\end{aligned} \tag{4.33}$$

Focusing on the integration with respect to  $x$  only, we have for the first integral with respect to  $x$ ,

$$\begin{aligned}
& \int_0^\infty \frac{\xi_i}{\sqrt{2\pi}} \exp\left(-\frac{x^2}{2}\right) \int_0^{\frac{x}{\xi_i}} \frac{1}{2a_i} \exp(-a_i A^2) dA dx \\
& = \int_0^\infty \frac{\xi_i}{\sqrt{2}} \exp\left(-\frac{x^2}{2}\right) \frac{1}{4a_i^{\frac{3}{2}}} \left[ \frac{2}{\sqrt{\pi}} \int_0^{\frac{x\sqrt{a_i}}{\xi_i}} \exp(-\tau^2) d\tau \right] dx \\
& = \int_0^\infty \frac{\xi_i}{4a_i^{\frac{3}{2}} \sqrt{2}} \exp\left(-\frac{x^2}{2}\right) \left[ \operatorname{erf}\left(\frac{x\sqrt{a_i}}{\xi_i}\right) \right] dx \\
& = \frac{\xi_i}{4a_i^{\frac{3}{2}} \sqrt{2}} \left[ \sqrt{\frac{\pi}{2}} - \sqrt{\frac{2}{\pi}} \tan^{-1}\left(\frac{\xi_i}{\sqrt{2a_i}}\right) \right]
\end{aligned} \tag{4.34}$$

and for the second integral with respect to  $x$

$$\int_0^\infty \frac{x}{2a_i \sqrt{2\pi}} \exp\left(-\frac{\gamma_i x^2}{2}\right) dx = \frac{-1}{2a_i \gamma_i \sqrt{2\pi}} \tag{4.35}$$

where  $\gamma_i$  is defined as



$$\gamma_i \equiv 1 + \frac{2a_i}{\xi_i^2} \quad (4.36)$$

Thus, Eq 4.29 becomes

$$\begin{aligned} & \int_{-\infty}^{\infty} A \sqrt{\frac{T_s}{2\pi N_0}} \int_0^{\frac{\pi}{8}} \exp\left(-\frac{A^2 T_s}{2N_0} f_i^2(\Gamma, \alpha, \beta)\right) g_i(\Gamma, \alpha, \beta) Q\left(A \sqrt{\frac{T_s}{N_0}} g_i(\Gamma, \alpha, \beta)\right) d\Gamma f_A(A) dA \\ &= \frac{1}{2\pi} \int_0^{\frac{\pi}{8}} \left[ \frac{\xi_i}{4A_0^2 a_i^{\frac{3}{2}}} \left\{ \frac{\pi}{\sqrt{2}} - \sqrt{2} \tan^{-1}\left(\frac{\xi_i}{\sqrt{2}a_i}\right) \right\} - \frac{1}{2a_i \gamma_i A_0^2} \right] d\Gamma \end{aligned} \quad (4.37)$$

From our previous definitions we can rewrite the expressions for  $a_i$  and  $\gamma_i$  as

$$\begin{aligned} a_i &= \rho_i + \frac{1}{2A_0^2} \\ &= \frac{T_s}{2N_0} f_i^2(\Gamma, \alpha, \beta) + \frac{1}{2A_0^2} \end{aligned} \quad (4.38)$$

and

$$\begin{aligned} \gamma_i &= 1 + \frac{2A}{\xi_i^2} \\ &= \frac{\frac{T_s}{N_0} f_i^2(\Gamma, \alpha, \beta) + \frac{1}{A_0^2}}{\frac{T_s}{N_0} g_i^2(\Gamma, \alpha, \beta)} \end{aligned} \quad (4.39)$$

Observe that the terms in Eq. 4.37 can be expressed in terms of the ratio of average signal energy to noise power spectral density as

$$\frac{\xi_i}{4A_0^2 a_i^{\frac{3}{2}}} = \frac{1}{\sqrt{2}} \sqrt{\frac{\bar{E}}{N_0}} \frac{g_i(\Gamma, \alpha, \beta)}{\left[ \frac{\bar{E}}{N_0} f_i^2(\Gamma, \alpha, \beta) + 1 \right]^{\frac{3}{2}}} \quad (4.40)$$

$$\frac{\xi_i}{\sqrt{2}a_i} = \frac{g_i(\Gamma, \alpha, \beta)}{\sqrt{f_i^2(\Gamma, \alpha, \beta) + \left(\frac{\bar{E}}{N_0}\right)^{-1}}} \quad (4.41)$$

and

$$2a_i\gamma_i A_0^2 = \left[ \frac{\bar{E}}{N_0} f_i^2(\Gamma, \alpha, \beta) + 1 \right] \left[ 1 + \frac{\frac{\bar{E}}{N_0} f_i^2(\Gamma, \alpha, \beta) + 1}{\frac{\bar{E}}{N_0} g_i(\Gamma, \alpha, \beta)} \right] \quad (4.42)$$

Using these results, the first term on the right hand side of Eq. 4.37 becomes

$$\frac{1}{2\pi} \int_0^{\frac{\pi}{8}} \frac{\xi_i}{4A_0^2 a_i^{\frac{3}{2}}} \frac{\pi}{\sqrt{2}} d\Gamma = \frac{1}{4} \sqrt{\frac{\bar{E}}{N_0}} \int_0^{\frac{\pi}{8}} \frac{g_i(\Gamma, \alpha, \beta)}{\left[ \frac{\bar{E}}{N_0} f_i^2(\Gamma, \alpha, \beta) + 1 \right]^{\frac{3}{2}}} d\Gamma \quad (4.43)$$

While the second term on the right hand side of Eq. 4.37 takes on the form

$$\begin{aligned} & -\frac{1}{2\pi} \int_0^{\frac{\pi}{8}} \frac{\xi_i}{4A_0^2 a_i^{\frac{3}{2}}} \left[ \sqrt{2} \tan^{-1} \left( \frac{\xi_i}{\sqrt{2} a_i} \right) \right] d\Gamma = \\ & -\frac{1}{2\pi} \sqrt{\frac{\bar{E}}{N_0}} \int_0^{\frac{\pi}{8}} \frac{g_i(\Gamma, \alpha, \beta)}{\left[ \frac{\bar{E}}{N_0} f_i^2(\Gamma, \alpha, \beta) + 1 \right]^{\frac{3}{2}}} \cdot \\ & \quad \tan^{-1} \left[ \frac{g_i(\Gamma, \alpha, \beta)}{\sqrt{f_i^2(\Gamma, \alpha, \beta) + \left( \frac{\bar{E}}{N_0} \right)^{-1}}} \right] d\Gamma \end{aligned} \quad (4.44)$$

Finally, from the third term on the right hand side of Eq. 4.37 takes on the form

$$\begin{aligned} & -\frac{1}{2\pi} \int_0^{\frac{\pi}{8}} \frac{1}{2a_i\gamma_i A_0^2} d\Gamma = \\ & -\frac{1}{2\pi} \int_0^{\frac{\pi}{8}} \left[ \frac{\bar{E}}{N_0} f_i^2(\Gamma, \alpha, \beta) + 1 \right]^{-1} \left[ 1 + \frac{\frac{\bar{E}}{N_0} f_i^2(\Gamma, \alpha, \beta) + 1}{\frac{\bar{E}}{N_0} g_i(\Gamma, \alpha, \beta)} \right]^{-1} d\Gamma \end{aligned} \quad (4.45)$$

so that the bit error probability for the third-most significant bit is obtained from the sum of Eqs. 4.28 and 4.43 - 4.45 . These integrals have not been expressed in closed form, however corresponding numerical evaluations can and have been carried out without difficulty. The total BER under Rayleigh fading conditions is finally given by

$$P_{b, Ray}\{e\} = \frac{1}{2} P_{Ray}\{1B \text{ incorrect}\} + \frac{1}{4} P_{Ray}\{2B \text{ incorrect}\} + \frac{1}{4} P_{Ray}\{3B \text{ incorrect}\} \quad (4.46)$$

Appendix C presents a listing of the FORTRAN computer program used to evaluate the BER under Rayleigh fading conditions for the 16-PSK DBD receiver. Data from this program is plotted and presented in Chapter 5.

### C. EFFECT ON BER OF MFSK/QPSK USING DBD RECEIVER

Recall that for the MFSK/QPSK DBD receiver, the BER is given by Eq. 3.99 as

$$P_b\{e\} = Q\left(\sqrt{\frac{E}{K_f N_0}}\right) \quad (4.47)$$

This expression must be rewritten as a function of the amplitude  $A$  in order to determine the effect of Rayleigh fading on receiver performance. Substituting Eq. 4.4 into Eq. 4.47 yields

$$\begin{aligned} P_b\{e\} &= Q\left(\sqrt{\frac{A^2 T_s}{2K_f N_0}}\right) \\ &= Q\left(A\sqrt{\frac{T_s}{NN_0}}\right) \end{aligned} \quad (4.48)$$

Weighting this probability by the Rayleigh p.d.f. and integrating over the variable  $A$ , the average bit error probability in the presence of signal fading is

$$P_{b, Ray}\{e\} = \int_{-\infty}^{\infty} Q\left(A\sqrt{\frac{T_s}{NN_0}}\right) f_A(A) dA \quad (4.49)$$

This integral can be evaluated using the identity of Eq. 4.9 as

$$P_{b, Ray}\{e\} = \frac{1}{2} \left[ 1 - \frac{1}{\sqrt{1 + \frac{NN_0}{\bar{E}}}} \right] = \frac{1}{2} \left[ 1 - \frac{1}{\sqrt{N \left( \frac{\bar{E}}{N_0} \right)^{-1} + 1}} \right] \quad (4.50)$$

#### D. EFFECT ON BER OF MFSK/QPSK USING THE OPTIMUM RECEIVER

Evaluation of the (non-fading) BER for MFSK/QPSK using the optimum receiver has been carried out in Chapter 3, Section C. Yet a different approach to determining the BER under Rayleigh fading conditions becomes more practical than using modifications to the approach previously used to evaluate the performance of the DBD receiver. Since the BER given in Eq. 3.81 as a function of  $s$ , the ratio of signal energy to noise variance, namely

$$s = \frac{\sqrt{E}}{\sigma} \quad (4.51)$$

where

$$\sigma = \sqrt{\frac{N_0}{2}} \quad (4.52)$$

has been previously evaluated, a transformation of variables is suggested to yield

$$\begin{aligned} s &= g(A) = \frac{\sqrt{E}}{\sigma} \\ &= \frac{\sqrt{\frac{A^2 T_s}{2}}}{\sqrt{\frac{N_0}{2}}} \\ &= A \sqrt{\frac{T_s}{N_0}} \end{aligned} \quad (4.53)$$

where the range of  $s$  is  $0 \leq s \leq \infty$ . Since the transformation is linear, the p.d.f. of  $s$  can be written as

$$\begin{aligned}
f_s(s) &= \frac{1}{|g'(A)|} f_A(g^{-1}(s)) \\
&= \frac{1}{\sqrt{\frac{T_s}{N_0}}} \frac{s \sqrt{\frac{N_0}{T_s}}}{A_0^2} \exp\left(-\frac{s^2 N_0}{2 T_s A_0^2}\right) u\left(s \sqrt{\frac{N_0}{T_s}}\right) \\
&= \frac{s N_0}{T_s A_0^2} \exp\left(-\frac{s^2 N_0}{2 T_s A_0^2}\right) u(s) \\
&= \frac{s}{S_0^2} \exp\left(-\frac{s^2}{2 S_0^2}\right) u(s)
\end{aligned} \tag{4.54}$$

where  $S_0^2$  is defined by

$$\begin{aligned}
S_0^2 &= A_0^2 \frac{T_s}{N_0} \\
&= \frac{\bar{E}}{N_0}
\end{aligned} \tag{4.55}$$

The BER under fading conditions can be evaluated by averaging the BER given by Eq. 3.81 over the range of the new random variable  $s$  as

$$\begin{aligned}
P_{b, Ray}\{e\} &= \\
&\int_{-\infty}^{\infty} \int_{-s}^{\infty} [1 - 2Q(y + s)]^{N-1} g(y) \frac{s}{S_0^2} \exp\left(-\frac{s^2}{2 S_0^2}\right) u(s) dy ds \\
&+ (N-1) \int_{-\infty}^{\infty} \int_0^{\infty} [1 - 2Q(y)]^{N-2} [1 - Q(y + s) - Q(y - s)] g(y) \frac{s}{S_0^2} \exp\left(-\frac{s^2}{2 S_0^2}\right) u(s) dy ds
\end{aligned} \tag{4.56}$$

This integration also requires numerical techniques, however the program presented in Appendix B can be used as a subroutine for the program listed in Appendix D which is used to evaluate Eq. 4.56. Data from the program of Appendix D is plotted and presented in Chapter 5.



## V. RESULTS

### A. PERFORMANCE COMPARISONS

The symbol error rate (SER) of the receiver for M-ary PSK signals is given by Eq. 1.4, while Eq. 1.8 is used to evaluate the SER of the receiver for M-ary FSK signals. The SER for MFSK/QPSK signals when using the optimum receiver of Figure 12 on page 32 is given by Eq. 3.48. Table 2 lists the ratio of bit energy to noise power spectral density (PSD) level,  $\frac{E_b}{N_0}$ , required to achieve symbol error rates of  $10^{-3}$  and  $10^{-5}$  for M-ary PSK, M-ary FSK, and MFSK/QPSK signaling schemes with  $k$  equal to 3 and 4 bits/symbol. The table shows the MFSK/QPSK signaling scheme yields slightly better performance than M-ary FSK with a nominal 0.2 dB difference, in terms of  $\frac{E_b}{N_0}$ , while outperforming M-ary PSK by an average  $\frac{E_b}{N_0}$  difference of 5.2 dB for  $k = 3$  and 10.4 dB for  $k = 4$ .

Table 2. PERFORMANCE COMPARISONS AT KEY SYMBOL ERROR RATES

| Modulation | Bits per Symbol | $\frac{E_b}{N_0}$ (dB) Required to Achieve |               |
|------------|-----------------|--|---------------|
|            |                 | $10^{-3}$ SER                              | $10^{-5}$ SER |
| 8-PSK      | 3               | 10.8                                       | 14.4          |
| 16-PSK     | 4               | 15.5                                       | 18.4          |
| 8-FSK      | 3               | 06.5                                       | 08.6          |
| 16-FSK     | 4               | 05.6                                       | 07.8          |
| 2FSK QPSK  | 3               | 06.2                                       | 08.5          |
| 4FSK QPSK  | 4               | 05.5                                       | 07.6          |

The BER for MFSK/QPSK signaling using the optimum receiver shown in Figure 11 on page 30 is evaluated using Eq. 3.81. Appendix B presents the FORTRAN computer program used to compute this optimum receiver's bit error probability by employing numerical integration in order to evaluate Eq. 3.81. That is,  $P_b\{e\}$  along with the union bound approximation to this probability as given by Eq. 3.82 is computed for varying values of  $\frac{E_b}{N_0}$ . The program is also used to evaluate  $P_b\{e\}$  for the MFSK/QPSK

DBD receiver, as given by Eq. 3.99. Data generated by this program is plotted in Figure 16 for  $k = 3$ , Figure 17 for  $k = 4$ , Figure 18 for  $k = 5$ , and Figure 19 for  $k = 6$ .

In all of the above referenced figures, numerical values for the BER obtained using the union bound approximation yield plots almost coinciding with the actual BER plots for the optimum receiver at moderate to high  $\frac{E_b}{N_0}$  values. This fact helps to confirm the appropriateness of the results of the numerical integration used to evaluate the actual receiver BER. From these plots, it becomes evident that the MFSK/QPSK DBD receiver suffers a performance penalty when compared to the performance of the optimum receiver. Table 3 lists  $\frac{E_b}{N_0}$  ratios required to achieve BER's of  $10^{-3}$  and  $10^{-6}$  for both the optimum and the DBD receiver structures for MFSK/QPSK modulation. The optimum receiver has an average 2.5 dB better performance than the DBD receiver for  $k = 3$  bits/symbol, which increases to an average value of 5 dB for  $k = 4$  in terms of  $\frac{E_b}{N_0}$  difference. For  $k = 6$ , the optimum receiver has an average 10 dB advantage over the DBD receiver.

Table 3. PERFORMANCE COMPARISONS OF MFSK/QPSK RECEIVERS

| Modulation/<br>Receivers | Bits per<br>Symbol | $\frac{E_b}{N_0}$ (dB) Required to Achieve |               |
|--------------------------|--------------------|--|---------------|
|                          |                    | $10^{-3}$ BER                              | $10^{-6}$ BER |
| 2FSK QPSK                | 3                  |  |               |
| Opt. Rcvr                |                    | 05.8                                       | 09.1          |
| DBD Rcvr                 |                    | 08.0                                       | 11.8          |
| 4FSK QPSK                | 4                  |  |               |
| Opt. Rcvr                |                    | 05.1                                       | 08.1          |
| DBD Rcvr                 |                    | 09.8                                       | 13.6          |
| 8FSK QPSK                | 5                  |  |               |
| Opt. Rcvr                |                    | 04.5                                       | 07.4          |
| DBD Rcvr                 |                    | 11.8                                       | 15.6          |
| 8FSK/QPSK                | 6                  |  |               |
| Opt. Rcvr                |                    | 04.1                                       | 06.8          |
| DBD Rcvr                 |                    | 14.0                                       | 17.8          |

The reasons for this increased performance penalty can be explained as follows. First, as can be seen by examining the DBD receiver BER curves as a function of  $\frac{E_b}{N_0}$ , the performance of the DBD receiver degrades as k, the number of bits per symbol is

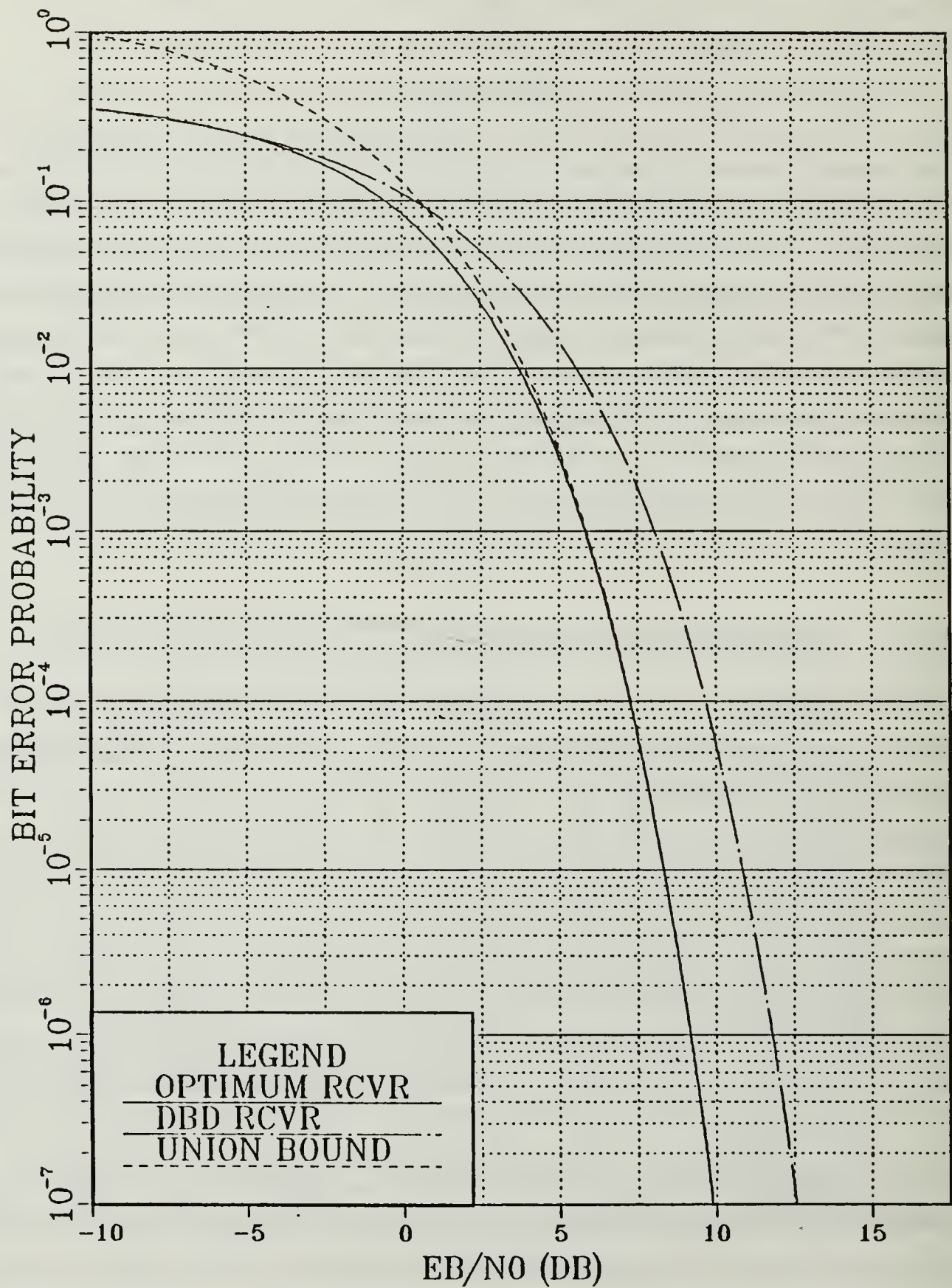


Figure 16. 2FSK/QPSK Bit Error Performance ( $k = 3$  bits/symbol)



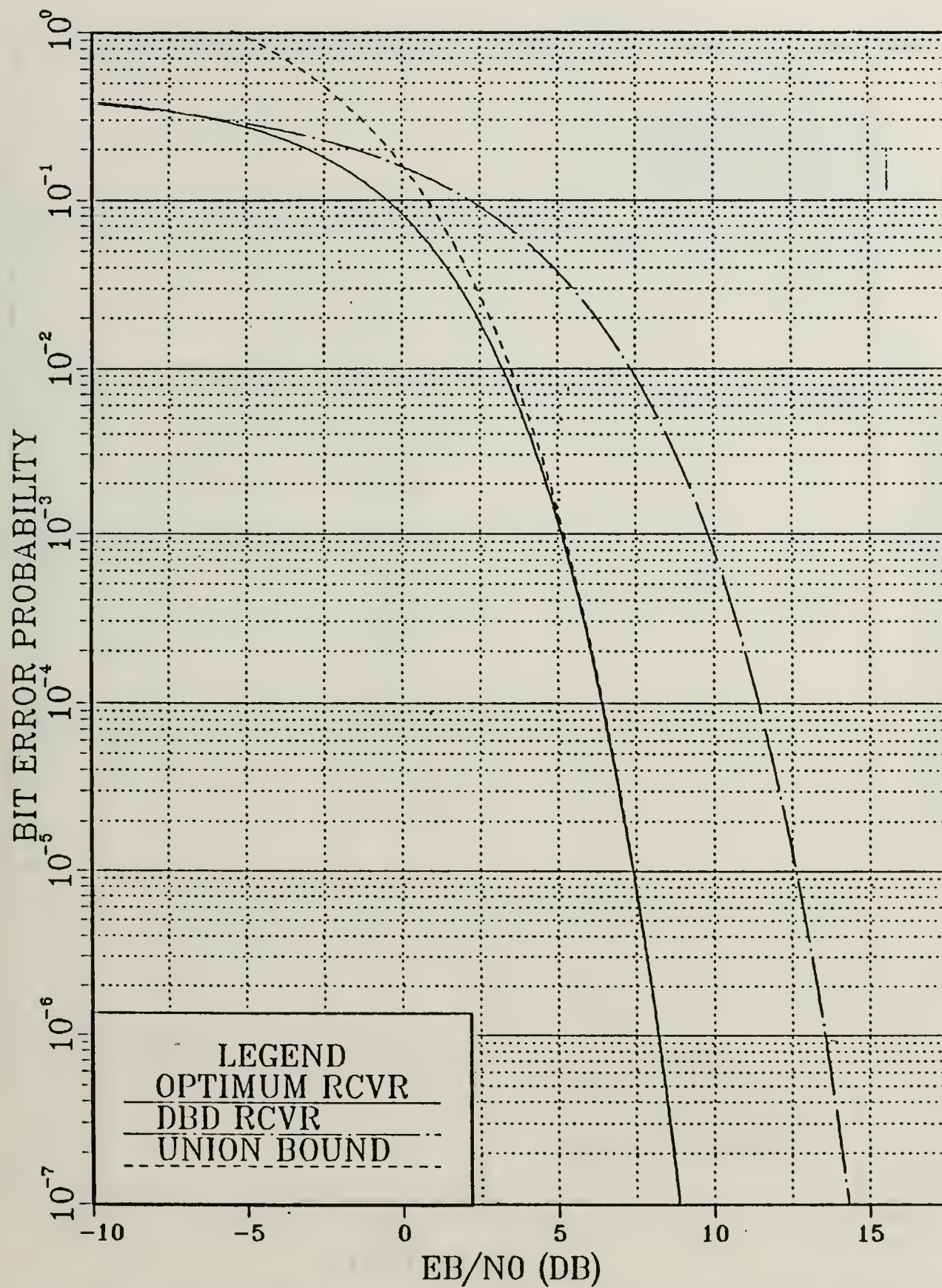


Figure 17. 4FSK/QPSK Bit Error Performance ( $k = 4$  bits/symbol)

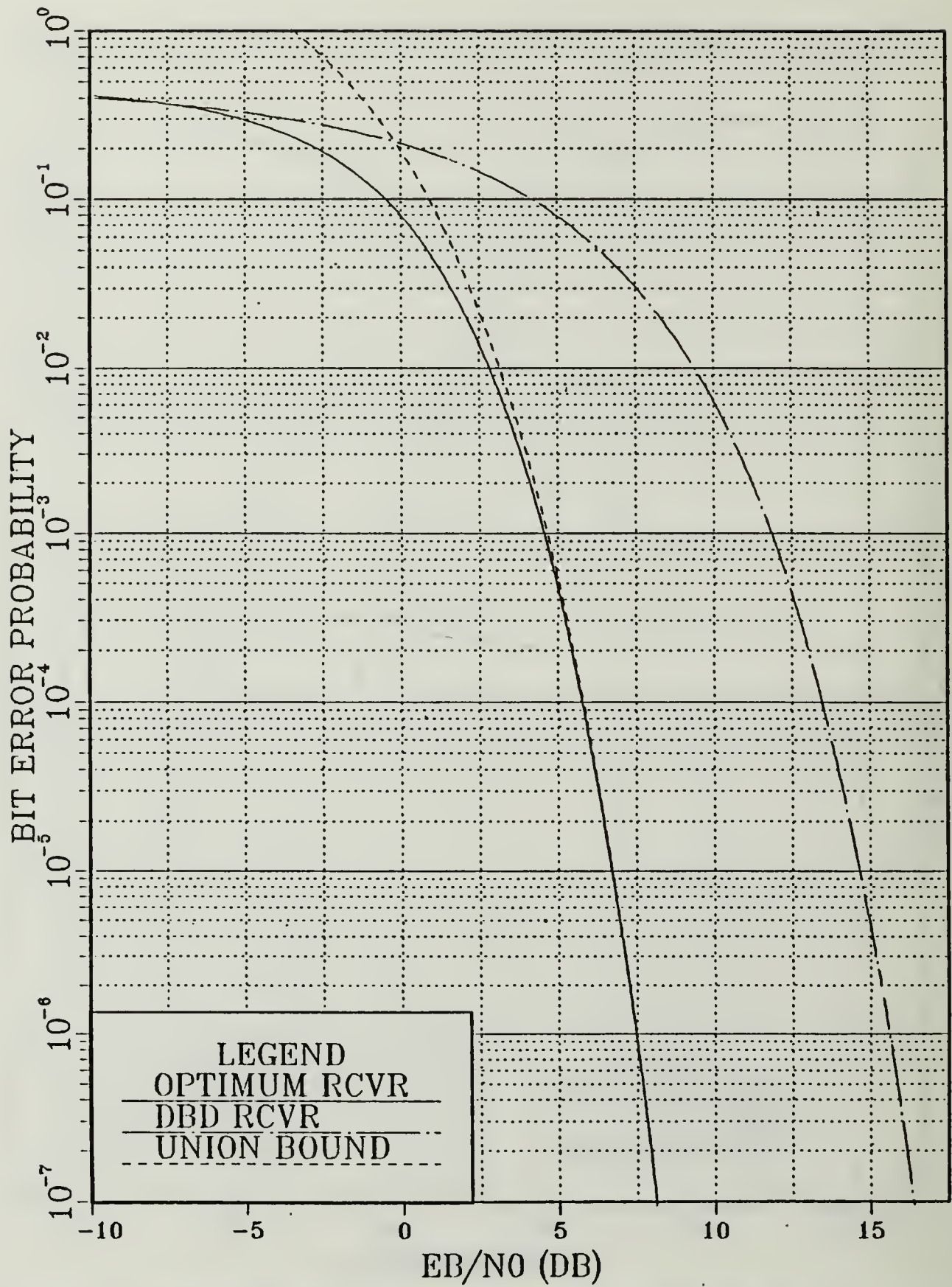


Figure 18. 8FSK/QPSK Bit Error Performance ( $k = 5$  bits/symbol)



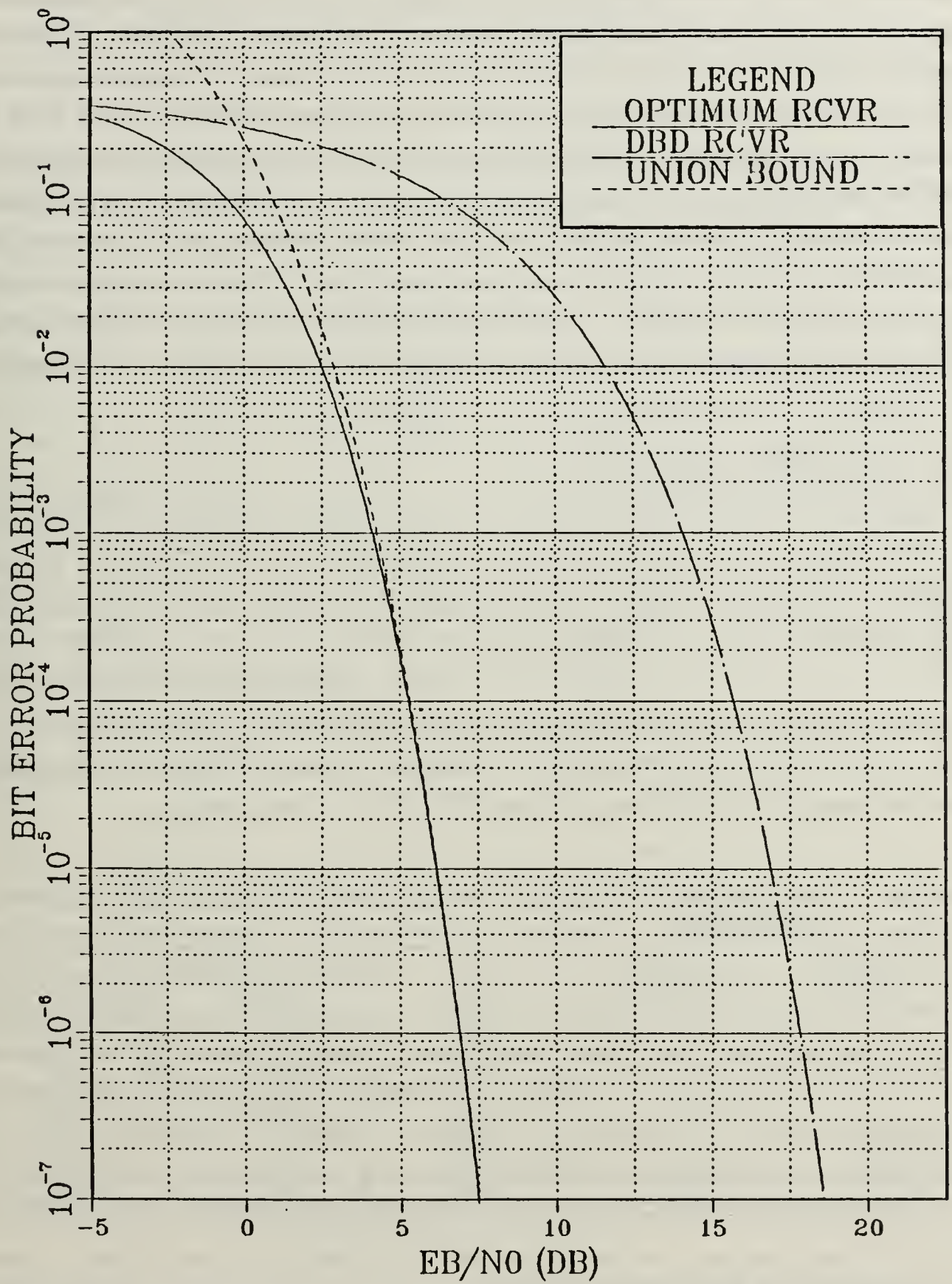


Figure 19. 16FSK/QPSK Bit Error Performance ( $k = 6$  bits/symbol)

increased. Recall from the BER analysis for the DBD receiver, that the variance for the summation output  $b_n$  is the sum of the variances of the correlator outputs  $r_j$ . When the number of bits ( and consequently the number of correlators ) is increased, there is a linear increase in the variance of  $b_n$  . This variance increase, which is strictly noise dependent, causes the bit error probability increase also. On the other hand, examination of the optimum receiver bit error curves reveals that, with increasing  $k$ , the optimum receiver exhibits improved performance. This improvement reflects the tradeoff that exists between bit error rate performance and signal bandwidth, as increasing  $k$  results in a greater signal bandwidth. Note however that this improved receiver performance would not be apparent if the bit error probability were plotted against unnormalized SNR instead of bit-normalized SNR, that is,  $\frac{E_b}{N_0}$  Ref. 6 [pp. 172-175].

### B. BANDWIDTH EFFICIENCY

The bandwidth efficiency for M-ary PSK, M-ary FSK, and MFSK/QPSK signaling is given by Eqs. 3.105, 3.106 and 3.107, respectively. Bandwidth efficiencies given in bits/Hz for values of  $k$  ranging from 2 to 6 bits/symbol are listed in Table 4 for these three signaling schemes. The table shows that M-ary PSK is more bandwidth efficient than both the M-FSK and MFSK/QPSK schemes. MFSK/QPSK is from three to four times as efficient as M-ary FSK, with the greater differences occuring at higher values of  $k$ . MFSK/QPSK operates at 67% the efficiency of M-ary PSK for  $k = 3$  bits/symbol, and at about 40% the efficiency of M-ary PSK for  $k = 4$  bits/symbol.

Table 4. BANDWIDTH EFFICIENCIES FOR M-ARY PSK, M-ARY FSK, AND MFSK/QPSK

| Number<br>of Bits | Number<br>of Signals | Bandwidth Efficiency |      |           |
|-------------------|----------------------|----------------------|------|-----------|
|                   |                      | MPSK                 | MFSK | MFSK QPSK |
| 2                 | 4                    | 1.00                 | 0.40 | ----      |
| 3                 | 8                    | 1.50                 | 0.33 | 1.00      |
| 4                 | 16                   | 2.00                 | 0.24 | 0.80      |
| 5                 | 32                   | 2.50                 | 0.15 | 0.56      |
| 6                 | 64                   | 3.00                 | 0.09 | 0.35      |

### C. EFFECTS OF RAYLEIGH FADING

The BER of the 8-PSK DBD receiver operating under Rayleigh fading signal conditions is given by Eq. 4.16 as a function of average  $\frac{E_b}{N_0}$  . This equation has been used

to evaluate receiver performance as a function of average  $\frac{E_b}{N_0}$  for various values of the angle  $\alpha$ . The plots shown in Figure 20 on page 72 demonstrate that the best receiver performance occurs for  $\alpha = 22.5^\circ$ . The curves for  $\alpha = 20.0^\circ$  and  $\alpha = 25.0^\circ$  and for  $\alpha = 17.5^\circ$  and  $\alpha = 27.5^\circ$  are coincident, and therefore appear as one line for each pair.

Appendix C presents the FORTRAN program used to evaluate via numerical integration the bit error probability under Rayleigh fading signal conditions for the 16-PSK DBD receiver. Data generated by this program is plotted in Figure 21 on page 73 for various values of the angle  $\alpha$  while, maintaining the relationship  $\beta = 45^\circ - \alpha$ . This plot shows the best receiver performance is achieved for  $\alpha = 11.25^\circ$ . Curves for  $\alpha = 9.75^\circ$  and  $\alpha = 12.75^\circ$  as well as for  $\alpha = 8.25^\circ$  and  $\alpha = 14.25^\circ$  are coincident and appear as only one line.

The receiver's BER for MFSK/QPSK using the DBD scheme, is given by Eq. 4.50 when Rayleigh fading signal conditions exist. Figure 22 on page 74 illustrates the plot of this BER for values of  $k$  ranging from 3 to 5 bits/symbol. The best performance is obtained for  $k$  equal to 3, and performance degrades with increasing values of  $k$ . The performance curve has a near linear characteristic for values of average  $\frac{E_b}{N_0}$  exceeding about 5 dB as opposed to the "waterfall" characteristic of the BER curves when Rayleigh fading conditions were not present.

The BER for MFSK/QPSK signaling using the optimum receiver under Rayleigh fading signal conditions is given by Eq. 4.56. Appendix D presents the listing of the FORTRAN program used to evaluate this BER, which involves double numerical integration. Data generated by this program is plotted in Figure 23 on page 75 for values of  $k$  ranging from 3 to 5 bits/symbol. The curves show a somewhat surprising result in that the best performance is obtained when  $k$  is equal to 3, and performance degrades with increasing values of  $k$ . This result is opposite to that encountered when Rayleigh fading conditions were not present, in which increasing  $k$  produced improved receiver performance. The curves of Figure 23 also exhibit nearly linear characteristics for values of average  $\frac{E_b}{N_0}$  greater than approximately 0 dB.

Table 5 on page 76 presents a summary of the average  $\frac{E_b}{N_0}$  values required to achieve bit error rates of  $10^{-1}$  and  $10^{-2}$  for all of the receivers discussed above, under both non-fading and Rayleigh fading signal conditions. For the MFSK/QPSK receivers, in order to simplify the comparisons, only the results for  $k = 3$  are presented. For the MFSK/QPSK receivers, the performance degradation is about the same for both the optimum and the DBD receivers. In order to achieve a BER of  $10^{-1}$  both receivers suffer a nominal 3 dB performance loss in terms of average  $\frac{E_b}{N_0}$  under Rayleigh fading condi-



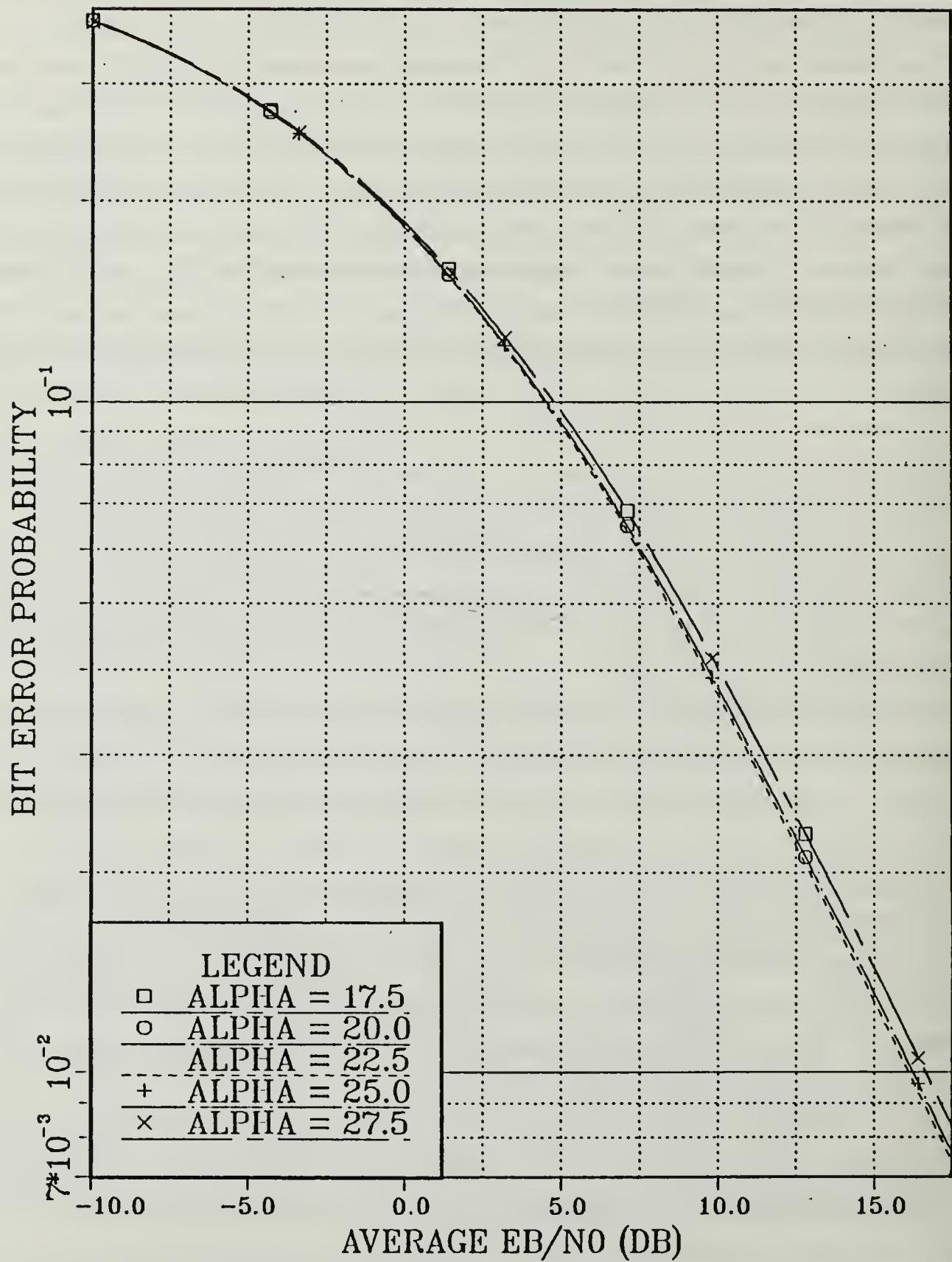


Figure 20. 8-PSK DBD Receiver Bit Error Performance in Rayleigh Fading

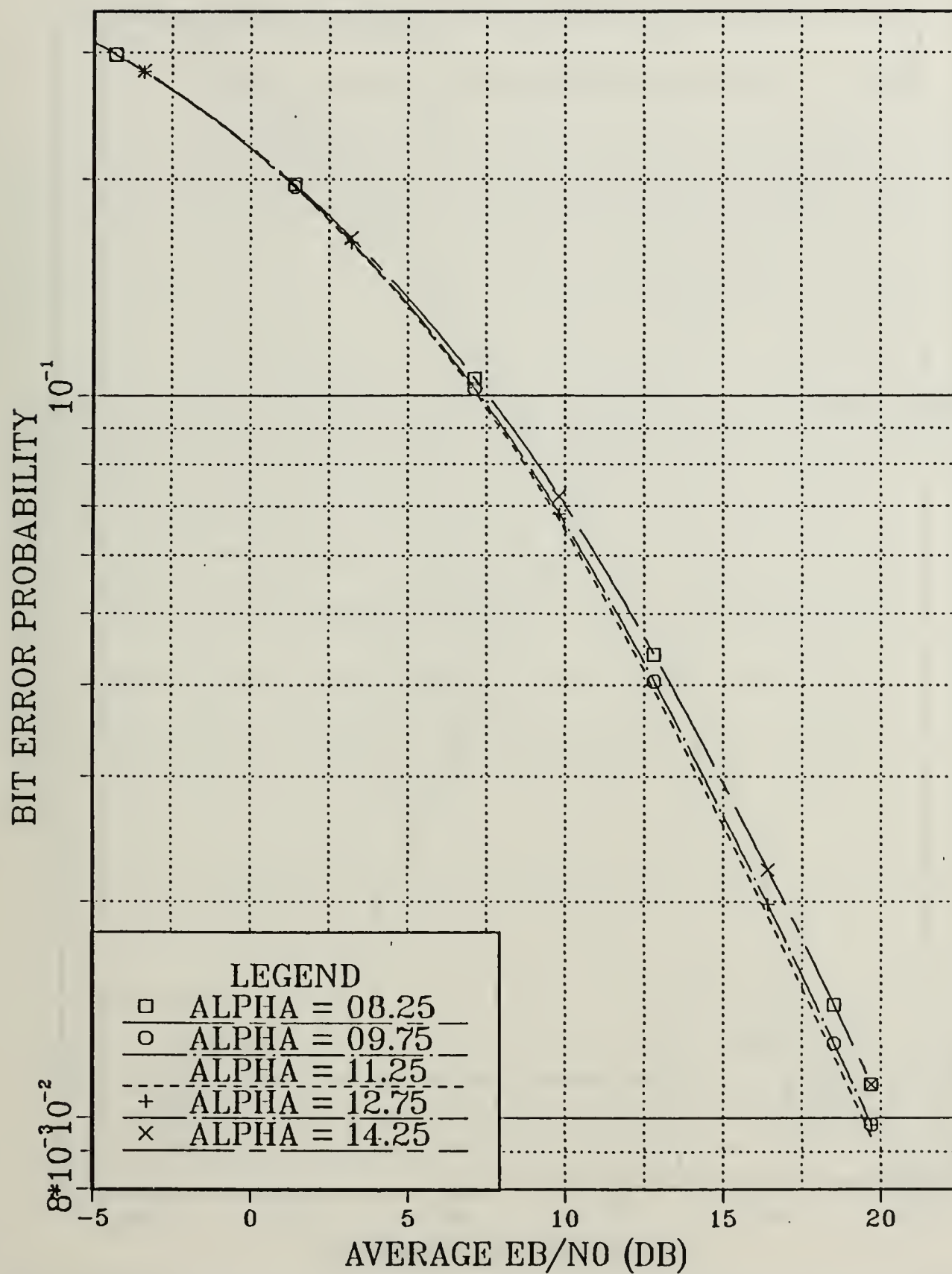


Figure 21. 16-PSK DBD Receiver Bit Error Performance in Rayleigh Fading

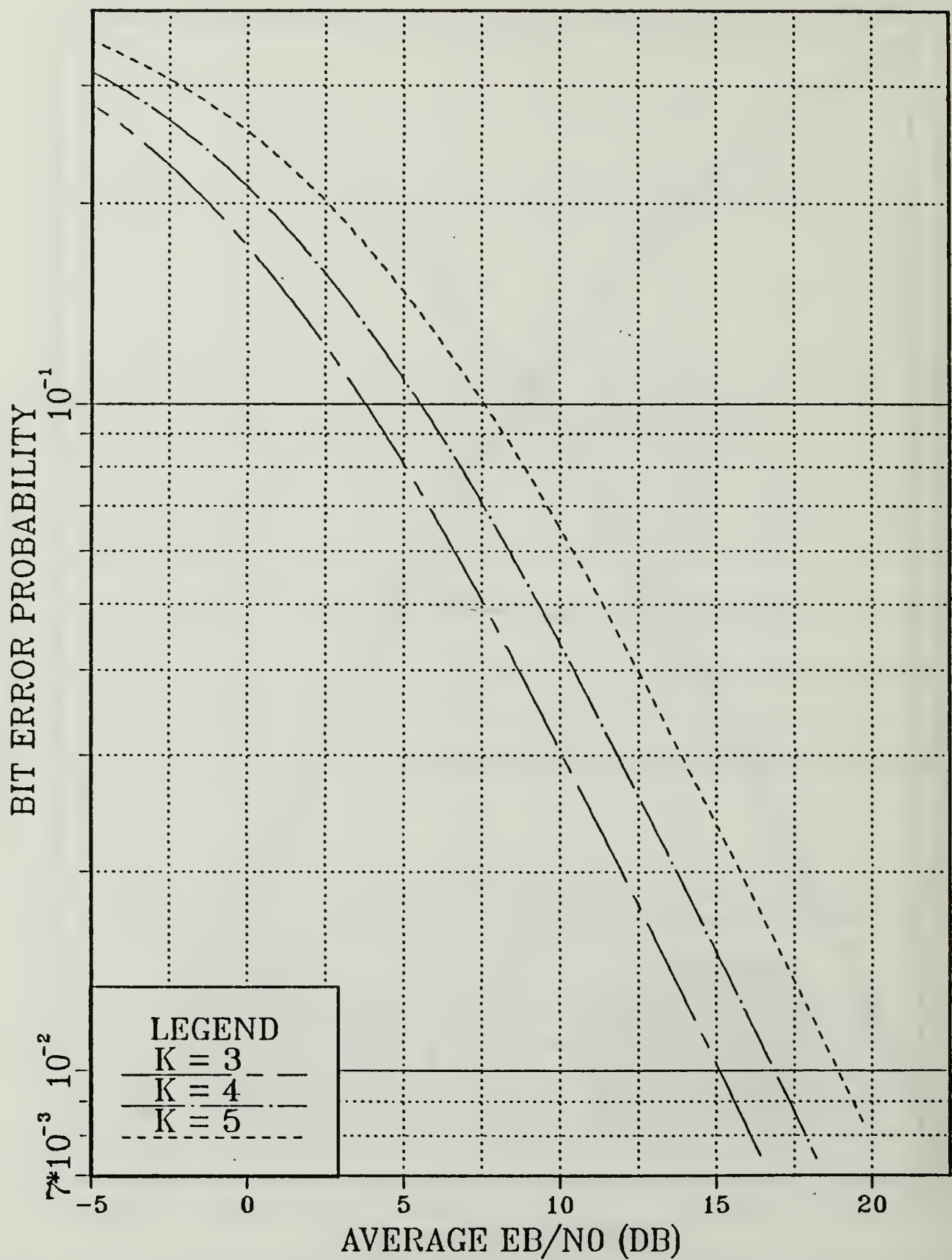


Figure 22. MFSK/QPSK DBD Rcvr. Bit Error Performance in Rayleigh Fading



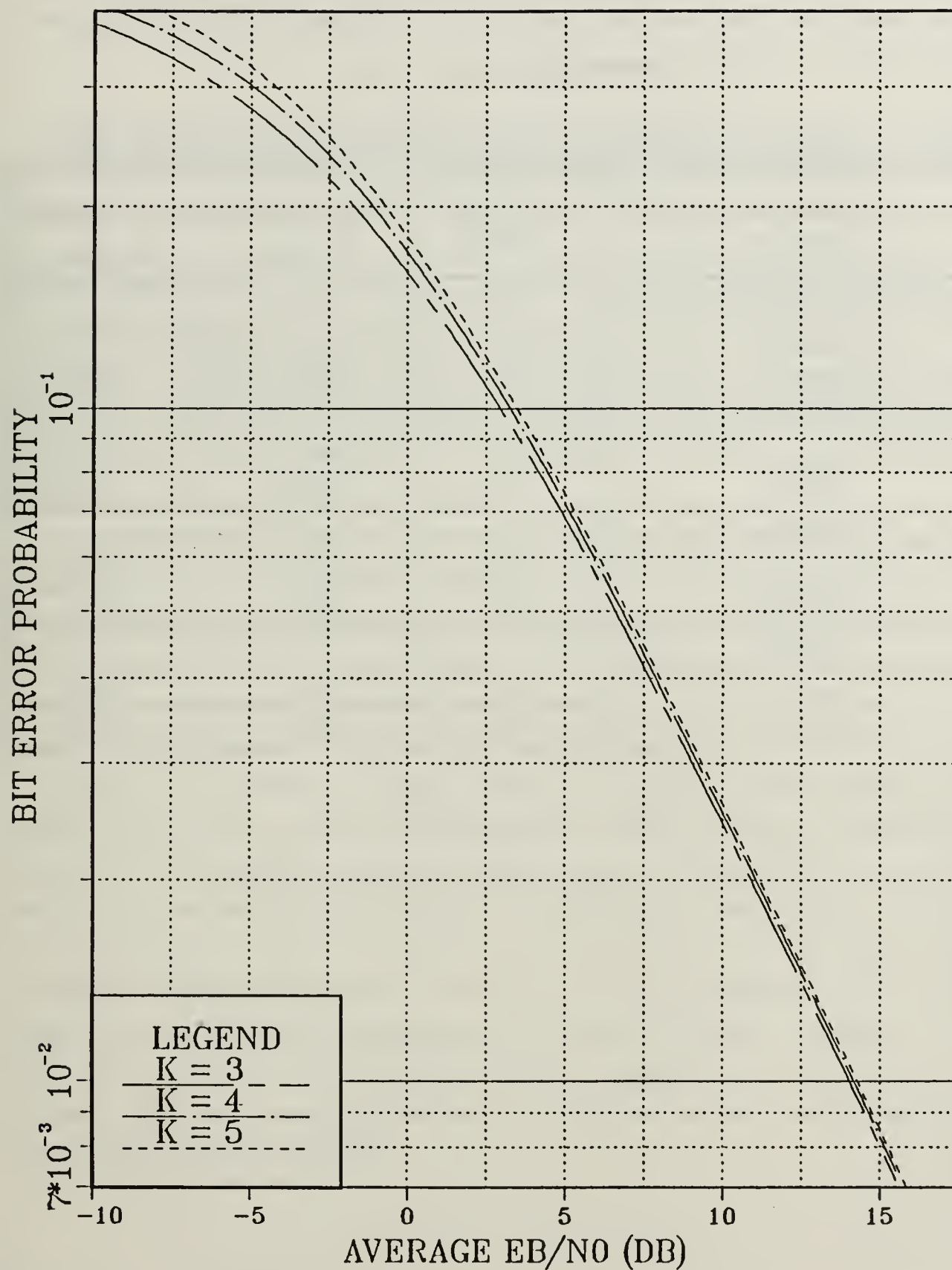


Figure 23. MFSK/QPSK Opt. Rcvr. Bit Error Performance in Rayleigh Fading

tions, and performance is correspondingly degraded by about 10 dB at a BER of  $10^{-2}$ . For the M-ary PSK DBD receivers, performance is degraded by about 4 dB and by 12 dB at a BER of  $10^{-1}$  and  $10^{-2}$ , respectively.

**Table 5. EFFECT OF RAYLEIGH FADING USING VARIOUS RECEIVERS**

| Modulation/<br>Receiver | Rayleigh<br>Fading | $\frac{E_b}{N_0}$ (dB) Required to Achieve |               |
|-------------------------|--------------------|--|---------------|
|                         |                    | $10^{-1}$ BER                              | $10^{-2}$ BER |
| 2FSK/QPSK               |                    |  |               |
| Optimum<br>Receiver     | No                 | -0.6                                       | 03.7          |
|                         | Yes                | 02.9                                       | 14.0          |
| 2FSK/QPSK               |                    |  |               |
| DBD<br>Receiver         | No                 | 00.4                                       | 05.6          |
|                         | Yes                | 03.6                                       | 15.1          |
| 8-PSK                   |                    |  |               |
| DBD<br>Receiver         | No                 | 00.1                                       | 03.9          |
|                         | Yes                | 04.4                                       | 16.0          |
| 16-PSK                  |                    |  |               |
| DBD<br>Receiver         | No                 | 03.6                                       | 07.4          |
|                         | Yes                | 07.2                                       | 19.4          |

## VI. CONCLUSIONS

The results presented show that MFSK/QPSK modulation is superior to M-ary FSK in aspects of error performance and bandwidth efficiency. While MFSK/QPSK has only slightly better error performance over M-ary FSK, MFSK/QPSK requires only one-third to one-fourth the bandwidth used by M-ary FSK signaling. Also, since the MFSK/QPSK receiver requires the use of only one fourth the number of synchronized carriers and integrate and dump circuits required by the M-ary FSK receiver, it can be argued that the MFSK/QPSK receiver is less complex than the M-ary FSK receiver. The results also show that MFSK/QPSK is comparable to M-ary PSK in the sense that it offers improved error performance over M-ary PSK, but does not reduce bandwidth efficiency as much as orthogonal signaling.

In comparing the different types of MFSK/QPSK receivers, the DBD receiver offers the ability to decode bits individually without symbol-to-bit mapping circuitry; however, this is accomplished at the expense of error performance. This error performance penalty becomes prohibitive for larger values of  $k$ . Since the advantage of receiver simplicity is no longer as attractive for larger  $k$ , the DBD receiver should be considered as an alternative to the optimum receiver only for smaller values of  $k$ .

Analysis of the effect of Rayleigh fading in M-ary FSK DBD receivers and in MFSK/QPSK receivers has generally demonstrated severe performance degradation in the sense of producing large increases in the bit energy to noise PSD ratios required to maintain only modest BER performance. The penalties increase rapidly for lower bit error probabilities. Unless fading effects can be overcome, all of the receivers studied become impractical in the presence of fading. The MFSK/QPSK receivers show a slight reduction in performance degradation over the M-ary PSK DBD receivers. For the M-ary PSK receivers, the same value of the angle adjustment  $\alpha$  which produced the minimum BER for a non-fading channel also produced the best overall performance under Rayleigh fading conditions.

## APPENDIX A. INTEGRAL IDENTITY

This appendix presents the proof for the integral identity used in the text as Eq. 4.13.

$$\int_{-\infty}^{\infty} Q(\alpha A)Q(\beta A)f_A(A)dA = \frac{1}{4} - \frac{\beta \tan^{-1} \left[ \frac{\sqrt{\beta^2 + \frac{1}{A_0^2}}}{\alpha} \right]}{2\pi \sqrt{\beta^2 + \frac{1}{A_0^2}}} - \frac{\alpha \tan^{-1} \left[ \frac{\sqrt{\alpha^2 + \frac{1}{A_0^2}}}{\beta} \right]}{2\pi \sqrt{\alpha^2 + \frac{1}{A_0^2}}} \quad (B.1)$$

We integrate by parts, i.e.,

$$\int_0^{\infty} u dv = uv \Big|_0^{\infty} + \int_0^{\infty} v du \quad (B.2)$$

with the following substitutions

$$u = Q(\alpha A)Q(\beta A) \quad (B.3)$$

and

$$\begin{aligned} dv &= f_A(A)dA \\ &= \frac{A}{A_0^2} \exp\left(-\frac{A^2}{2A_0^2}\right)dA \end{aligned} \quad (B.4)$$

Differentiating Eq. B.3 with respect to  $A$ , yields

$$\frac{du}{dA} = Q(\alpha A)\dot{Q}(\beta A) + \dot{Q}(\alpha A)Q(\beta A) \quad (B.5)$$

where

$$\begin{aligned}
\dot{Q}(\alpha A) &= \frac{d}{dA} Q(\alpha A) \\
&= \frac{d}{dA} \int_{\alpha A}^{\infty} \frac{1}{\sqrt{2\pi}} \exp\left(-\frac{y^2}{2}\right) dy \\
&= -\frac{\alpha}{\sqrt{2\pi}} \exp\left(-\frac{\alpha^2 A^2}{2}\right)
\end{aligned} \tag{B.6}$$

where the last equality is obtained using Liebnitz rule to differentiate the integral. Similar results hold for  $\dot{Q}(\beta A)$ , thus yielding

$$du = -\left[ Q(\alpha A) \frac{\beta}{\sqrt{2\pi}} \exp\left(-\frac{\beta^2 A^2}{2}\right) + Q(\beta A) \frac{\alpha}{\sqrt{2\pi}} \exp\left(-\frac{\alpha^2 A^2}{2}\right) \right] dA \tag{B.7}$$

Now, integrating Eq. B.4 to obtain  $v$  results in

$$\begin{aligned}
v &= \int \frac{A}{A_0^2} \exp\left(-\frac{A^2}{2A_0^2}\right) dA \\
&= -\exp\left(-\frac{A^2}{2A_0^2}\right)
\end{aligned} \tag{B.8}$$

Solving for the first term on the right hand side of Eq. B.2 yields

$$\begin{aligned}
uv|_0^\infty &= \left[ -Q(\alpha A) Q(\beta A) \exp\left(-\frac{A^2}{2A_0^2}\right) \right]_0^\infty = Q^2(0) \\
&= \frac{1}{4}
\end{aligned} \tag{B.9}$$

For the second term on the right hand side of Eq. B.2 , we have

$$\begin{aligned}
\int_0^\infty v du &= \int_0^\infty \exp\left(-\frac{A^2}{2A_0^2}\right) \cdot \\
&\quad \left[ Q(\alpha A) \frac{\beta}{\sqrt{2\pi}} \exp\left(-\frac{\beta^2 A^2}{2}\right) + Q(\beta A) \frac{\alpha}{\sqrt{2\pi}} \exp\left(-\frac{\alpha^2 A^2}{2}\right) \right] dA \\
&= \int_0^\infty \left[ Q(\alpha A) \frac{\beta}{\sqrt{2\pi}} \exp(-z_1^2 A^2) + Q(\beta A) \frac{\alpha}{\sqrt{2\pi}} \exp(-z_2^2 A^2) \right] dA
\end{aligned} \tag{B.10}$$



where  $z_1$  and  $z_2$  are defined as

$$z_1 \equiv \sqrt{\frac{\beta^2}{2} + \frac{1}{2A_0^2}} \quad (B.11)$$

and

$$z_2 \equiv \sqrt{\frac{\alpha^2}{2} + \frac{1}{2A_0^2}} \quad (B.12)$$

The form of these integrals is similar to the identity given by [Ref. 9: pp. 1-20] as

$$\int_0^\infty \text{Erfc}(ax) \exp(b^2 x^2) dx = \frac{1}{2b\sqrt{\pi}} \ln \left[ \frac{a+b}{a-b} \right] \quad (B.13)$$

where  $a$  and  $b$  may be complex, and

$$\left| \tan^{-1} \left[ \frac{\text{Real}(a)}{\text{Imag}(a)} \right] \right| < \frac{\pi}{4} \quad (B.14)$$

Using this identity and the equality

$$Q(x) = \frac{1}{2} \text{Erfc} \left( \frac{x}{\sqrt{2}} \right) \quad (B.15)$$

produces an equivalent form, namely

$$\int_0^\infty Q(ax) \exp(b^2 x^2) dx = \frac{1}{4b\sqrt{\pi}} \ln \left[ \frac{a+b\sqrt{2}}{a-b\sqrt{2}} \right] \quad (B.16)$$

Using Eq. B.16 to solve Eq. B.10 yields

$$\int_0^\infty v du = \frac{\beta}{j4\pi z \sqrt{2}} \ln \left[ \frac{\alpha + jz_1 \sqrt{2}}{\alpha - jz_1 \sqrt{2}} \right] + \frac{\alpha}{j4\pi z \sqrt{2}} \ln \left[ \frac{\beta + jz_2 \sqrt{2}}{\beta - jz_2 \sqrt{2}} \right] \quad (B.17)$$

Focusing on the argument of the first log function and converting to complex exponential notation produces



$$\begin{aligned}
\frac{\alpha + jz_1\sqrt{2}}{\alpha - jz_1\sqrt{2}} &= \frac{\sqrt{\alpha^2 + 2z_1^2} \exp\left[j \tan^{-1}\left(\frac{z_1\sqrt{2}}{\alpha}\right)\right]}{\sqrt{\alpha^2 + 2z_1^2} \exp\left[j \tan^{-1}\left(\frac{-z_1\sqrt{2}}{\alpha}\right)\right]} \\
&= \exp\left[j\left\{\tan^{-1}\left(\frac{z_1\sqrt{2}}{\alpha}\right) - \tan^{-1}\left(\frac{-z_1\sqrt{2}}{\alpha}\right)\right\}\right] \\
&= \exp\left[j2 \tan^{-1}\left(\frac{z_1\sqrt{2}}{\alpha}\right)\right]
\end{aligned} \tag{B.18}$$

where the last equality holds by restricting both  $\alpha$  and  $z_1$  to be positive, which is indeed the case. Using this result in Eq. B.17 yields

$$\int_0^\infty v du = \frac{\beta \tan^{-1}\left[\frac{\sqrt{\beta^2 + \frac{1}{A_0^2}}}{\alpha}\right]}{2\pi \sqrt{\beta^2 + \frac{1}{A_0^2}}} + \frac{\alpha \tan^{-1}\left[\frac{\sqrt{\alpha^2 + \frac{1}{A_0^2}}}{\beta}\right]}{2\pi \sqrt{\alpha^2 + \frac{1}{A_0^2}}} \tag{B.19}$$

Finally, substituting Eqs. B.9 and B.19 into Eq. B.2 yields the right hand side of Eq. B.1, thus proving the identity.

## APPENDIX B. MFSK/QPSK BER COMPUTER PROGRAM

```

*****
*
*   PROGRAM TO COMPUTE THE BIT ERROR RATES FOR THE BI-ORTHOGONAL
*   SIGNAL SET (BOSS) FOR THE OPTIMUM RCVR AND FOR THE MFSK/QPSK
*   DIRECT BIT DETECTION (DBD) RCVR.
*
*****

```

PROGRAM PRBTER

```

IMPLICIT CHARACTER*1 (A-Z)
DOUBLE PRECISION EBNODB,INIT,FINAL,DLTADB
DOUBLE PRECISION EBDVNO,SREDSEI
DOUBLE PRECISION PRBTCT,PRBER,INTGL1,INTGL2,INTGL3
DOUBLE PRECISION DBDPBE,UBAPBE
DOUBLE PRECISION DCADRE,F1,A1,B1,AERR,RERR,ERROR
DOUBLE PRECISION F2,A2,B2,F3
DOUBLE PRECISION PIE,SQR2PI,SQR8PI,ONE
INTEGER I,K,N,M,F,IER,NUMPTS
INTEGER LEVEL,LEVOLD

EXTERNAL F1,F2,F3
COMMON SREDSEI,N

```

```

C                                     INITIALIZE CONSTANTS
PIE      = 3.141592654D0
SQR2PI   = DSQRT(2*PIE)
SQR8PI   = DSQRT(8*PIE)
K        = 6
M        = 2**K
N        = 2** (K-1)
F        = 2** (K-2)
A2       = 00.0D0
B1       = 20.0D0
B2       = 20.0D0
ONE      = 01.0D0
NUMPTS   = 101
INIT     = -10.0D0
FINAL    = 8.0D0
DLTADB   = (FINAL - INIT)/(NUMPTS-1)
AERR     = 0.0
RERR     = .0000001

```

```

C                                     SUPPRESS ALL ERROR MESSAGES.
LEVEL = 0

```

```
CALL UERSET(LEVEL,LEVOLD)
CALL XUFLOW(0)
```

```
C
C
C      COMPUTE PROBABILITY OF BIT ERROR
      FOR VALUES OF EB/NO IN THE RANGE OF:
      INIT < EBNODB < FINAL
```

```
      WRITE(8,100) K,F
      WRITE(8,*) ' '
      WRITE(8,*) '
&   UNION BOUND'
      WRITE(8,*) '
&   APPROXIMATION'
      WRITE(8,*) 'INDEX   EB/NO (DB)   PROBABILITY   PROBABILITY
&   BIT ERROR'
      EBNODB = INIT
      DO 10 I=1,NUMPTS
        EBDVNO = 10.0D0**((EBNODB/10)
        SREDISI = DSQRT(2*EBDVNO*K)
        A1      = -SREDISI
        INTGL1 = DCADRE(F1,A1,B1,AERR,RERR,ERROR,IER) / SQR2PI
        INTGL2 = DCADRE(F2,A2,B2,AERR,RERR,ERROR,IER) / SQR8PI
        INTGL3 = DCADRE(F3,A1,B2,AERR,RERR,ERROR,IER) / SQR8PI
        IF(INTGL3.GT.0.0D0) THEN
          PRBTCL = (N-1)*(INTGL2+INTGL3) + INTGL1
        ELSE
          PRBTCL = (N-1)*INTGL2 + (N-1)*INTGL3 + INTGL1
        ENDIF
        PRBERR = ONE - PRBTCL
        DBDPBE = DERFC( DSQRT(2*K*EBDVNO/M) ) / 2
        UBAPBE = ( (M - 2)*DERFC( DSQRT(K*EBDVNO/2) )
&               + DERFC( DSQRT(K*EBDVNO) ) ) / 4
        WRITE(8,101) I,EBNODB,PRBERR,DBDPBE,UBAPBE
        EBNODB = EBNODB + DLTADB
10  CONTINUE
```

```
100 FORMAT(2X,'NUMBER OF BITS: ',2X,I1,6X,'NUMBER OF FREQUENCIES: ',
&         2X,I1)
101 FORMAT(2X,I3,3X,F10.5,3X,E14.5E2,3X,E14.5E2,3X,E14.5E2)
      STOP
      END
```

```
*****
      DOUBLE PRECISION FUNCTION F1(Y)
```

```
      DOUBLE PRECISION Y,SREDISI,SQRT2
      INTEGER          N
```

```
      COMMON           SREDISI,N
```

```
C
C      INITIALIZE CONSTANT
      SQRT2 = DSQRT(2.0D0)
```

```

C                                COMPUTE F1(Y,SREDSI,N)

F1  =  DERF( (Y+SREDSI)/SQRT2 )**(N-1) * DEXP(-(Y**2)/2)

RETURN
END

```

```

*****
DOUBLE PRECISION FUNCTION F2(Y)
DOUBLE PRECISION  Y,FACTR1,FACTR2,SREDSI
DOUBLE PRECISION  SQRT2
INTEGER           N

```

```
COMMON          SREDSI,N
```

```

C                                INITIALIZE CONSTANTS

SQRT2  =  DSQRT(2.0D0)

```

```

C                                COMPUTE F2(Y,SREDSI,N)

```

```

FACTR1 = DERF( Y/SQRT2 )**(N-2)
FACTR2 = DERF( (Y+SREDSI)/SQRT2 )
F2      = FACTR1*FACTR2*DEXP(-(Y**2)/2)

```

```

RETURN
END

```

```

*****
DOUBLE PRECISION FUNCTION F3(Y)
DOUBLE PRECISION  Y,FACTR1,FACTR2,SREDSI
DOUBLE PRECISION  SQRT2
INTEGER           N

```

```
COMMON          SREDSI,N
```

```

C                                INITIALIZE CONSTANTS

SQRT2  =  DSQRT(2.0D0)

```

```

C                                COMPUTE F3(Y,SREDSI,N)

```

```

FACTR1 = DERF( (Y+SREDSI)/SQRT2 )**(N-2)
FACTR2 = DERF( Y/SQRT2 )
F3      = FACTR1*FACTR2*DEXP(-(Y+SREDSI)**2/2 )

```

```

RETURN
END

```

# APPENDIX C. 16-PSK RAYLEIGH FADING BER COMPUTER PROGRAM

```

*****
*
*
*   PROGRAM TO COMPUTE THE PROBABILITY OF A BIT ERROR FOR 16-PSK USING
*   THE DIRECT BIT DETECTION (DBD) RECEIVER IN THE RAYLEIGH FADING
*   ENVIROMENT.
*
*****

```

```

PROGRAM      DBDRAY

```

```

IMPLICIT CHARACTER*1 (A-Z)
DOUBLE PRECISION  EBNODB,INIT,FINAL,DLTADB,PBERAY
DOUBLE PRECISION  EBDVNO,AVESNR,ALPHA,AL$DEG,BETA
DOUBLE PRECISION  P1BERY,V1$FTN(4),ARGMNT
DOUBLE PRECISION  P2BERY,V2$FTN(4),ARG$1,ARG$2
DOUBLE PRECISION  P3BERY,INTGRL(8),TERM$1,TERM$2,TERM$3
DOUBLE PRECISION  F1,A,B,ERRABS,ERRREL,INTGL1,ERREST
DOUBLE PRECISION  F2,F3,INTGL2,INTGL3
DOUBLE PRECISION  PI,ONE,SUM$1,SUM$2
INTEGER           I,INDEX,NUMPTS,IRULE

EXTERNAL          F1,F2,F3
COMMON            AVESNR,ALPHA,BETA,INDEX

```

```

C                                     SUPPRESS IMSL10 ERROR MESSAGES.
CALL ERSET(3,0,-1)

```

```

C                                     INITIALIZE CONSTANTS

```

```

PI      = 3.141592654D0
ONE     = 1.0D0
AL$DEG  = 14.25D0
ALPHA   = AL$DEG * PI/180
BETA    = PI/4 - ALPHA

V1$FTN(1) = DCOS(ALPHA)
V1$FTN(2) = DCOS(BETA)
V1$FTN(3) = DSIN(ALPHA)
V1$FTN(4) = DSIN(BETA)

V2$FTN(1) = DCOS(ALPHA) - DSIN(ALPHA)
V2$FTN(2) = DCOS(ALPHA) + DSIN(ALPHA)
V2$FTN(3) = DCOS(BETA) - DSIN(BETA)

```



V2\$FTN(4) = DCOS(BETA) + DSIN(BETA)

NUMPTS = 101  
 INIT = -10.000  
 FINAL = 20.000  
 DLTADB = (FINAL - INIT)/(NUMPTS-1)

A = 0.000  
 B = PI/8  
 ERRABS = 0.000  
 ERRREL = 0.0001  
 IRULE = 2

C COMPUTE PROBABILITY OF BIT ERROR  
 C FOR VALUES OF EBNODB IN THE RANGE OF:  
 C INIT < EBNODB < FINAL

WRITE(8,\*)'EFFECT OF RAYLEIGH FADING ON 16-PSK, DBD RCVR'  
 WRITE(8,100) AL\$DEG  
 WRITE(8,\*)' '  
 WRITE(8,\*)' DBD RCVR'  
 WRITE(8,\*)' BIT ERROR'  
 WRITE(8,\*)' INDEX EB/NO (DB) PROBABILITY'  
 EBNODB = INIT

C BEGIN MAIN LOOP.

DO 70 I=1,NUMPTS  
 EBDVNO = 10.000\*\*\*(EBNODB/10)  
 AVESNR = 2 \* EBDVNO

C CALCULATE PROBABILITY OF 1B ERROR

SUM\$1 = 0.000  
 DO 10 INDEX=1,4  
 ARG\$1 = EBDVNO / (4 \* EBDVNO \* V1\$FTN(INDEX)\*\*2 + ONE)  
 SUM\$1 = SUM\$1 + V1\$FTN(INDEX) \* DSQRT(ARG\$1)  
 10 CONTINUE  
 P1BERY = (2.000 - SUM\$1)/4

C CALCULATE PROBABILITY OF 2B ERROR

SUM\$1 = 0.000  
 DO 20 INDEX=1,4  
 ARG\$1 = EBDVNO / (EBDVNO \* V2\$FTN(INDEX)\*\*2 + ONE/2)  
 SUM\$1 = SUM\$1 + V2\$FTN(INDEX) \* DSQRT(ARG\$1)  
 20 CONTINUE  
 SUM\$2 = 0.000  
 DO 30 INDEX=1,4  
 ARG\$1 = DSQRT( V2\$FTN(INDEX)\*\*2 + ONE / (2\*EBDVNO) )  
 ARG\$2 = ARG\$1 / V2\$FTN( INDEX - (-1)\*\*(INDEX) )  
 SUM\$2 = SUM\$2 + V2\$FTN(INDEX) \* DATAN(ARG\$2) / ARG\$1  
 30 CONTINUE  
 P2BERY = ONE/2 - SUM\$1/4 + SUM\$2/(2\*PI)

C CALCULATE PROBABILITY OF 3B ERROR

```

      DO 40 INDEX=1,8
      CALL DQDAG (F1,A,B,ERRABS,ERRREL,IRULE,INTGL1,ERREST)
      TERM$1 = DSQRT(AVESNR)*INTGL1/4
      CALL DQDAG (F2,A,B,ERRABS,ERRREL,IRULE,INTGL2,ERREST)
      TERM$2 = INTGL2
      CALL DQDAG (F3,A,B,ERRABS,ERRREL,IRULE,INTGL3,ERREST)
      TERM$3 = DSQRT(AVESNR)*INTGL3
      INTGRL(INDEX) = TERM$1 - (TERM$2 + TERM$3)/(4*PI)
40    CONTINUE

      SUM$1 = 0.0D0
      DO 50 INDEX=5,8
      SUM$1 = SUM$1 + INTGRL(INDEX)
50    CONTINUE

      SUM$2 = 0.0D0
      DO 60 INDEX=1,4
      SUM$2 = SUM$2 + INTGRL(INDEX)
60    CONTINUE

      P3BERY = ONE/2 + SUM$1 - SUM$2
      PBERAY = P1BERY/2 + P2BERY/4 + P3BERY/4
      WRITE(8,101) I,EBNODB,PBERAY
      EBNODB = EBNODB + DLTADB
70    CONTINUE
C                                     END MAIN LOOP

100  FORMAT(2X,'ALPHA =',1X,F5.2,1X,'DEGREES. ')
101  FORMAT(2X,I3,3X,F10.5,3X,E14.5E2,3X,E14.5E2,3X,E14.5E2)

      STOP
      END

*****
      DOUBLE PRECISION FUNCTION  F1(GAMMA)

      IMPLICIT CHARACTER*1 (A-Z)
      DOUBLE PRECISION  GAMMA,AVESNR,ALPHA,BETA
      DOUBLE PRECISION  TERM$1,FINDEX,GINDEX
      INTEGER            INDEX

      COMMON              AVESNR,ALPHA,BETA,INDEX

C                                     COMPUTE F1(INDEX,GAMMA,AVESNR,ALPHA,BETA)
C
      GO TO (10,20,30,40,50,60,70,80) INDEX

10  FINDEX = DSIN(GAMMA - ALPHA)
      GINDEX = DCOS(GAMMA - ALPHA)
      GO TO 100

```

```

20 FINDEX = DCOS(GAMMA - ALPHA)
   GINDEX = DSIN(GAMMA - ALPHA)
   GO TO 100

30 FINDEX = DCOS(GAMMA + ALPHA)
   GINDEX = DSIN(GAMMA + ALPHA)
   GO TO 100

40 FINDEX = DSIN(GAMMA + ALPHA)
   GINDEX = DCOS(GAMMA + ALPHA)
   GO TO 100

50 FINDEX = DSIN(GAMMA - BETA)
   GINDEX = DCOS(GAMMA - BETA)
   GO TO 100

60 FINDEX = DCOS(GAMMA - BETA)
   GINDEX = DSIN(GAMMA - BETA)
   GO TO 100

70 FINDEX = DCOS(GAMMA + BETA)
   GINDEX = DSIN(GAMMA + BETA)
   GO TO 100

80 FINDEX = DSIN(GAMMA + BETA)
   GINDEX = DCOS(GAMMA + BETA)

100 TERM$1 = AVESNR * FINDEX**2 + 1.0D0/2
    F1      = GINDEX / TERM$1 / DSQRT(TERM$1)

    RETURN
    END

```

\*\*\*\*\*

```
DOUBLE PRECISION FUNCTION F2(GAMMA)
```

```
IMPLICIT CHARACTER*1 (A-Z)
```

```
DOUBLE PRECISION GAMMA, AVESNR, ALPHA, BETA
```

```
DOUBLE PRECISION TERM$1, TERM$2, FINDEX, GINDEX
```

```
INTEGER INDEX
```

```
COMMON AVESNR, ALPHA, BETA, INDEX
```

```

C                                     COMPUTE F2( INDEX, GAMMA, AVESNR, ALPHA, BETA)
C

```

```
GO TO (10,20,30,40,50,60,70,80) INDEX
```

```

10 FINDEX = DSIN(GAMMA - ALPHA)
   GINDEX = DCOS(GAMMA - ALPHA)
   GO TO 100

```

```
20 FINDEX = DCOS(GAMMA - ALPHA)
```

```

    GINDEX = DSIN(GAMMA - ALPHA)
    GO TO 100

30  FINDEX = DCOS(GAMMA + ALPHA)
    GINDEX = DSIN(GAMMA + ALPHA)
    GO TO 100

40  FINDEX = DSIN(GAMMA + ALPHA)
    GINDEX = DCOS(GAMMA + ALPHA)
    GO TO 100

50  FINDEX = DSIN(GAMMA - BETA)
    GINDEX = DCOS(GAMMA - BETA)
    GO TO 100

60  FINDEX = DCOS(GAMMA - BETA)
    GINDEX = DSIN(GAMMA - BETA)
    GO TO 100

70  FINDEX = DCOS(GAMMA + BETA)
    GINDEX = DSIN(GAMMA + BETA)
    GO TO 100

80  FINDEX = DSIN(GAMMA + BETA)
    GINDEX = DCOS(GAMMA + BETA)

100 TERM$1 = AVESNR * FINDEX**2    + 1.0D0/2
    TERM$2 = AVESNR * GINDEX**2
    F2     = TERM$2 / (TERM$1*TERM$2 + TERM$1**2)

    RETURN
    END

```

\*\*\*\*\*

```

    DOUBLE PRECISION FUNCTION F3(GAMMA)

```

```

    IMPLICIT CHARACTER*1 (A-Z)
    DOUBLE PRECISION GAMMA,AVESNR,ALPHA,BETA
    DOUBLE PRECISION TERM$1,TERM$2,FACTR1,FACTR2,FINDEX,GINDEX
    INTEGER INDEX

```

```

    COMMON AVESNR,ALPHA,BETA,INDEX

```

```

C                                     COMPUTE F3(INDEX,GAMMA,AVESNR,ALPHA,BETA)
C

```

```

    GO TO (10,20,30,40,50,60,70,80) INDEX

```

```

10  FINDEX = DSIN(GAMMA - ALPHA)
    GINDEX = DCOS(GAMMA - ALPHA)
    GO TO 100

```

```

20  FINDEX = DCOS(GAMMA - ALPHA)

```

```

    GINDEX = DSIN(GAMMA - ALPHA)
    GO TO 100

30  FINDEX = DCOS(GAMMA + ALPHA)
    GINDEX = DSIN(GAMMA + ALPHA)
    GO TO 100

40  FINDEX = DSIN(GAMMA + ALPHA)
    GINDEX = DCOS(GAMMA + ALPHA)
    GO TO 100

50  FINDEX = DSIN(GAMMA - BETA)
    GINDEX = DCOS(GAMMA - BETA)
    GO TO 100

60  FINDEX = DCOS(GAMMA - BETA)
    GINDEX = DSIN(GAMMA - BETA)
    GO TO 100

70  FINDEX = DCOS(GAMMA + BETA)
    GINDEX = DSIN(GAMMA + BETA)
    GO TO 100

80  FINDEX = DSIN(GAMMA + BETA)
    GINDEX = DCOS(GAMMA + BETA)

100 TERMS1 = AVESNR * FINDEX**2 + 1.0D0/2
    TERM$2 = AVESNR * GINDEX**2
    FACTR1 = GINDEX / TERMS1 / DSQRT(TERM$1)
    FACTR2 = DATAN( DSQRT(TERM$2/TERMS1) )
    F3      = FACTR1 * FACTR2

    RETURN
    END

```



# APPENDIX D. MFSK/QPSK RAYLEIGH FADING BER COMPUTER PROGRAM

```

*****
*
*
*   PROGRAM TO COMPUTE THE BIT ERROR RATES FOR THE BI-ORTHOGONAL
*   SIGNAL SET (BOSS) FOR THE OPTIMUM RCVR WHEN SUBJECTED TO RAYLEIGH
*   FADING.
*
*
*****

```

PROGRAM PBTERA

```

IMPLICIT CHARACTER*1 (A-Z)
DOUBLE PRECISION EBNODB,INIT,FINAL,DLTADB
DOUBLE PRECISION EBDVNO,SOSQRD,S
DOUBLE PRECISION PBCRAY,PBERAY
DOUBLE PRECISION DCADR2,INTGND,LIL,UIL,AERR,RERR,ERROR
DOUBLE PRECISION ONE
INTEGER I,K,N,M,F,IER,NUMPTS
INTEGER LEVEL,LEVOLD

EXTERNAL INTGND
COMMON SOSQRD,S,N

```

C INITIALIZE CONSTANTS

```

K      = 5
M      = 2**K
N      = 2**(K-1)
F      = 2**(K-2)
LIL    = 00.0D0
ONE    = 01.0D0
NUMPTS = 101
INIT   = -10.0D0
FINAL  = 20.0D0
DLTADB = (FINAL - INIT)/(NUMPTS-1)
AERR   = 0.0
RERR   = .0001

```

C SUPPRESS ALL ERROR MESSAGES.

```

LEVEL = 0
CALL UERSET(LEVEL,LEVOLD)
C     CALL XUFLOW(0)

```

C  
C  
C

COMPUTE PROBABILITY OF BIT ERROR  
FOR VALUES OF EB/NO IN THE RANGE OF:  
INIT < EBNODB < FINAL

```

WRITE(8,*) 'EFFECT OF RAYLEIGH FADING ON BOSS'
WRITE(8,*) ' '
WRITE(8,100) K,F
WRITE(8,*) ' '
WRITE(8,*) '
WRITE(8,*) '
WRITE(8,*) ' INDEX    EB/NO (DB)    OPTIMUM RCVR'
WRITE(8,*) '                                BIT ERROR '
WRITE(8,*) '                                PROBABILITY '
EBNODB = INIT
DO 10 I=1,NUMPTS
    EBDVNO = 10.0D0**((EBNODB/10))
    SOSQRD = EBDVNO * K
    UIL     = MIN(18.5D0,10*DSQRT(SOSQRD) )
    PBERAY = DCADR2(INTGND,LIL,UIL,AERR,RERR,ERROR,IER) / SOSQRD
    WRITE(8,101) I,EBNODB,PBERAY
    EBNODB = EBNODB + DLTADB
10 CONTINUE

100 FORMAT(2X,'NUMBER OF BITS: ',2X,I1,6X,'NUMBER OF FREQUENCIES: ',
&          2X,I1)
101 FORMAT(2X,I3,3X,F10.5,3X,E14.5E2,3X,E14.5E2,3X,E14.5E2)

STOP
END

```

\*\*\*\*\*

DOUBLE PRECISION FUNCTION INTGND(SRED SI)

```

IMPLICIT CHARACTER*1 (A-Z)
DOUBLE PRECISION EBDVNO,SRED SI,SOSQRD,S,THRHL
DOUBLE PRECISION PRBTGR,PRBTER,ORTERM,APTERM
DOUBLE PRECISION INTGL1,INTGL2,INTGL3
DOUBLE PRECISION DCADRE,F1,A1,B1,AERR,RERR,ERROR
DOUBLE PRECISION F2,A2,B2,F3
DOUBLE PRECISION PIE,SQR2PI,SQR8PI,ONE
INTEGER N,IER

EXTERNAL F1,F2,F3
COMMON SOSQRD,S,N

```

C

INITIALIZE CONSTANTS

```

THRHL = 6.2D0
PIE    = 3.141592654D0
ONE    = 1.00D0
SQR2PI = DSQRT(2*PIE)
SQR8PI = DSQRT(8*PIE)
AERR   = 0.0
RERR   = .0000001

```

```

A2      = 00.0D0
B1      = 20.0D0
B2      = 20.0D0

```

```

C          COMPUTE PROBABILITY OF BIT ERROR AS A
C          FUNCTION OF SREDSI AND N

```

```

IF(SREDSI.GT.THRHLD) THEN

```

```

C          USE UNION BOUND APPROXIMATION

```

```

ORTERM = (2*N - 2)*DERFC( SREDSI/2 )
APTERM = DERFC( SREDSI / DSQRT(2.0D0) )
PRBTER = ( ORTERM + APTERM ) / 4
ELSE

```

```

C          USE EXACT CALCULATION

```

```

S      = SREDSI
A1     = -SREDSI
INTGL1 = DCADRE(F1,A1,B1,AERR,RERR,ERROR,IER) / SQR2PI
INTGL2 = DCADRE(F2,A2,B2,AERR,RERR,ERROR,IER) / SQR8PI
INTGL3 = DCADRE(F3,A1,B2,AERR,RERR,ERROR,IER) / SQR8PI
IF( INTGL3.GT.0.0D0 ) THEN
    PRBTCL = INTGL1 + (N-1)*(INTGL2+INTGL3)
ELSE
    PRBTCL = INTGL1 + (N-1)*INTGL2 + (N-1)*INTGL3
ENDIF
PRBTER = ONE - PRBTCL

```

```

ENDIF

```

```

C          COMPUTE INTGND(SREDSI,SQSQRD,N).

```

```

INTGND = PRBTER * SREDSI * DEXP( -(SREDSI**2) / (2 * SOSQRD) )

```

```

RETURN
END

```

```

*****
DOUBLE PRECISION FUNCTION F1(Y)

```

```

DOUBLE PRECISION  Y,SQSQRD,S,SQRT2
INTEGER           N

```

```

COMMON           SOSQRD,S,N

```

```

C          INITIALIZE CONSTANT

```

```

SQRT2 = DSQRT(2.0D0)

```

```

C          COMPUTE F1(Y,S,N)

```

```

F1 = DERF( (Y+S)/SQRT2 )**(N-1) * DEXP(-(Y**2)/2)

```

```

RETURN
END

```

\*\*\*\*\*

```
DOUBLE PRECISION FUNCTION F2(Y)
DOUBLE PRECISION  Y,FACTR1,FACTR2,SQSQRD,S
DOUBLE PRECISION  SQRT2
INTEGER           N
```

```
COMMON           SOSQRD,S,N
```

```
C               INITIALIZE CONSTANTS
SQRT2  = DSQRT(2.0D0)
```

```
C               COMPUTE F2(Y,S,N)
```

```
FACTR1 = DERF( Y/SQRT2 )**(N-2)
FACTR2 = DERF( (Y+S)/SQRT2 )
F2      = FACTR1*FACTR2*DEXP(-(Y**2)/2)
```

```
RETURN
END
```

\*\*\*\*\*

```
DOUBLE PRECISION FUNCTION F3(Y)
DOUBLE PRECISION  Y,FACTR1,FACTR2,SQSQRD,S
DOUBLE PRECISION  SQRT2
INTEGER           N
```

```
COMMON           SOSQRD,S,N
```

```
C               INITIALIZE CONSTANTS
SQRT2  = DSQRT(2.0D0)
```

```
C               COMPUTE F3(Y,S,N)
```

```
FACTR1 = DERF( (Y+S)/SQRT2 )**(N-2)
FACTR2 = DERF( Y/SQRT2 )
F3      = FACTR1*FACTR2*DEXP(-(Y+S)**2/2 )
```

```
RETURN
END
```

## LIST OF REFERENCES

1. Bukofzer, Daniel C., "A Two Channel Direct-Bit Detection Receiver for 16-PSK Modulated Signals," *IEE Proceedings*, Part F, pp. 461-470, October 1988.
2. Frostenson, Nels A. and Sonnefeld, Michael D., *2 FSK/QPSK Transmitter and Receiver: Design and Performance*, Master's Thesis, Naval Postgraduate School, Monterey, CA, December 1987.
3. Ziemer, Rodger E. and Peterson, Roger L., *Digital Communications and Spread Spectrum Systems*, Macmillan, 1985.
4. Myers, G. A. and Bukofzer, Daniel C., "A Simple Two-Channel Receiver for 8-PSK which Provides Direct Bit Detection and Has Optimum Performance," submitted to *IEEE Transactions on Communications*.
5. Wozencraft, John M. and Jacobs, Irwin M., *Principles of Communication Engineering*, John Wiley & Sons, Inc., 1965.
6. Sklar, Bernard, *Digital Communications Fundamentals and Applications*, Prentice-Hall, 1988.
7. Papoulis, Athanasios, *Probability, Random Variables, and Stochastic Processes*, McGraw-Hill, 1984.
8. Bukofzer, Daniel C., "Bit Error Rates in QAM Systems and the Effect of Rayleigh Fading," paper presented at the Sixth International Conference on Systems Engineering, Coventry, England, September 1988.
9. Ng, Edward W., and Geller, Murray, "A Table of Integrals of the Error Functions," *Journal of Research of the National Bureau of Standards - B. Mathematical Sciences*, v. 73 B, No. 1, January-March 1969.



## INITIAL DISTRIBUTION LIST

|  | No. Copies |
|--|------------|
| 1. Defense Technical Information Center<br>Cameron Station<br>Alexandria, VA 22304-6145  | 2          |
| 2. Library, Code 0142<br>Naval Postgraduate School<br>Monterey, CA 93943-5002  | 2          |
| 3. Chairman, Code 62<br>Electrical and Computer Engineering Department<br>Naval Postgraduate School<br>Monterey, CA 93943-5000                 | 1          |
| 4. Dr. Daniel C. Bukofzer, Code 62Bh<br>Electrical and Computer Engineering Department<br>Naval Postgraduate School<br>Monterey, CA 93943-5000 | 5          |
| 5. Dr. Glen A. Myers, Code 62Mv<br>Electrical and Computer Engineering Department<br>Naval Postgraduate School<br>Monterey, CA 93943-5000      | 1          |
| 6. Commandant (G-PTE)<br>United States Coast Guard<br>2100 Second Street, N.W.<br>Washington, DC 20593   | 2          |
| 7. Commanding Officer<br>U.S. Coast Guard Station<br>7323 Telegraph Rd.<br>Attn: LT Larry Rudy<br>Alexandria, VA 22310-3999                    | 2          |















Th  
R8  
c.  
Thesis  
R8375  
c.1 Rudy

The performance of  
conventional and DBD  
receivers for MFSK/QPSK  
modulation when opera-  
ting in the presence of  
noise and Rayleigh  
fading.

Thesis

R8375 Rudy  
c.1

The performance of  
conventional and DBD  
receivers for MFSK/QPSK  
modulation when opera-  
ting in the presence of  
noise and Rayleigh  
fading.



thesR8375

The performance of conventional and DBD



3 2768 000 81493 3

DUDLEY KNOX LIBRARY C.1